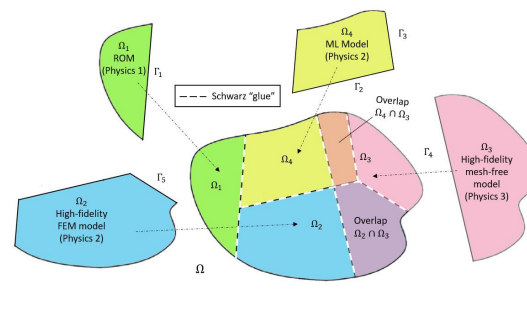
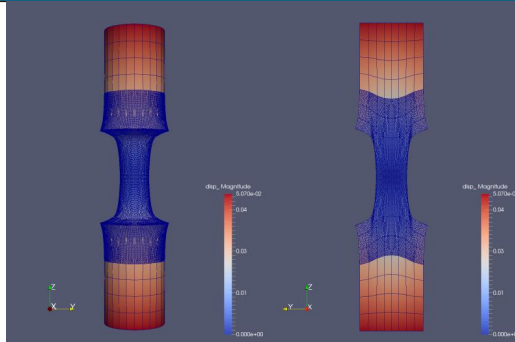
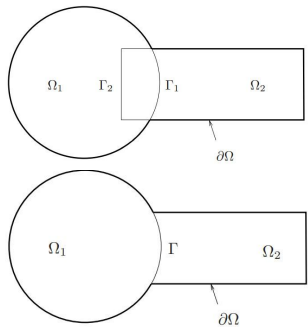


Accelerating mod/sim workflows through hybrid domain decomposition-based models and the Schwarz alternating method



Irina Tezaur¹, Alejandro Mota¹, Coleman Alleman¹, Greg Phlipot²,
Chris Wentland¹, Francesco Rizzi³, Joshua Barnett⁴

¹Sandia National Laboratories, ²MSC Software, ³NexGen Analytics,
⁴Cadence Design Systems

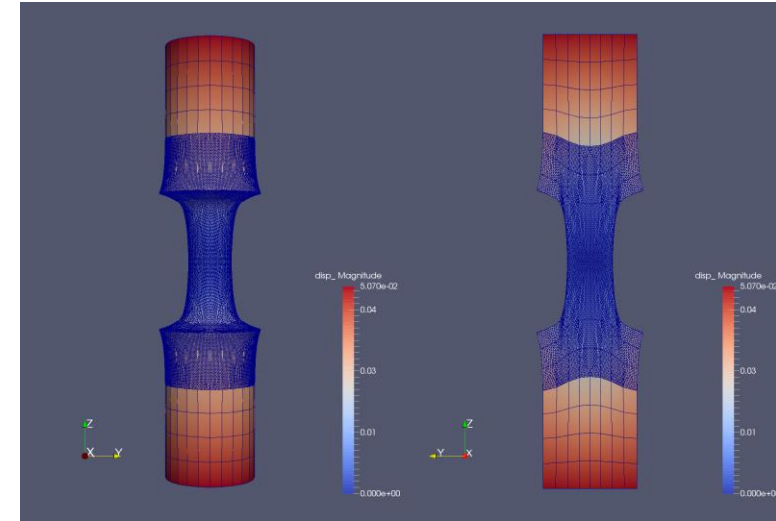
ESCO 2024

June 10-14, 2024

SAND2024-06735C

1. Schwarz Alternating Method for Coupling of Full Order Models (FOMs) in Solid Mechanics

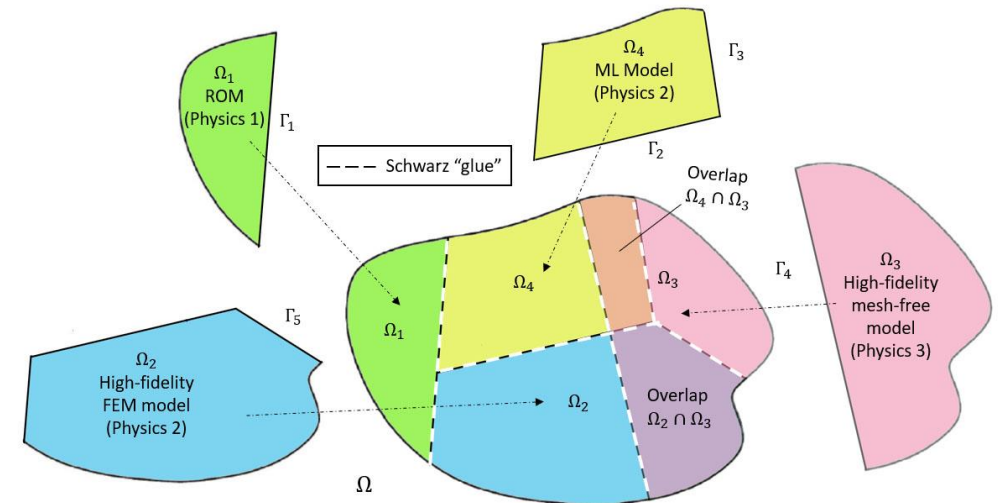
- Motivation & Background
- Quasistatic Formulation
 - Numerical Examples
- Extension to Dynamics
 - Numerical Examples



2. Schwarz Alternating Method for FOM-ROM* and ROM-ROM Coupling

- Motivation & Background
- Formulation
- Numerical Examples

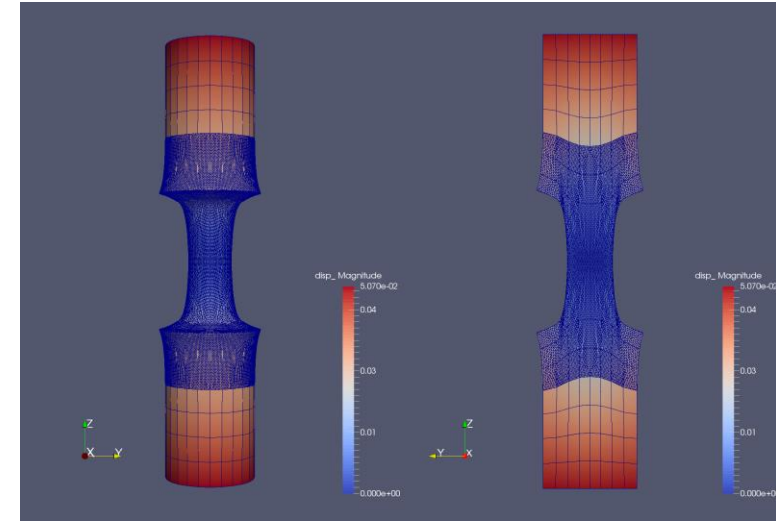
3. Summary and Future Work



* Projection-based Reduced Order Model

1. Schwarz Alternating Method for Coupling of Full Order Models (FOMs) in Solid Mechanics

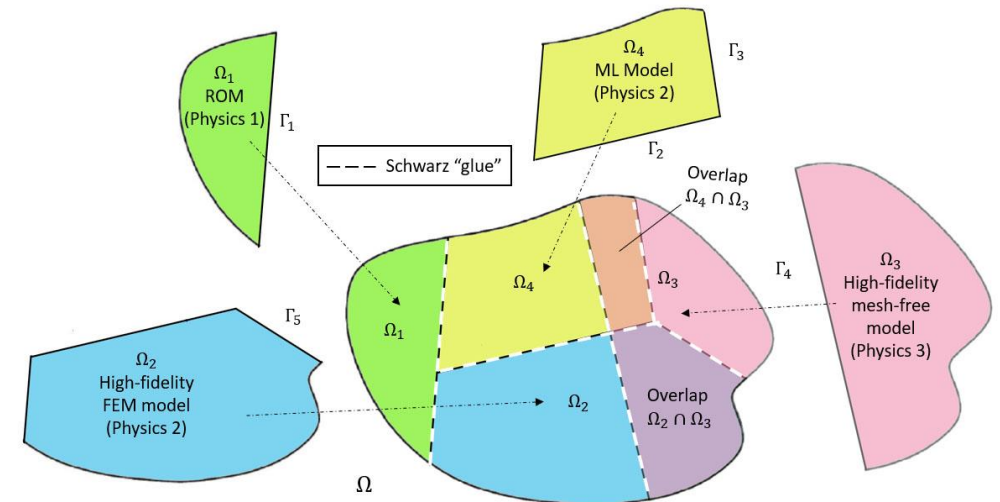
- Motivation & Background
- Quasistatic Formulation
 - Numerical Examples
- Extension to Dynamics
 - Numerical Examples



2. Schwarz Alternating Method for FOM-ROM* and ROM-ROM Coupling

- Motivation & Background
- Formulation
- Numerical Examples

3. Summary and Future Work



* Projection-based Reduced Order Model

Motivation for Coupling in Solid Mechanics

Concurrent multiscale coupling for predicting failure

- **Large scale** structural **failure** frequently originates from **small scale** phenomena such as defects, microcracks, inhomogeneities and more, which grow quickly in unstable manner
- Failure occurs due to **tightly coupled interaction** between small scale (stress concentrations, material instabilities, cracks, etc.) and large scale (vibration, impact, high loads and other perturbations)
- **Concurrent multiscale methods** are **essential** for understanding and prediction of behavior of engineering systems when a **small scale failure** determines the performance of the entire system

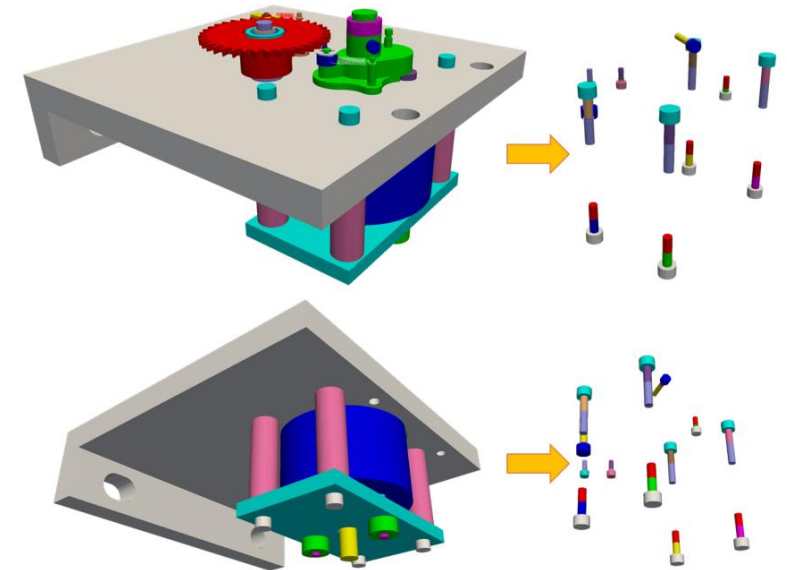
Simplification of mesh generation

- Creating a **high-quality mesh** for a **single component** can take **weeks**, making it “the single biggest bottleneck in analyses” [Sandia Lab News, 2020]!

Goal: develop a **concurrent multiscale coupling method** that is **minimally-intrusive** to implement into large HPC codes and can **simplify** the task of **meshing** complex geometries.



Roof failure of Boeing 737 aircraft due to fatigue cracks. From *imechanica.org*

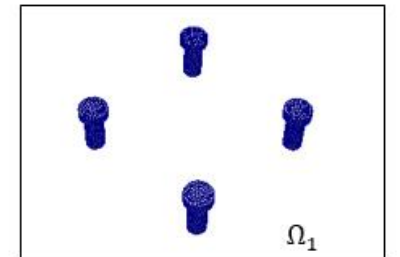
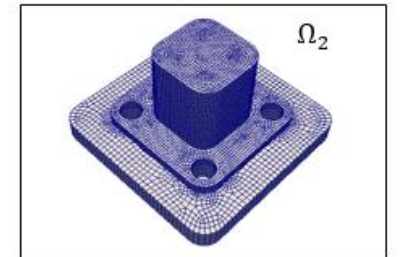
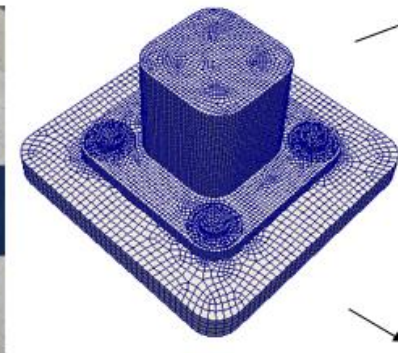


Schematic of difficult-to-mesh ratcheting mechanism with multiple threaded fasteners. From Parish *et al.*, 2024.

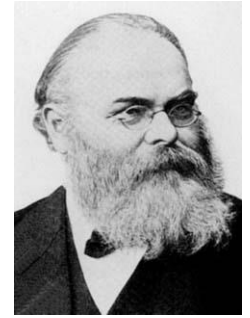
Requirements for Multiscale Coupling Method



- Coupling is *concurrent* (two-way)
- *Ease of implementation* into existing massively-parallel HPC codes
- “*Plug-and-play*” *framework*: simplifies task of meshing complex geometries
 - Ability to couple regions with *different non-conformal meshes*, *different element types* and *different levels of refinement*
 - Ability to use *different solvers/time-integrators* in different regions
- *Scalable, fast, robust* (we target *real* engineering problems, e.g., analyses involving failure of bolted components!)
- Coupling does not introduce *nonphysical artifacts*
- *Theoretical* convergence properties/ guarantees



6 Schwarz Alternating Method for Domain Decomposition



H. Schwarz (1843-1921)



- Proposed in 1870 by H. Schwarz for solving Laplace PDE on irregular domains.

Crux of Method: if the solution is known in regularly shaped domains, use those as pieces to iteratively build a solution for the more complex domain.

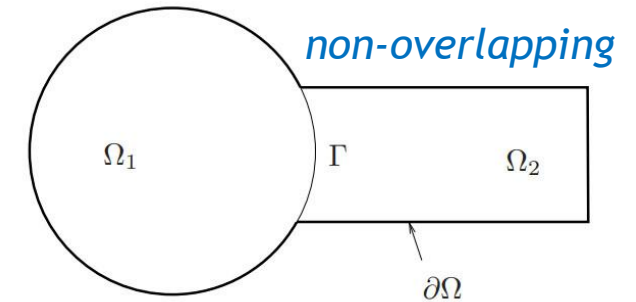
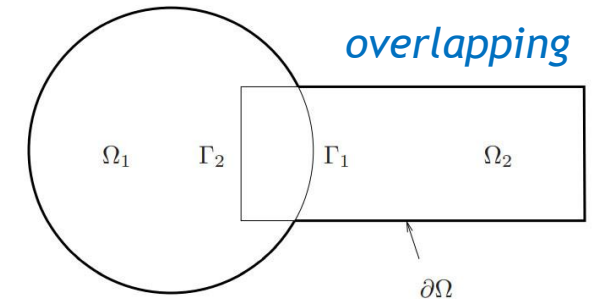
Basic Schwarz Algorithm

Initialize:

- Solve PDE by any method on Ω_1 w/ initial guess for transmission BCs on Γ_1 .

Iterate until convergence:

- Solve PDE by any method on Ω_2 w/ transmission BCs on Γ_2 based on values just obtained for Ω_1 .
- Solve PDE by any method on Ω_1 w/ transmission BCs on Γ_1 based on values just obtained for Ω_2 .

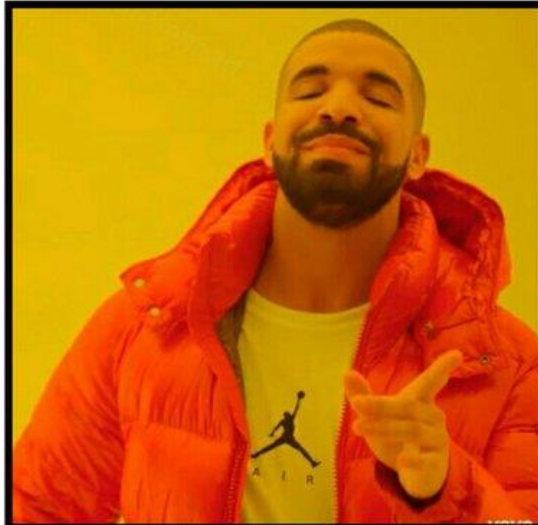


- Schwarz alternating method most commonly used as a **preconditioner** for Krylov iterative methods to solve linear algebraic equations.

Idea behind this work: using the Schwarz alternating method as a **discretization method** for solving multi-scale or multi-physics partial differential equations (PDEs).



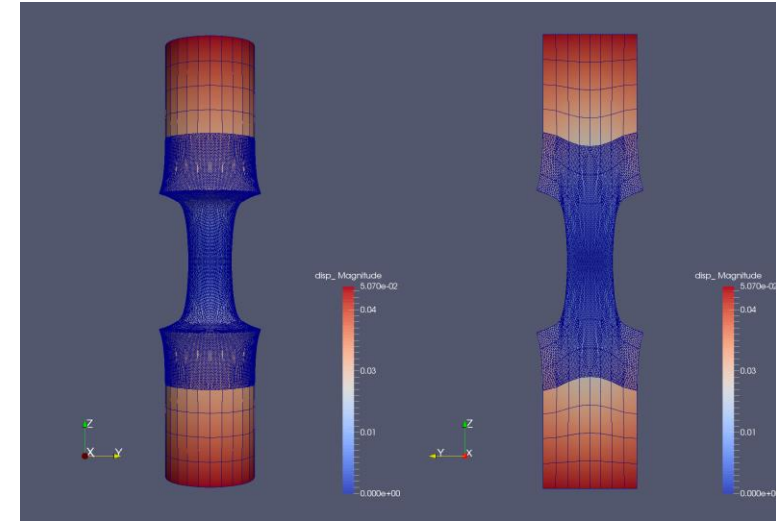
AS A *PRECONDITIONER*
FOR THE LINEARIZED
SYSTEM



AS A *SOLVER* FOR THE
COUPLED
FULLY NONLINEAR
PROBLEM

1. Schwarz Alternating Method for Coupling of Full Order Models (FOMs) in Solid Mechanics

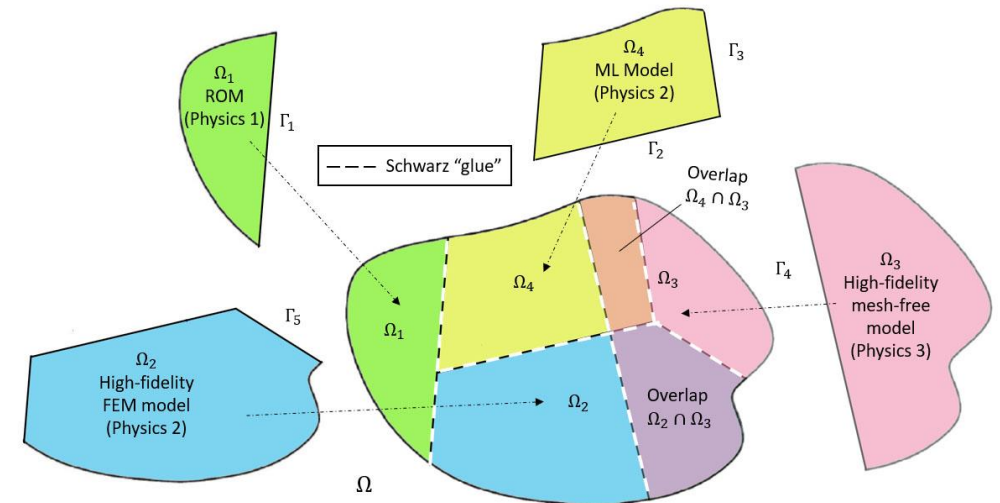
- Motivation & Background
- **Quasistatic Formulation**
 - Numerical Examples
- Extension to Dynamics
 - Numerical Examples



2. Schwarz Alternating Method for FOM-ROM* and ROM-ROM Coupling

- Motivation & Background
- Formulation
- Numerical Examples

3. Summary and Future Work



* Projection-based Reduced Order Model

Quasistatic Solid Mechanics Formulation



- Energy functional defining weak form of the governing PDEs

$$\Phi[\boldsymbol{\varphi}] := \int_{\Omega} A(\mathbf{F}, \mathbf{Z}) dV - \int_{\Omega} \rho \mathbf{B} \cdot \boldsymbol{\varphi} dV$$

- $A(\mathbf{F}, \mathbf{Z})$: Helmholtz free-energy density
 - $\mathbf{F} := \nabla \boldsymbol{\varphi}$: deformation gradient
 - \mathbf{Z} : collection of internal variables (for plastic materials)
 - ρ : density, \mathbf{B} : body force, $\mathbf{P} = \partial A / \partial \mathbf{F}$: Piola-Kirchhoff stress
- Euler-Lagrange equations, obtained by minimizing $\Phi[\boldsymbol{\varphi}]$:

$$\begin{cases} \text{Div } \mathbf{P} + \rho \mathbf{B} = \mathbf{0}, & \text{in } \Omega \\ \boldsymbol{\varphi} = \boldsymbol{\chi}, & \text{on } \partial\Omega \end{cases}$$
- Quasistatics solves **sequence of problems** in which loading (body force) \mathbf{B} is incremented quasistatically w.r.t. pseudo time t_i :

For $i = 1, \dots, n$

Solve $\text{Div } \mathbf{P} + \rho \mathbf{B}(t_i) = \mathbf{0}$ with appropriate boundary conditions (BCs)

Increment pseudo time t_i to obtain t_{i+1}

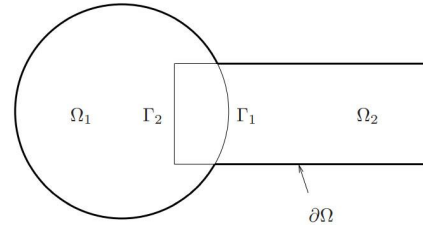
Spatial Coupling via (Multiplicative) Alternating Schwarz



Overlapping Domain Decomposition

$$\begin{cases} \text{Div } \mathbf{P}_1^{(n+1)} + \rho \mathbf{B}(t_i) = \mathbf{0}, & \text{in } \Omega_1 \\ \varphi_1^{(n+1)} = \chi, & \text{on } \partial\Omega_1 \setminus \Gamma_1 \\ \varphi_1^{(n+1)} = \varphi_2^{(n)} & \text{on } \Gamma_2 \end{cases}$$

$$\begin{cases} \text{Div } \mathbf{P}_2^{(n+1)} + \rho \mathbf{B}(t_i) = \mathbf{0}, & \text{in } \Omega_2 \\ \varphi_2^{(n+1)} = \chi, & \text{on } \partial\Omega_2 \setminus \Gamma_2 \\ \varphi_2^{(n+1)} = \varphi_1^{(n+1)} & \text{on } \Gamma_2 \end{cases}$$



Model PDE:

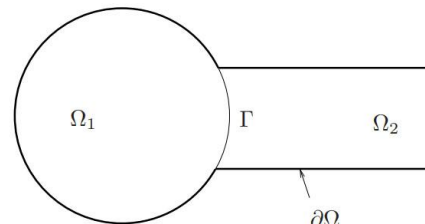
$$\begin{cases} \text{Div } \mathbf{P} + \rho \mathbf{B} = \mathbf{0}, & \text{in } \Omega \\ \varphi = \chi, & \text{on } \partial\Omega \end{cases}$$

- Dirichlet-Dirichlet transmission BCs [Schwarz, 1870; Lions, 1988]

Non-overlapping Domain Decomposition

$$\begin{cases} \text{Div } \mathbf{P}_1^{(n+1)} + \rho \mathbf{B}(t_i) = \mathbf{0}, & \text{in } \Omega_1 \\ \varphi_1^{(n+1)} = \chi, & \text{on } \partial\Omega_1 \setminus \Gamma \\ \varphi_1^{(n+1)} = \lambda_{n+1} & \text{on } \Gamma \end{cases}$$

$$\begin{cases} \text{Div } \mathbf{P}_2^{(n+1)} + \rho \mathbf{B}(t_i) = \mathbf{0}, & \text{in } \Omega_2 \\ \varphi_2^{(n+1)} = \chi, & \text{on } \partial\Omega_2 \setminus \Gamma \\ \mathbf{P}_2^{(n+1)} \mathbf{n} = \mathbf{P}_2^{(n+1)} \mathbf{n}, & \text{on } \Gamma \end{cases}$$



$$\lambda_{n+1} = \theta \varphi_2^{(n)} + (1 - \theta) \lambda_n, \text{ on } \Gamma, \text{ for } n \geq 1$$

- Relevant for multi-material and multi-physics coupling
- Alternating Dirichlet-Neumann transmission BCs [Zanolli *et al.*, 1987]
- Robin-Robin transmission BCs also lead to convergence [Lions, 1990]
- $\theta \in [0,1]$: relaxation parameter (can help convergence)

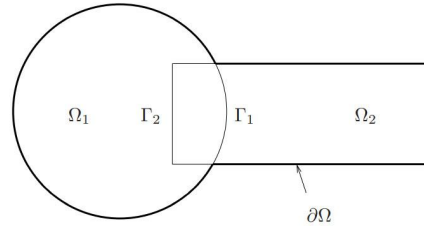
Spatial Coupling via (Multiplicative) Alternating Schwarz



Overlapping Domain Decomposition

$$\begin{cases} \text{Div } \mathbf{P}_1^{(n+1)} + \rho \mathbf{B}(t_i) = \mathbf{0}, & \text{in } \Omega_1 \\ \boldsymbol{\varphi}_1^{(n+1)} = \boldsymbol{\chi}, & \text{on } \partial\Omega_1 \setminus \Gamma_1 \\ \boldsymbol{\varphi}_1^{(n+1)} = \boldsymbol{\varphi}_2^{(n)} & \text{on } \Gamma_2 \end{cases}$$

$$\begin{cases} \text{Div } \mathbf{P}_2^{(n+1)} + \rho \mathbf{B}(t_i) = \mathbf{0}, & \text{in } \Omega_2 \\ \boldsymbol{\varphi}_2^{(n+1)} = \boldsymbol{\chi}, & \text{on } \partial\Omega_2 \setminus \Gamma_2 \\ \boldsymbol{\varphi}_2^{(n+1)} = \boldsymbol{\varphi}_1^{(n+1)} & \text{on } \Gamma_2 \end{cases}$$



Model PDE:

$$\begin{cases} \text{Div } \mathbf{P} + \rho \mathbf{B} = \mathbf{0}, & \text{in } \Omega \\ \boldsymbol{\varphi} = \boldsymbol{\chi}, & \text{on } \partial\Omega \end{cases}$$

- Dirichlet-Dirichlet transmission BCs [Schwarz, 1870; Lions, 1988]

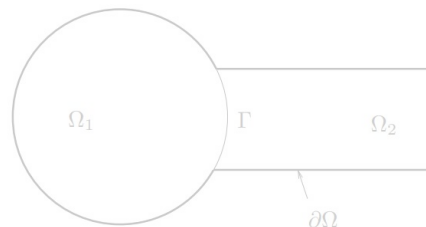
Part 1 of talk

Non-overlapping Domain Decomposition

Part 2 of talk

$$\begin{cases} \text{Div } \mathbf{P}_1^{(n+1)} + \rho \mathbf{B}(t_i) = \mathbf{0}, & \text{in } \Omega_1 \\ \boldsymbol{\varphi}_1^{(n+1)} = \boldsymbol{\chi}, & \text{on } \partial\Omega_1 \setminus \Gamma \\ \boldsymbol{\varphi}_1^{(n+1)} = \boldsymbol{\lambda}_{n+1} & \text{on } \Gamma \end{cases}$$

$$\begin{cases} \text{Div } \mathbf{P}_2^{(n+1)} + \rho \mathbf{B}(t_i) = \mathbf{0}, & \text{in } \Omega_2 \\ \boldsymbol{\varphi}_2^{(n+1)} = \boldsymbol{\chi}, & \text{on } \partial\Omega_2 \setminus \Gamma \\ \mathbf{P}_2^{(n+1)} \mathbf{n} = \mathbf{P}_2^{(n+1)} \mathbf{n}, & \text{on } \Gamma \end{cases}$$



$$\boldsymbol{\lambda}_{n+1} = \theta \boldsymbol{\varphi}_2^{(n)} + (1 - \theta) \boldsymbol{\lambda}_n, \text{ on } \Gamma, \text{ for } n \geq 1$$

- Relevant for multi-material and multi-physics coupling
- Alternating Dirichlet-Neumann transmission BCs [Zanolli *et al.*, 1987]
- Robin-Robin transmission BCs also lead to convergence [Lions, 1990]
- $\theta \in [0, 1]$: relaxation parameter (can help convergence)

Multiplicative Overlapping Schwarz

$$\begin{cases} \text{Div } \mathbf{P}_1^{(n+1)} + \rho \mathbf{B}(t_i) = \mathbf{0}, & \text{in } \Omega_1 \\ \boldsymbol{\varphi}_1^{(n+1)} = \boldsymbol{\chi}, & \text{on } \partial\Omega_1 \setminus \Gamma_1 \\ \boldsymbol{\varphi}_1^{(n+1)} = \boldsymbol{\varphi}_2^{(n)} & \text{on } \Gamma_2 \end{cases}$$

$$\begin{cases} \text{Div } \mathbf{P}_2^{(n+1)} + \rho \mathbf{B}(t_i) = \mathbf{0}, & \text{in } \Omega_2 \\ \boldsymbol{\varphi}_2^{(n+1)} = \boldsymbol{\chi}, & \text{on } \partial\Omega_2 \setminus \Gamma_2 \\ \boldsymbol{\varphi}_2^{(n+1)} = \boldsymbol{\varphi}_1^{(n+1)} & \text{on } \Gamma_2 \end{cases}$$

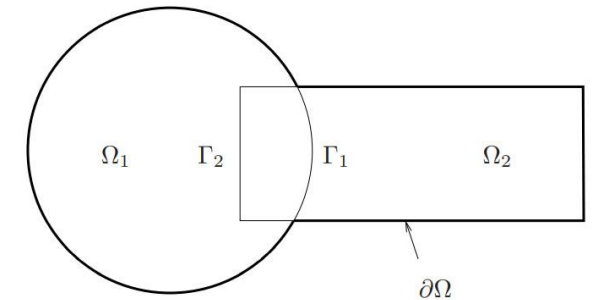
Additive Overlapping Schwarz

$$\begin{cases} \text{Div } \mathbf{P}_1^{(n+1)} + \rho \mathbf{B}(t_i) = \mathbf{0}, & \text{in } \Omega_1 \\ \boldsymbol{\varphi}_1^{(n+1)} = \boldsymbol{\chi}, & \text{on } \partial\Omega_1 \setminus \Gamma_1 \\ \boldsymbol{\varphi}_1^{(n+1)} = \boldsymbol{\varphi}_2^{(n)} & \text{on } \Gamma_2 \end{cases}$$

$$\begin{cases} \text{Div } \mathbf{P}_2^{(n+1)} + \rho \mathbf{B}(t_i) = \mathbf{0}, & \text{in } \Omega_2 \\ \boldsymbol{\varphi}_2^{(n+1)} = \boldsymbol{\chi}, & \text{on } \partial\Omega_2 \setminus \Gamma_2 \\ \boldsymbol{\varphi}_2^{(n+1)} = \boldsymbol{\varphi}_1^{(n+1)} & \text{on } \Gamma_2 \end{cases}$$

Model PDE:

$$\begin{cases} \text{Div } \mathbf{P} + \rho \mathbf{B} = \mathbf{0}, & \text{in } \Omega \\ \boldsymbol{\varphi} = \boldsymbol{\chi}, & \text{on } \partial\Omega \end{cases}$$



- **Multiplicative Schwarz:** solves subdomain problems **sequentially** (in serial)
- **Additive Schwarz:** advance subdomains in **parallel**, communicate boundary condition data later
 - Typically requires a few more **Schwarz iterations**, but does not degrade **accuracy**
 - **Parallelism** helps balance additional **cost** due to Schwarz iterations
 - Applicable to both **overlapping** and **non-overlapping** Schwarz



Part 1 of talk

Multiplicative Overlapping Schwarz

$$\begin{cases} \text{Div } \mathbf{P}_1^{(n+1)} + \rho \mathbf{B}(t_i) = \mathbf{0}, & \text{in } \Omega_1 \\ \varphi_1^{(n+1)} = \chi, & \text{on } \partial\Omega_1 \setminus \Gamma_1 \\ \varphi_1^{(n+1)} = \varphi_2^{(n)} & \text{on } \Gamma_2 \end{cases}$$

$$\begin{cases} \text{Div } \mathbf{P}_2^{(n+1)} + \rho \mathbf{B}(t_i) = \mathbf{0}, & \text{in } \Omega_2 \\ \varphi_2^{(n+1)} = \chi, & \text{on } \partial\Omega_2 \setminus \Gamma_2 \\ \varphi_2^{(n+1)} = \varphi_1^{(n+1)} & \text{on } \Gamma_2 \end{cases}$$

Part 2 of talk

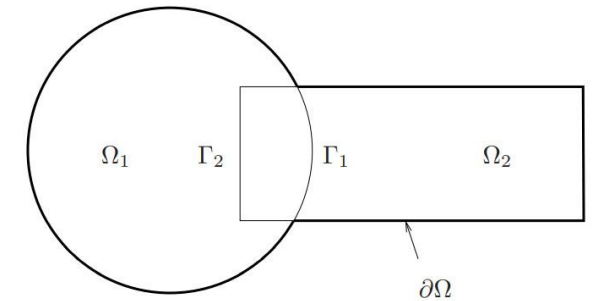
Additive Overlapping Schwarz

$$\begin{cases} \text{Div } \mathbf{P}_1^{(n+1)} + \rho \mathbf{B}(t_i) = \mathbf{0}, & \text{in } \Omega_1 \\ \varphi_1^{(n+1)} = \chi, & \text{on } \partial\Omega_1 \setminus \Gamma_1 \\ \varphi_1^{(n+1)} = \varphi_2^{(n)} & \text{on } \Gamma_2 \end{cases}$$

$$\begin{cases} \text{Div } \mathbf{P}_2^{(n+1)} + \rho \mathbf{B}(t_i) = \mathbf{0}, & \text{in } \Omega_2 \\ \varphi_2^{(n+1)} = \chi, & \text{on } \partial\Omega_2 \setminus \Gamma_2 \\ \varphi_2^{(n+1)} = \varphi_1^{(n+1)} & \text{on } \Gamma_2 \end{cases}$$

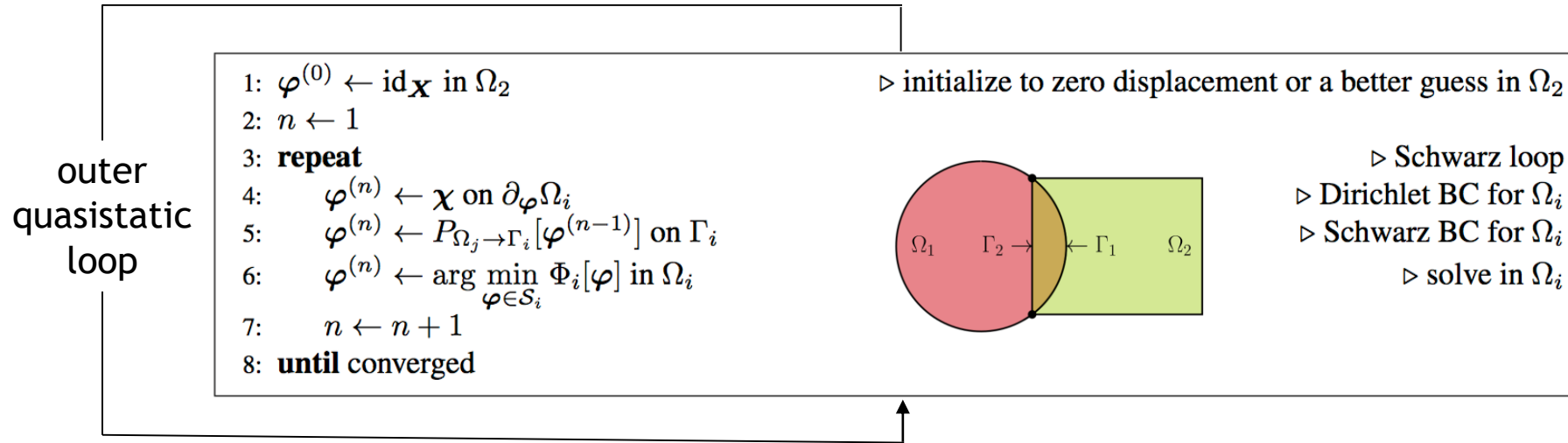
Model PDE:

$$\begin{cases} \text{Div } \mathbf{P} + \rho \mathbf{B} = \mathbf{0}, & \text{in } \Omega \\ \varphi = \chi, & \text{on } \partial\Omega \end{cases}$$



- **Multiplicative Schwarz:** solves subdomain problems **sequentially** (in serial)
- **Additive Schwarz:** advance subdomains in **parallel**, communicate boundary condition data later
 - Typically requires a few more **Schwarz iterations**, but does not degrade **accuracy**
 - **Parallelism** helps balance additional **cost** due to Schwarz iterations
 - Applicable to both **overlapping** and **non-overlapping** Schwarz

Overlapping Schwarz Coupling in Quasistatics



Advantages:

- Conceptually very *simple*.
- Allows the coupling of regions with *different non-conforming meshes*, *different element types*, and *different levels of refinement*.
- Information is exchanged among two or more regions, making coupling *concurrent*.
- *Different solvers* can be used for the different regions.
- *Different material models* can be coupled if they are compatible in the overlap region.
- Simplifies the task of *meshing complex geometries* for the different scales.

Convergence Proof*



2 Formulation of the Schwarz Alternating Method

We start by defining the standard finite deformation variational formulation to establish notation before presenting the formulation of the coupling method.

2.1 Variational Formulation on a Single Domain

Consider a body as the open set $\Omega \subset \mathbb{R}^2$ undergoing a motion described by the mapping $\varphi = \varphi(X; t) : \Omega \times [0, \infty) \rightarrow \mathbb{R}^2$. Assume that the boundary of the body is $\partial\Omega = \partial\Omega_D \cup \partial\Omega_N$ with $\partial\Omega_D \cap \partial\Omega_N = \emptyset$, where $\partial\Omega_D$ is a displacement boundary, $\partial\Omega_N$ is a traction boundary, and $\partial\Omega_D \cup \partial\Omega_N = \partial\Omega$. The prescribed boundary displacements or tractions boundary conditions are $\varphi_D|_{\partial\Omega_D} = \bar{\varphi}_D$ and $t|_{\partial\Omega_N} = \bar{t}$. The prescribed boundary tractions or Neumann boundary conditions are $T \cdot \nu|_{\partial\Omega_N} = \bar{t}$, $\nu \in \mathbb{R}^2$. Let $F = \text{Grad} \varphi$ be the deformation gradient. Let also $\Omega \subset \mathbb{R}^2 \rightarrow \mathbb{R}^2$ be the body force, with f the mass density in the reference configuration. Furthermore, introduce the energy functional

$$\Phi[\varphi] := \int_{\Omega} A(F, Z) dV - \int_{\Omega} Bb \cdot \varphi dV - \int_{\partial\Omega_D} T \cdot \varphi dS, \quad (1)$$

in which $A(F, Z)$ is the Helmholtz free energy density and Z is a collection of internal variables. The weak form of the problem is obtained by minimizing the energy functional $\Phi[\varphi]$ over the Sobolev space $W^{1,2}(\Omega)$ that is composed of all functions that are square-integrable and have square-integrable first derivatives. Define

$$S := \{ \varphi \in W^{1,2}(\Omega) : \varphi = \chi \text{ on } \partial\Omega_D \} \quad (2)$$

and

$$V := \{ \xi \in W^{1,2}(\Omega) : \xi = 0 \text{ on } \partial\Omega_D \} \quad (3)$$

where $\xi \in V$ is a test function. The potential energy is minimized if and only if $\Phi[\varphi] \leq \Phi[\varphi + \xi]$ for all $\xi \in V$ and $\varphi \in S$. It is straightforward to show that the minimum of $\Phi[\varphi]$ is the mapping $\varphi \in S$ that satisfies

$$D\Phi[\varphi] \cdot \xi = \int_{\Omega} P \cdot \text{Grad} \xi dV - \int_{\Omega} Bb \cdot \xi dV - \int_{\partial\Omega_N} T \cdot \xi dS = 0, \quad (4)$$

where $P = \partial A / \partial F$ denotes the first Piola-Kirchhoff stress. The Euler-Lagrange equation corresponding to the variational statement (4) is

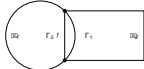


Figure 1: Two subdomains Ω_1 and Ω_2 and the corresponding boundaries Γ_1 and Γ_2 , used by the Schwarz alternating method.

that is $\ell = 1$ and $\ell = 2$ if n is odd, and $\ell = 2$ and $\ell = 1$ if n is even. Introduce the following definitions for each subdomain i :

- Closure $\bar{\Omega}_i := \Omega_i \cup \partial\Omega_i$
- Disjointed boundary $\partial\Omega_i := \partial\Omega_i \setminus \partial\Omega$
- Neumann boundary $\partial\Omega_i^N := \partial\Omega_i \setminus \partial\Omega_i^D$
- Schwarz boundary $\Gamma_i := \partial\Omega_i^D \cap \partial\Omega_j^D$

Note that with these definitions we guarantee that $\partial\Omega_1 \cap \partial\Omega_2 = \emptyset$, $\partial\Omega_1 \cap \Gamma_1 = \emptyset$ and $\partial\Omega_2 \cap \Gamma_2 = \emptyset$. Now define the spaces

$$S_i := \{ \varphi \in W^{1,2}(\Omega_i) : \varphi = \chi \text{ on } \partial\Omega_i^D \} \quad (5)$$

and

$$V_i := \{ \varphi \in W^{1,2}(\Omega_i) : \varphi = 0 \text{ on } \partial\Omega_i^D \} \quad (6)$$

where the symbol $P_{\Omega_i} : \mathbb{R}^2 \rightarrow \mathbb{R}^2$ denotes the projection from the subdomain Ω_i onto the Schwarz boundary Γ_i . This projection operator plays a central role in the Schwarz alternating method. Its form and implementation are discussed in subsequent sections. For the moment it is sufficient to assume that the operator is able to project a field φ from one subdomain to the Schwarz boundary of the other subdomain.

The Schwarz alternating method solves a sequence of problems on Ω_1 and Ω_2 . The solution $\varphi^{(n)}$ for the

1. $\varphi_i^{(n)} \in X_i^{(n)}$ with $\varphi_i^{(n)} = \chi _{\partial\Omega_i^D}$ on $\partial\Omega_i^D$.	• iterate for i
2. $\varphi_i^{(n)} \in X_i^{(n)}$ with $\varphi_i^{(n)} = \chi _{\partial\Omega_i^D}$ on $\partial\Omega_i^D$.	• constraint (6)
3. $\varphi_i^{(n)} \in X_i^{(n)}$ with $\varphi_i^{(n)} = \chi _{\partial\Omega_i^D}$ on $\partial\Omega_i^D$.	• Neumann boundary
4. $\varphi_i^{(n)} \in X_i^{(n)}$ with $\varphi_i^{(n)} = \chi _{\partial\Omega_i^D}$ on $\partial\Omega_i^D$.	• linear system
5. $\varphi_i^{(n)} \in X_i^{(n)}$ with $\varphi_i^{(n)} = \chi _{\partial\Omega_i^D}$ on $\partial\Omega_i^D$.	
6. $\varphi_i^{(n)} \in X_i^{(n)}$ with $\varphi_i^{(n)} = \chi _{\partial\Omega_i^D}$ on $\partial\Omega_i^D$.	
7. $\varphi_i^{(n)} \in X_i^{(n)}$ with $\varphi_i^{(n)} = \chi _{\partial\Omega_i^D}$ on $\partial\Omega_i^D$.	• right inverse

[15, 34, 4]. Although we do not provide here formal convergence proofs for the remaining variants of the Schwarz method, we offer some numerical results illustrating their convergence in Section 4.

Consider the energy functional $\Phi[\varphi]$ defined in (1). We will denote by φ the L^2 -inner product over Ω , that is,

$$(\varphi, \psi) := \int_{\Omega} \varphi \cdot \psi dV. \quad (35)$$

For $\varphi_1, \varphi_2 \in H^1(\Omega)$, with corresponding norm $\|\cdot\|$. The proof of the convergence of the Schwarz alternating method requires that the functional $\Phi[\varphi]$ satisfy the following properties over the space S defined in (2).

1. $\Phi[\varphi]$ is convex.
2. $\Phi[\varphi]$ is Fréchet differentiable, with $\Phi'[\varphi]$ denoting its Fréchet derivative.
3. $\Phi[\varphi]$ is strictly convex.
4. $\Phi[\varphi]$ is lower semi-continuous.
5. $\Phi'[\varphi]$ is uniformly continuous on K_R , where

$$K_R := \{ \varphi \in S : \Phi[\varphi] \leq R, \forall R \in \mathbb{R}, R < \infty \}. \quad (36)$$

It can be shown that the energy functional $\Phi[\varphi]$ defined in (1) is strictly convex in S . Property 1) provided that the bilinearity form (φ, ψ) is a non-degenerate bilinear form. The bilinear form is non-

Remark that [15]

$$\delta_n = \varphi^{(n+1)} + \varphi, \quad \text{for } \varphi^{(n+1)} \in \delta_{n+1} \Rightarrow \varphi^{(n+1)} \in \delta_n. \quad (40)$$

Theorem 1. Assume that the energy functional $\Phi[\varphi]$ satisfies properties 1–5 above. Consider the Schwarz alternating method of Section 2, defined by (9)–(13) and its equivalent form (39). Then

- (a) $\Phi[\varphi^{(n)}] \geq \Phi[\varphi^{(n+1)}] \geq \dots \geq \Phi[\varphi^{(n-1)}] \geq \Phi[\varphi^{(n)}] \geq \dots \geq \Phi[\varphi]$, where φ is the minimizer of $\Phi[\varphi]$ over S .
- (b) the sequence $\{\varphi^{(n)}\}$ defined in (39) converges to the minimizer φ of $\Phi[\varphi]$ in S .
- (c) the Schwarz minimum value $\Phi[\varphi^{(n)}]$ converges monotonically to the minimum value $\Phi[\varphi]$ in S starting from any initial guess $\varphi^{(0)}$.
- (d) if $\Phi'[\varphi]$ is Lipschitz continuous in a neighborhood of φ , then the sequence $\{\varphi^{(n)}\}$ converges geometrically to the minimizer φ .

Proof. See Appendix A. \square

Finally, while most of our work until now present their analysis for the specific case of two subdomains, extension to multiple subdomains is in general straightforward. The case of multiple subdomains is considered specifically in Lions [13], Baoin [1], and Li-Sun and Evans [14].

4 Numerical Examples

In this section, we present numerical examples of the behavior of the Schwarz alternating method for two different implementations. First, we briefly describe the two implementations, one in MATLAB and the other in the open-source ABAQUS finite element code [12]. Next, we discuss the error measures used throughout the numerical examples. Then, we continue with four examples that demonstrate different features of the Schwarz alternating method and our implementation. The first example, a one-dimensional singular bar, is used to demonstrate the behavior of the four Schwarz variants of Section 2.4. The second example, a cuboid body of square base, aims to study the effect of the size of the overlap region on the convergence of the method. The objective of the third example, a meshed cylinder, is to analyze the numerical error in the results and to demonstrate the ability of the method to compute different domain subdomains. The last example, a bar

Theorem 1. Assume that the energy functional $\Phi[\varphi]$ satisfies properties 1–5 above. Consider the Schwarz alternating method of Section 2 defined by (9)–(13) and its equivalent form (39). Then

- (a) $\Phi[\varphi^{(0)}] \geq \Phi[\varphi^{(1)}] \geq \dots \geq \Phi[\varphi^{(n-1)}] \geq \Phi[\varphi^{(n)}] \geq \dots \geq \Phi[\varphi]$, where φ is the minimizer of $\Phi[\varphi]$ over S .
- (b) The sequence $\{\varphi^{(n)}\}$ defined in (39) converges to the minimizer φ of $\Phi[\varphi]$ in S .
- (c) The Schwarz minimum values $\Phi[\varphi^{(n)}]$ converge monotonically to the minimum value $\Phi[\varphi]$ in S starting from any initial guess $\varphi^{(0)}$.

Remark 1. The convexity of $\Phi[\varphi]$ follows from the LeFort theorem that a unique minimizer to this functional over S exists, i.e., the minimization of $\Phi[\varphi]$ is well-posed.

Remark 2. By the Stampacchia theorem, the minimization of $\Phi[\varphi]$ in S is equivalent to finding $\varphi \in S$ such that

$$(\Phi'[\varphi], \xi) \geq 0 \quad (51)$$

for all $\xi \in S$.

Remark 3. Recall that the strict convexity property of $\Phi[\varphi]$ can be written as

$$\Phi[\varphi] - \Phi[\psi] - (\Phi'[\psi], \varphi - \psi) \geq 0 \quad (52)$$

where $\varphi, \psi \in S$. From (51), remark that if $\Phi[\varphi]$ is strictly convex over S for $R \in \mathbb{R}$ such that $R < \infty$, we can find $\alpha > 0$ such that $\Phi[\varphi] - \Phi[\psi] \geq \alpha \|\varphi - \psi\|$.

Remark 4. Property 5, the uniform continuity of $\Phi'[\varphi]$, thus exists a modulus of continuity $\omega > 0$, with $\omega : K_R \rightarrow K_R$, such that

$$\|\Phi'[\varphi] - \Phi'[\psi]\| \leq \omega(\|\varphi - \psi\|). \quad (54)$$

where $\varphi, \psi \in K_R$. By definition, $\omega(\cdot) \rightarrow 0$ as $\cdot \rightarrow 0$.

Remark 5. It was shown in [15] that in the case $\Omega_1 \cap \Omega_2 \neq \emptyset$, $\forall \varphi \in S$, there exist $C_1 \in S_1$ and $C_2 \in S_2$ such that

$$\varphi = C_1 + C_2. \quad (55)$$

and

$$\|\varphi\| \leq C_3 \|\varphi\|. \quad (56)$$

for some $C_3 > 0$ independent of φ .

Remark 6. Note that (56) can be written as

$$\|\varphi^{(n)}\| \leq C_3 \|\varphi^{(n)}\| \quad (57)$$

for $\ell \in \{1, 2\}$ and $n \in \{0, 1, 2, \dots\}$ (recall from (5) the selection between 1 and 2). This is due to the uniqueness of the solution to each minimization problem over S_i , and the definition of $\varphi^{(n)}$ as the minimizer of $\Phi[\varphi]$ over S_i .

Remark 7. Let $\varphi^{(n)} \in S_n$, and let $\xi \in S$. By Remark 5, there exist $C_1 \in S_1$ and $C_2 \in S_2$ such that

$$(\Phi'[\varphi^{(n)}], \xi) = (\Phi'[\varphi^{(n)}], C_1 + C_2). \quad (58)$$

Again using (57) and also (54) in (58) leads to

$$(\Phi'[\varphi^{(n)}] - \Phi'[\varphi^{(n-1)}], C_2) = (\Phi'[\varphi^{(n)}] - \Phi'[\varphi^{(n-1)}], C_2) \cdot \|C_2\|, \quad (61)$$

and substituting (61) into (58) we finally obtain that

$$(\Phi'[\varphi^{(n)}] - \Phi'[\varphi^{(n-1)}], C_1) \leq C_3 \|(\Phi'[\varphi^{(n)}] - \Phi'[\varphi^{(n-1)}], C_2)\|, \quad (62)$$

$\forall \xi \in S$.

Remark 8. For part (a) of Theorem 1, recall the definition of geometric convexity:

$$K_R \subseteq C K_R, \quad (63)$$

where $K \subseteq \{0, 1, 2, \dots\}$ for some $C > 0$, where

$$K_n := \|\varphi^{(n+1)} - \varphi^{(n)}\|. \quad (64)$$

Remark 9. Recall from the definition of continuity that if $\Phi'[\varphi]$ is Lipschitz continuous at $\varphi^{(n)}$ near φ , then there exists a constant $K \geq 0$ such that

$$\frac{\|\Phi'[\varphi^{(n)}] - \Phi'[\varphi]\|}{\|\varphi^{(n)} - \varphi\|} \leq K. \quad (65)$$

Considering that $\Phi'[\varphi] = 0$ since φ is the minimizer of $\Phi[\varphi]$, (65) is equivalent to

$$\|\Phi'[\varphi^{(n)}]\| \leq K \|\varphi^{(n)} - \varphi\|. \quad (66)$$

Proof of Theorem 1

Proof of (a). Let $\varphi^{(0)} = \arg \min_{\varphi \in S} \Phi[\varphi]$. By (40), $\varphi^{(0)} \in S_1$. Let $\varphi^{(1)}$ be the minimizer of $\Phi[\varphi]$ over S_2 and suppose $\varphi^{(1)} \in S_2$. But this is a contradiction, since we can take $\varphi^{(1)} = \varphi^{(0)}$. Hence, it cannot be that $\varphi^{(1)} \in S_2$ where $\varphi^{(0)} = \arg \min_{\varphi \in S} \Phi[\varphi]$. It follows by induction that

$$\varphi^{(n)} \in S_n \quad (67)$$

for $n \in \{1, 2, 3, \dots\}$. Now let φ be the minimizer of $\Phi[\varphi]$ over S . Since the problem is well-posed in S , hence $\Phi[\varphi] \leq \Phi[\varphi^{(n)}]$ for all $n \in \{1, 2, 3, \dots\}$. \square

$$\lim_{n \rightarrow \infty} \|\varphi^{(n)} - \varphi^{(n-1)}\| = 0. \quad (69)$$

from which we can conclude that $\varphi^{(n)} = \varphi^{(n-1)} = 0$ as $n \rightarrow \infty$.

We must now show that $\varphi^{(n)}$ converges to φ , the minimizer of $\Phi[\varphi]$ on S . By (55) with $\varphi_1 = \varphi$ and $\varphi_2 = \varphi^{(n)}$, we have

$$\|\varphi - \varphi^{(n)}\|^2 \leq \frac{1}{\alpha} (\Phi[\varphi] - \Phi[\varphi^{(n)}]) + (\Phi'[\varphi^{(n)}], \varphi - \varphi^{(n)}). \quad (70)$$

Since φ is the minimum of $\Phi[\varphi]$, by (a) we have that $\Phi[\varphi] \leq \Phi[\varphi^{(n)}]$. It follows that

$$\|\varphi - \varphi^{(n)}\|^2 \leq (\Phi'[\varphi^{(n)}], \varphi - \varphi^{(n)}) \leq (\Phi'[\varphi^{(n)}], \varphi - \varphi^{(n)}) = (\Phi'[\varphi^{(n)}], \varphi^{(n)} - \varphi). \quad (71)$$

Substituting (71) into (70) we have

$$\|\varphi - \varphi^{(n)}\|^2 \leq \frac{1}{\alpha} (\Phi'[\varphi^{(n)}], \varphi^{(n)} - \varphi). \quad (72)$$

Now by (62) (Remark 7),

$$(\Phi'[\varphi^{(n)}], \varphi^{(n)} - \varphi) \leq C_3 \|(\Phi'[\varphi^{(n)}] - \Phi'[\varphi^{(n-1)}]), \varphi^{(n)} - \varphi\|. \quad (73)$$

Substituting (73) into (72) leads to

$$\|\varphi - \varphi^{(n)}\|^2 \leq \frac{C_3}{\alpha} \|(\Phi'[\varphi^{(n)}] - \Phi'[\varphi^{(n-1)}]), \varphi^{(n)} - \varphi\|. \quad (74)$$

Applying the uniform continuity assumption (64), we obtain

$$\|\varphi - \varphi^{(n)}\|^2 \leq \frac{C_3}{\alpha} \omega(\|\varphi^{(n)} - \varphi^{(n-1)}\|). \quad (75)$$

By (69), $\|\varphi^{(n)} - \varphi^{(n-1)}\| \rightarrow 0$ as $n \rightarrow \infty$. From this we obtain the result, namely that $\varphi^{(n)} \rightarrow \varphi$ as $n \rightarrow \infty$. \square

Proof of (b). This follows immediately from (a) and (b). \square

Proof of (c). By (b), for large enough n , there exists some $C_1 > 0$ independent of n such that

$$\|\varphi^{(n)} - \varphi\| \leq C_1 \|\varphi^{(n-1)} - \varphi^{(n)}\|. \quad (76)$$

Let us choose C_2 such that $C_1 > \alpha_2 R$, where R is the Lipschitz continuity constant in (66). Combining (76) with (75) leads to

$$\frac{1}{\alpha} (\Phi'[\varphi^{(n)}] - \Phi'[\varphi^{(n-1)}]), \varphi^{(n)} - \varphi \geq \frac{1}{C_1} \|\varphi^{(n)} - \varphi\|^2. \quad (77)$$

$$(\Phi'[\varphi^{(n)}] - \Phi'[\varphi^{(n-1)}]), \varphi^{(n)} - \varphi \geq (\Phi'[\varphi^{(n)}] - \Phi'[\varphi^{(n-1)}]), \varphi^{(n)} - \varphi^{(n-1)} + \alpha_2 (\varphi^{(n)} - \varphi^{(n-1)}) \cdot (\varphi^{(n)} - \varphi) \quad (79)$$

since $\alpha_2 \geq 0$. Now, by the Cauchy-Schwarz inequality followed by the application of the Lipschitz continuity of $\Phi'[\varphi]$ (66) we can write

$$(\Phi'[\varphi^{(n)}], \varphi - \varphi^{(n)}) \leq \|(\Phi'[\varphi^{(n)}])\| \cdot \|\varphi - \varphi^{(n)}\| \leq R \|\varphi - \varphi^{(n)}\|. \quad (80)$$

Hence, from (79),

$$\Phi'[\varphi^{(n)}] - \Phi'[\varphi] \leq R \|\varphi^{(n)} - \varphi\|. \quad (81)$$

Moreover, by (53) since $\Phi'[\varphi] = 0$,

$$\Phi'[\varphi^{(n)}] - \Phi'[\varphi] \geq \alpha \|\varphi^{(n)} - \varphi\|. \quad (82)$$

Using (81) and (82) we obtain

$$(\Phi'[\varphi^{(n)}] - \Phi'[\varphi]), \varphi^{(n)} - \varphi \leq R \|\varphi^{(n)} - \varphi\|^2 + \alpha \|\varphi^{(n)} - \varphi\|^2. \quad (83)$$

Combining (83) and (77) leads to

$$\frac{\alpha}{C_1} \|\varphi^{(n)} - \varphi\|^2 \leq (\Phi'[\varphi^{(n)}] - \Phi'[\varphi]), \varphi^{(n)} - \varphi \leq R \|\varphi^{(n)} - \varphi\|^2 + \alpha \|\varphi^{(n)} - \varphi\|^2. \quad (84)$$

or

$$\|\varphi^{(n)} - \varphi\| \leq R \|\varphi^{(n)} - \varphi\| \quad (85)$$

with

$$R := \frac{1}{\alpha} \left(\frac{R}{C_1} + \alpha \right). \quad (86)$$

and $R \in \mathbb{R}$ as we chose $C_1 > \alpha_2 R$. Furthermore, since the sequence $\{\varphi^{(n)}\}$ converges monotonically to the minimizer φ of $\Phi[\varphi]$ by (a) and (b), it follows that $\ell \in \{0, 1\}$. Define C as $1 + \alpha_2 R$ in (85), then (85) can be recast as

$$\|\varphi^{(n+1)} - \varphi^{(n)}\| \leq C \|\varphi^{(n)} - \varphi^{(n-1)}\| \quad (87)$$

whereupon the claim is proven. \square

B Analytic Solution for Linear-Elastic Singular Bar

As reference, herein we provide the solution of the singular bar of Section 4.1 for linear elasticity. The equilibrium equation is

$$P = \sigma(X)A(X) = \text{const.}, \quad \sigma(X) = B\sigma(X), \quad \sigma(X) = \sigma(X), \quad A(X) = A_0 \left(\frac{X}{L} \right)^{-1}. \quad (88)$$

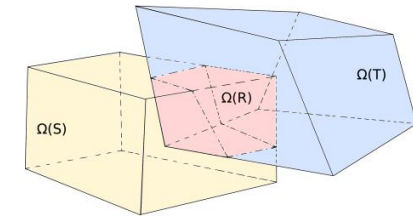
Implementation in *Albany-LCM* and *Sierra/SM* HPC Codes



The overlapping Schwarz alternating method has been implemented in two Sandia HPC codes: *Albany-LCM* and *Sierra/SM*

Albany-LCM¹

- *Open-source* parallel, C++, *multi-physics*, finite element code that relies heavily on Trilinos² libraries
- Parallel implementation of Schwarz alternating method uses the *Data Transfer Kit (DTK)*³



Data Transfer Kit (DTK)

Sierra/Solid Mechanics (Sierra/SM)

- Sandia proprietary production *Lagrangian 3D code* for finite element analysis of solids & structures
- Schwarz alternating method was “*implemented*” in *Sierra/SM* using *Arpeggio* iterative coupling framework

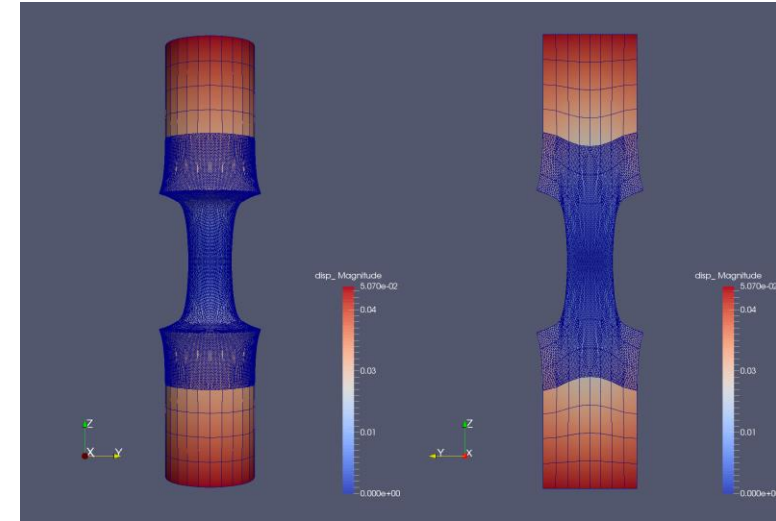
We did not have to write any code in Sierra/SM to implement Schwarz!



¹<https://github.com/sandialabs/LCM.git>. ²<http://github.com/trilinos/Trilinos.git>. ³<https://github.com/ORNL-CEES/DataTransferKit>.

1. Schwarz Alternating Method for Coupling of Full Order Models (FOMs) in Solid Mechanics

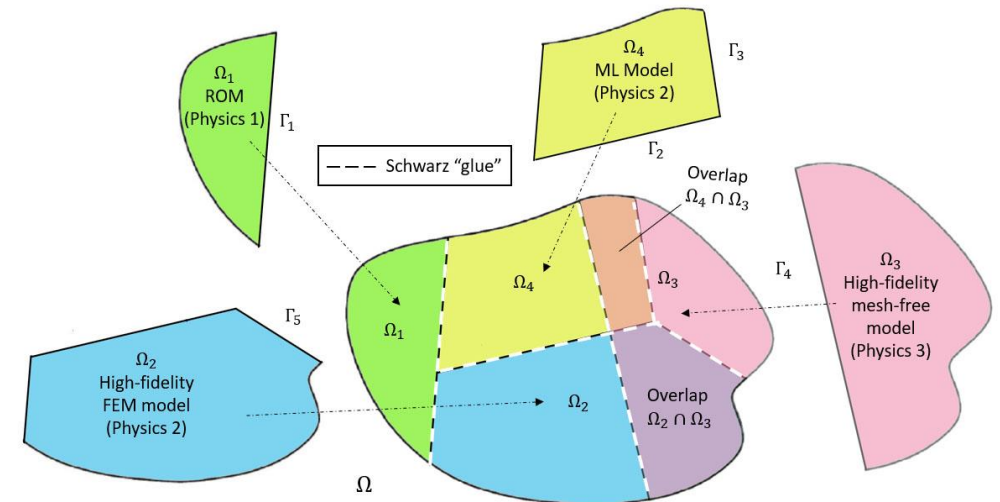
- Motivation & Background
- Quasistatic Formulation
 - Numerical Examples
- Extension to Dynamics
 - Numerical Examples



2. Schwarz Alternating Method for FOM-ROM* and ROM-ROM Coupling

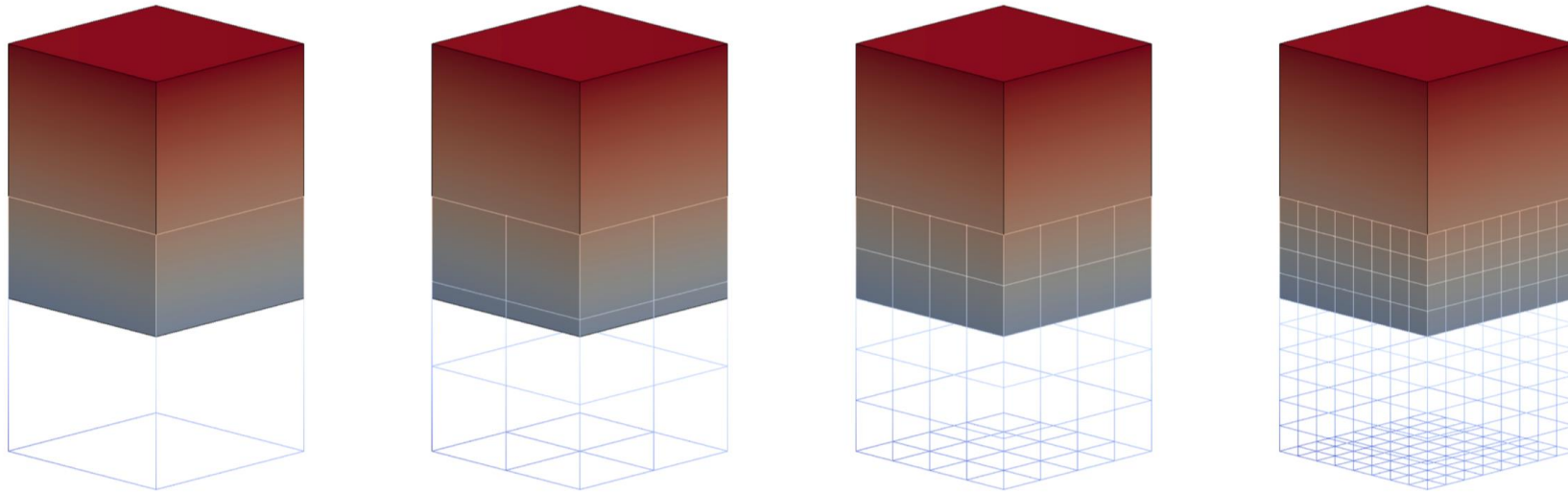
- Motivation & Background
- Formulation
- Numerical Examples

3. Summary and Future Work

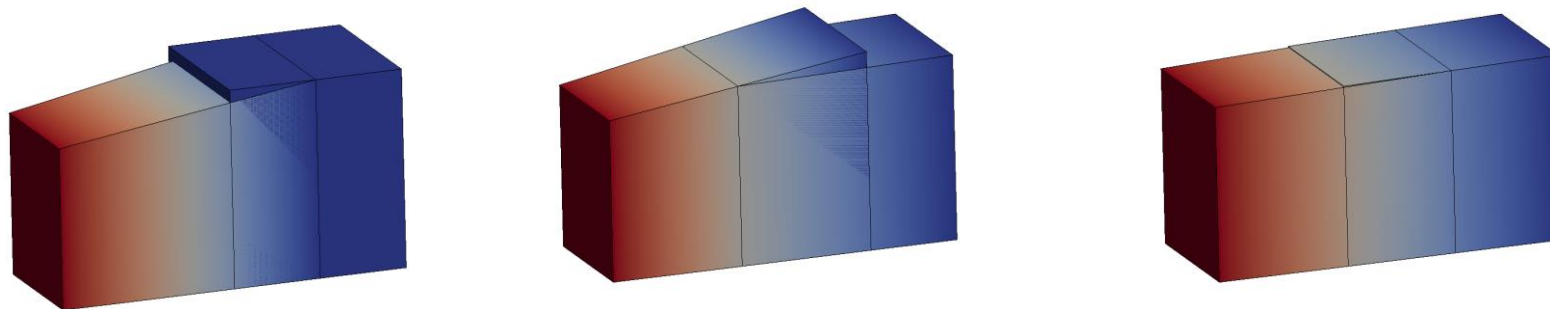


* Projection-based Reduced Order Model

Cuboid Problem



- Coupling of *two cuboids* with square base (above).
- *Neohookean*-type material model.



Schwarz Iteration

Cuboid Problem: Convergence and Accuracy

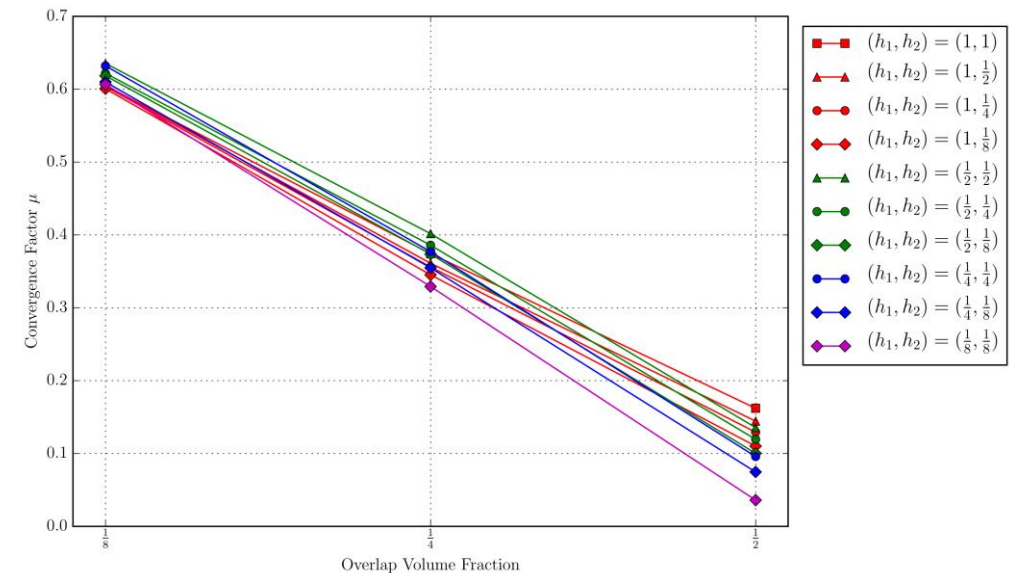
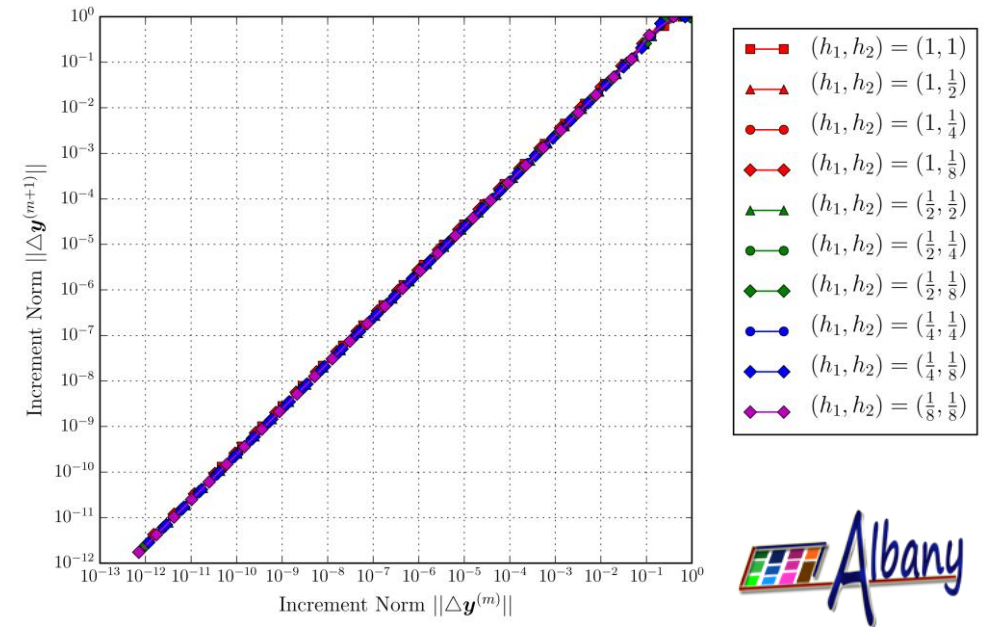


- **Top right:** convergence of the cuboid problem for *different mesh sizes* and *fixed overlap volume fraction*. The Schwarz alternating method converges *linearly*.
- **Bottom right:** convergence factor μ as a function of overlap volume and different mesh. There is *faster linear convergence* with increasing *overlap volume fraction*.

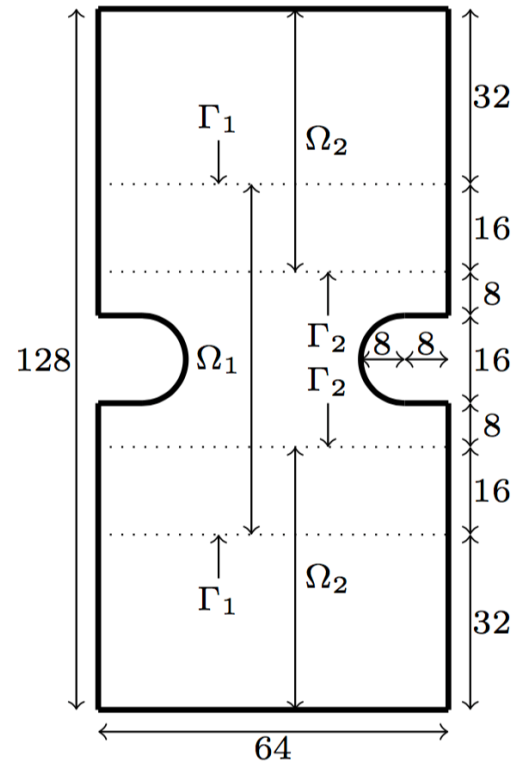
$$\Delta y^{(m+1)} \leq \mu \Delta y^{(m)}$$

- **Below:** *relative errors* in displacement and stress w.r.t. single-domain reference solution. Errors are on the order of *machine precision*.

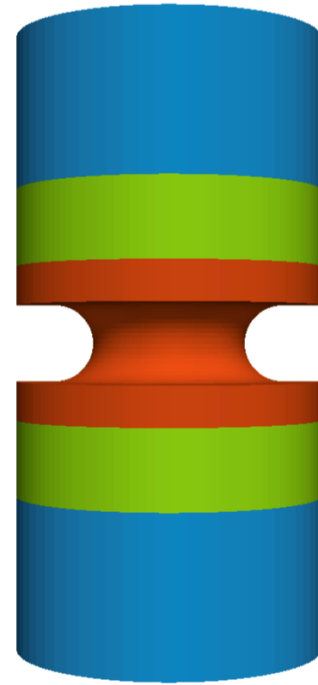
Subdomain	u_3 relative error	σ_{33} relative error
Ω_1	1.24×10^{-14}	2.31×10^{-13}
Ω_2	7.30×10^{-15}	3.06×10^{-13}



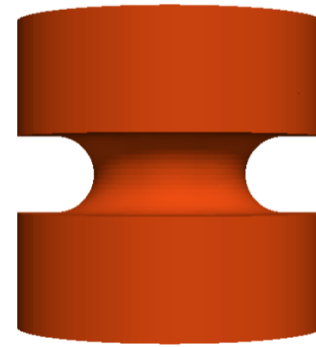
Notched Cylinder



(a) Schematic



(b) Entire Domain Ω



(c) Fine Region Ω_1



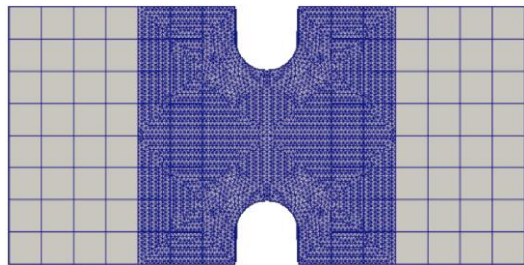
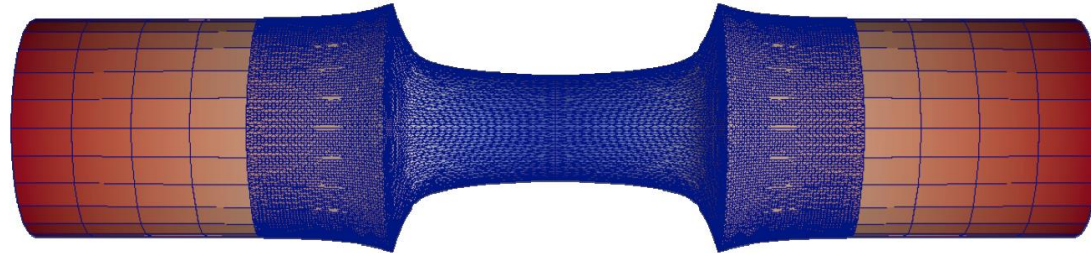
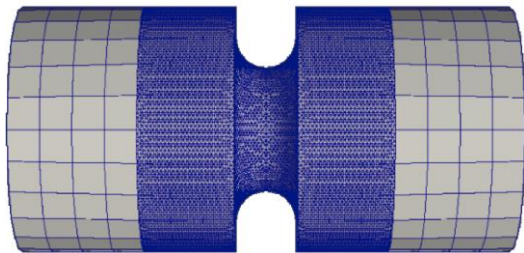
(d) Coarse Region Ω_2

- **Notched cylinder** that is stretched along its axial direction.
- Domain decomposed into **two subdomains**.
- **Neohookean**-type material model.

Notched Cylinder: TET - HEX Coupling



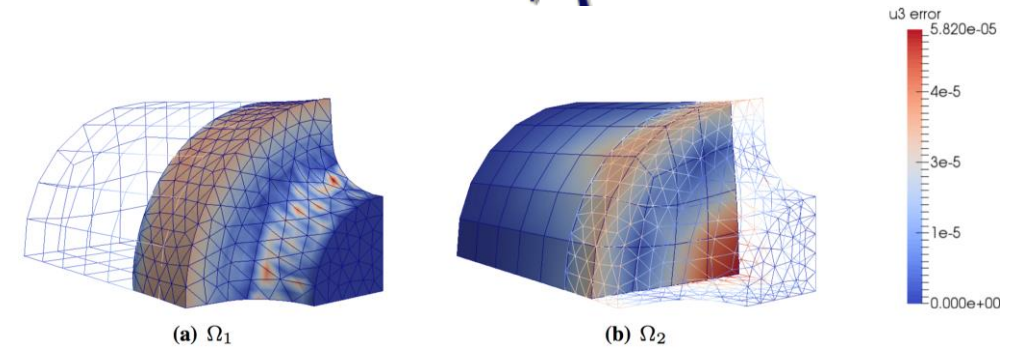
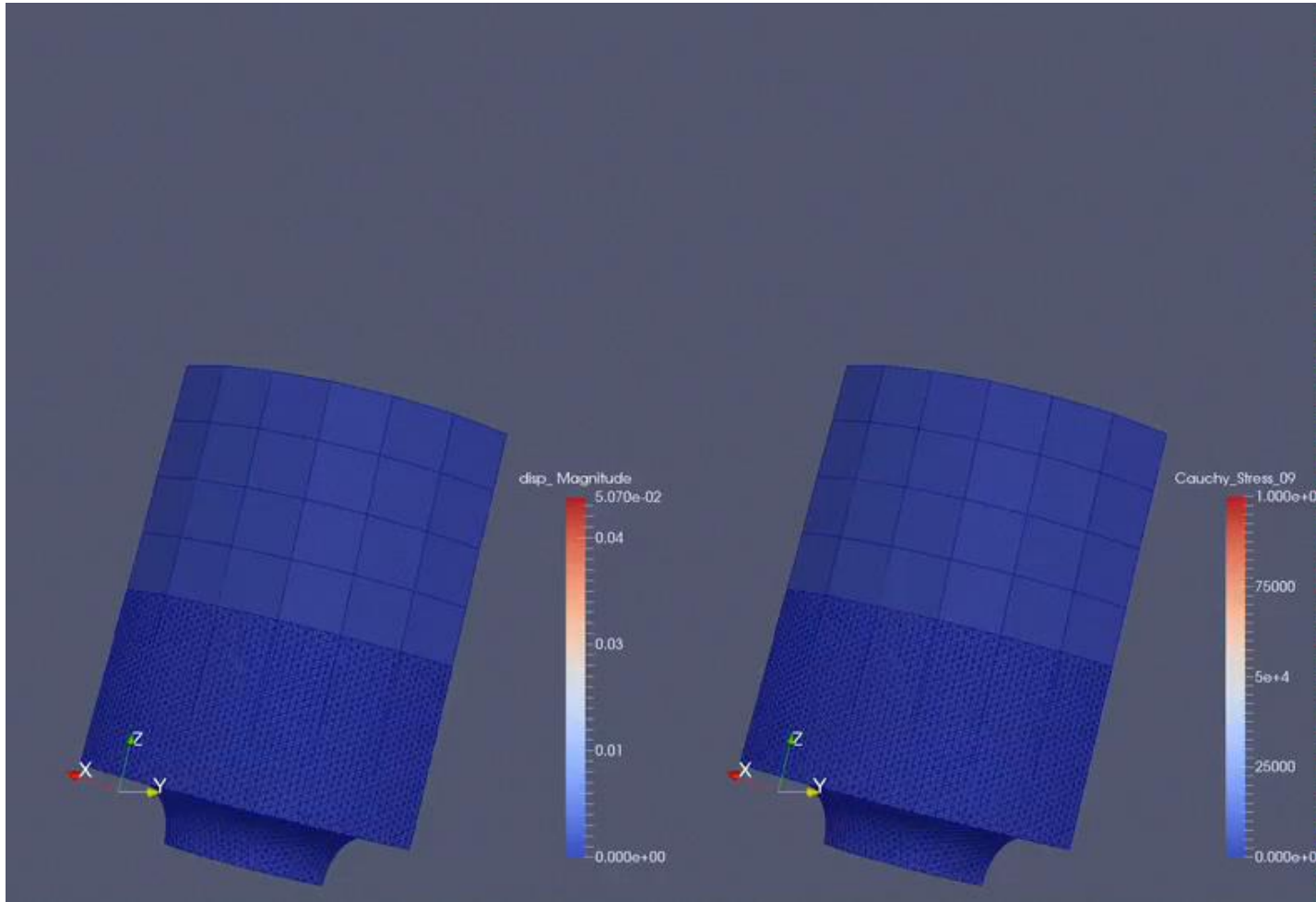
- The Schwarz alternating method is capable of coupling *different mesh topologies*.
- The notched region, where stress concentrations are expected, is *finely* meshed with *tetrahedral* elements.
- The top and bottom regions, presumably of less interest, are meshed with *coarser hexahedral* elements.



Notched Cylinder: TET - HEX Coupling



Albany



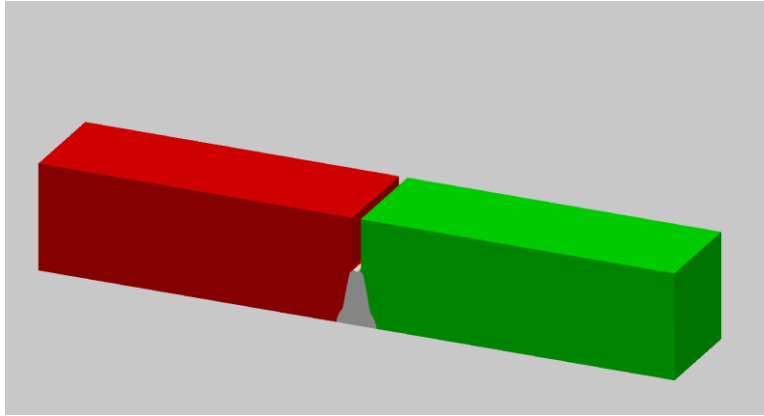
Absolute residual tolerance	u_3 relative error	
	Ω_1	Ω_2
1.0×10^{-14}	9.27×10^{-3}	3.70×10^{-3}

- Relative errors in displacement w.r.t. single-domain reference solution are dominated by **geometric** (rather than coupling) **error**.

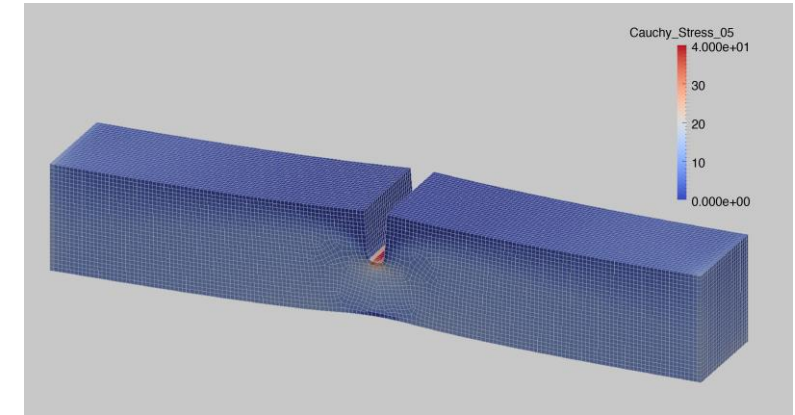
Laser Weld (Albany/LCM)



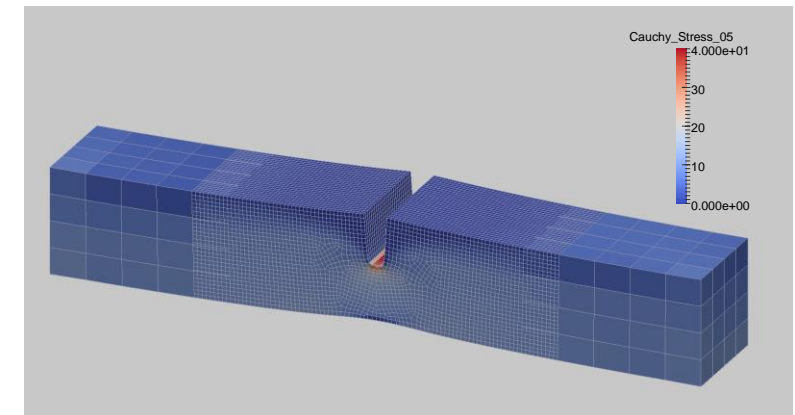
Laser weld specimen



Single domain discretization

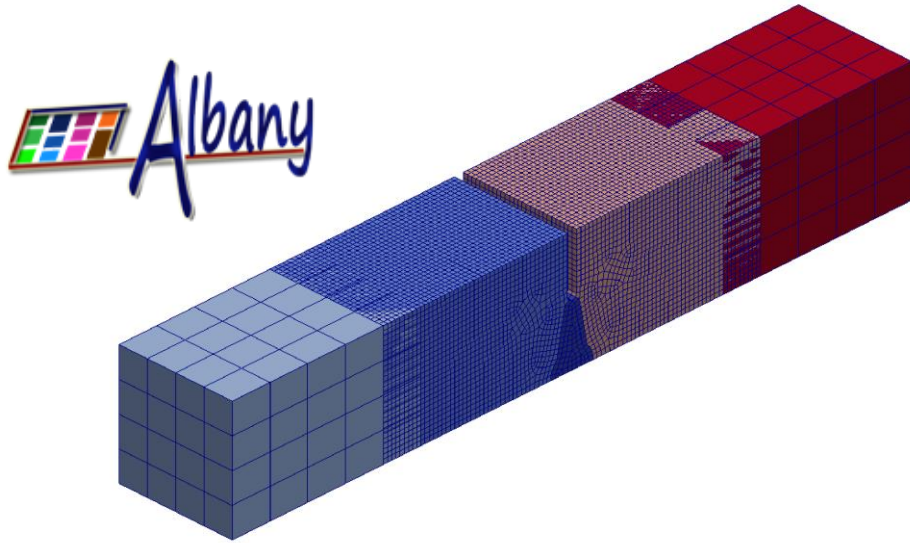


Coupled Schwarz discretization
(50% reduction in model size)

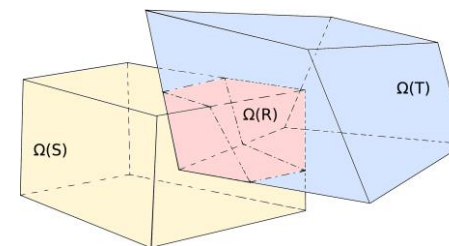
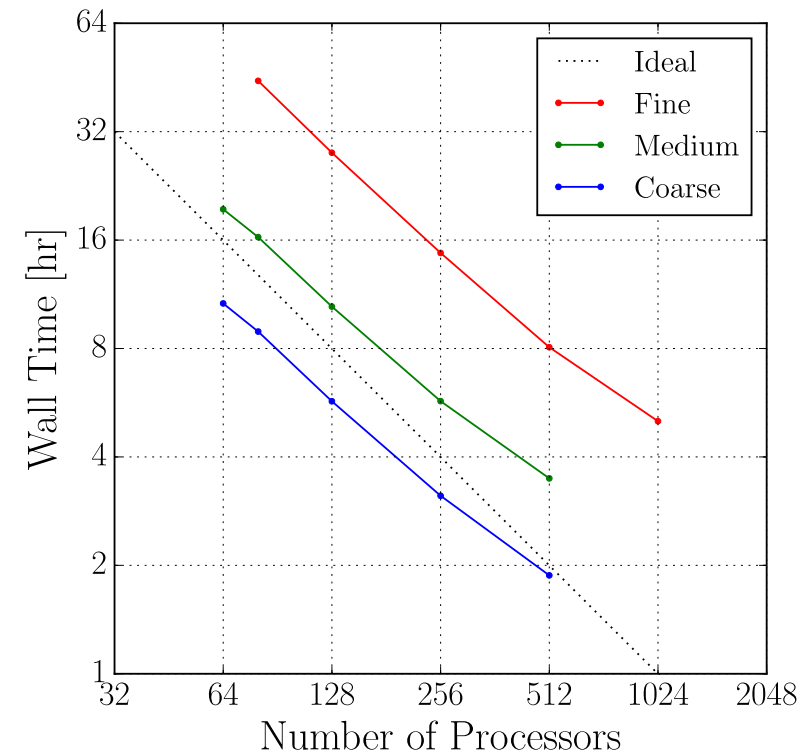
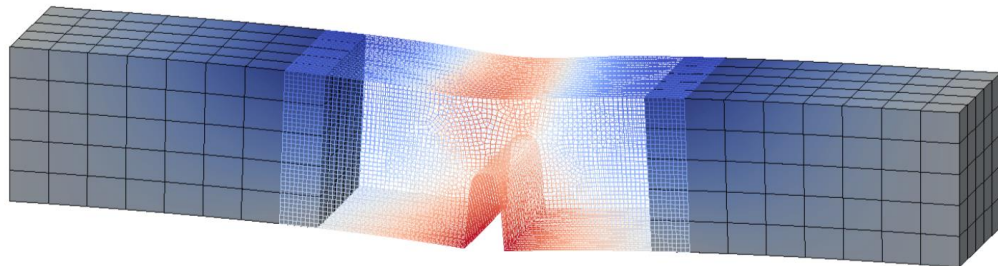


- Problem of *practical scale*.
- *Isotropic elasticity* and J_2 *plasticity* with linear isotropic hardening.
- *Identical parameters* for weld and base materials for proof of concept, to become independent models.

Laser Weld (Albany/LCM): Strong Scalability of Parallel Schwarz with DTK



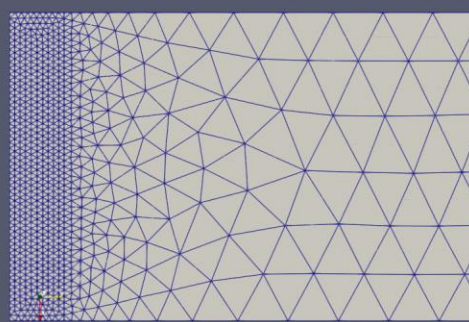
- *Near-ideal linear speedup (64-1024 cores).*



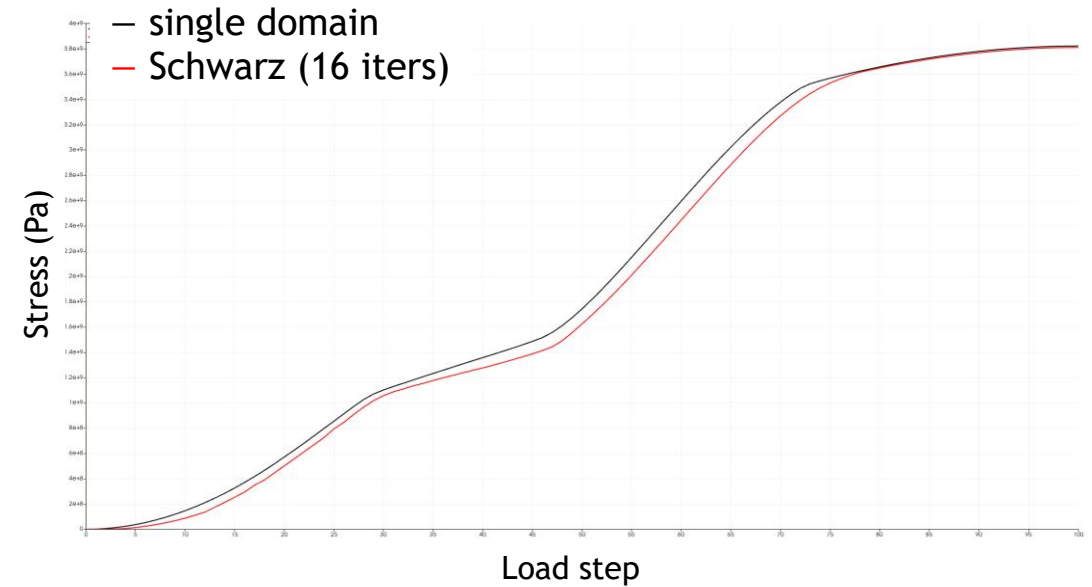
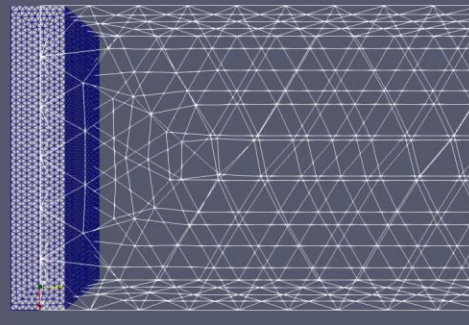
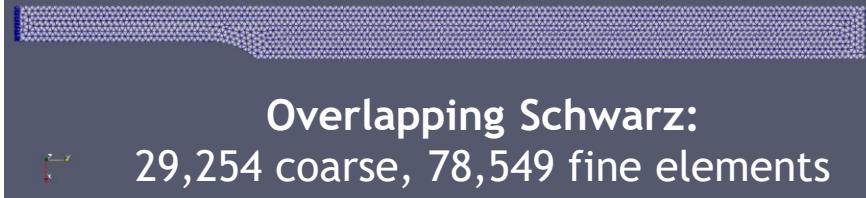
Data Transfer Kit (DTK)



Single domain:
123,425 elements



Overlapping Schwarz:
29,254 coarse, 78,549 fine elements

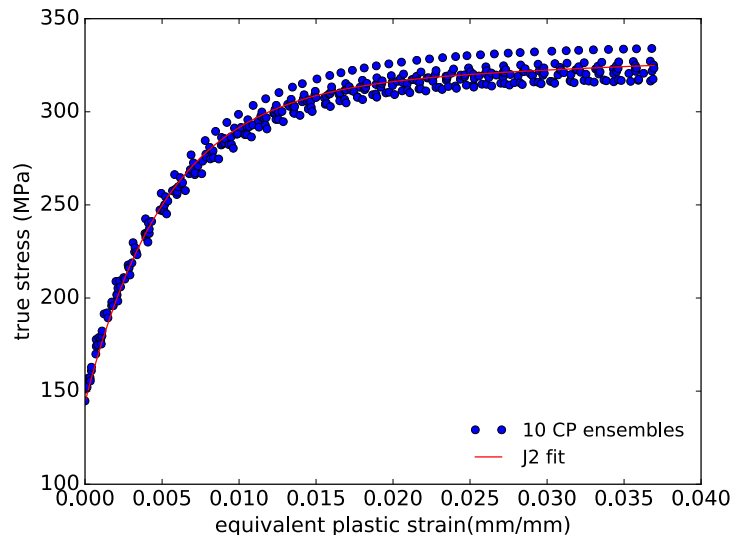


- The domains for Schwarz coupling are **meshed independently**
- This provides the ability to try **different meshing schemes** for each subdomain
- **No need to re-mesh** entire domain
- Schwarz gives **accurate prediction** of stress states if tight enough Schwarz tolerance is used
 - **Tight Schwarz tolerance** needed due to **large disparity** between **element sizes**
- For now, Schwarz is **slower** on this problem, but we are optimizing this

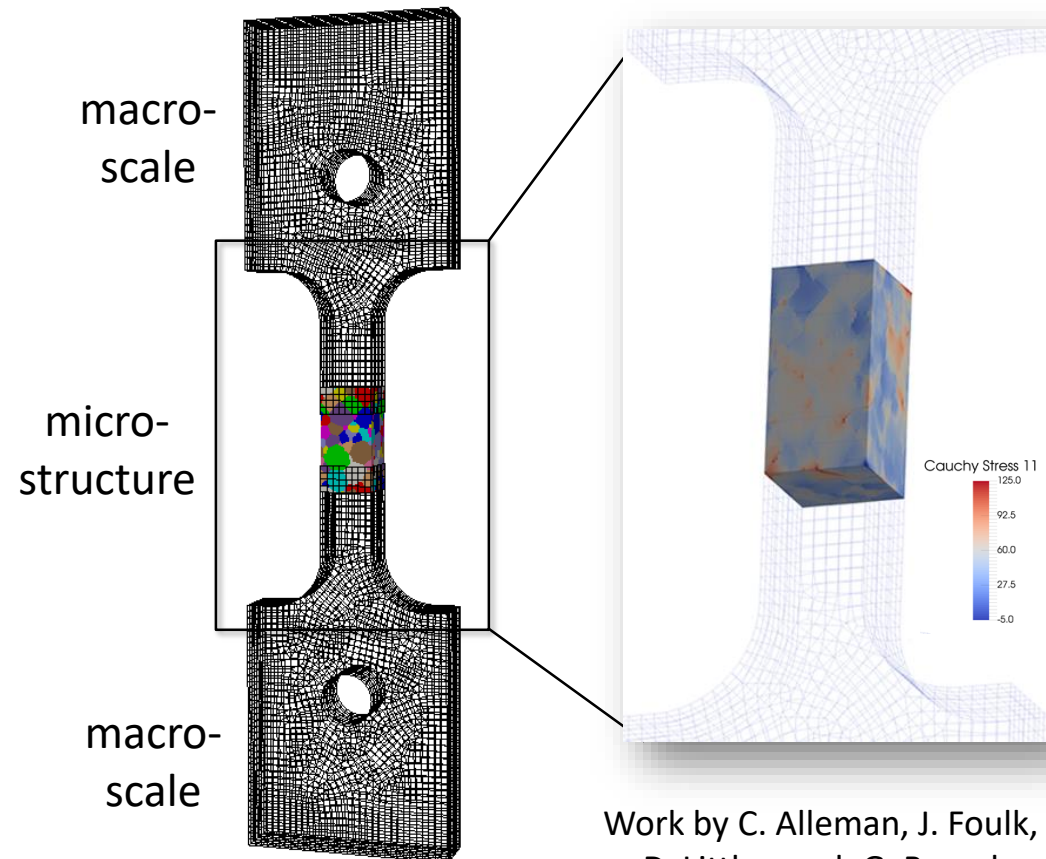


The alternating Schwarz method can be used as part of a *homogenization* (upscaling) process to bridge gap b/w *microscopic* and *macroscopic* regions

- *Microstructure* embedded in ASTM tensile geometry (right).
- Fix microstructure, investigate *ensemble* of uniaxial loads.
- Fit flow curves with a *macroscale* J_2 plasticity model (below).



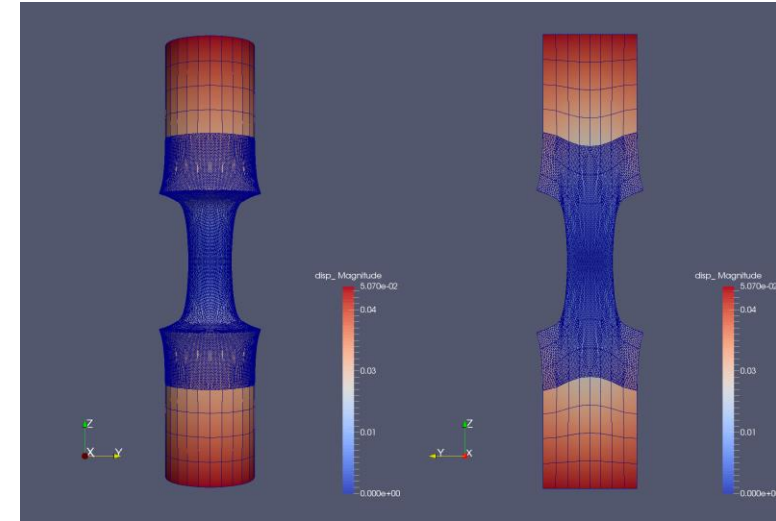
Goal: study strain localization in microstructure.



Work by C. Alleman, J. Foulk,
D. Littlewood, G. Bergel

1. Schwarz Alternating Method for Coupling of Full Order Models (FOMs) in Solid Mechanics

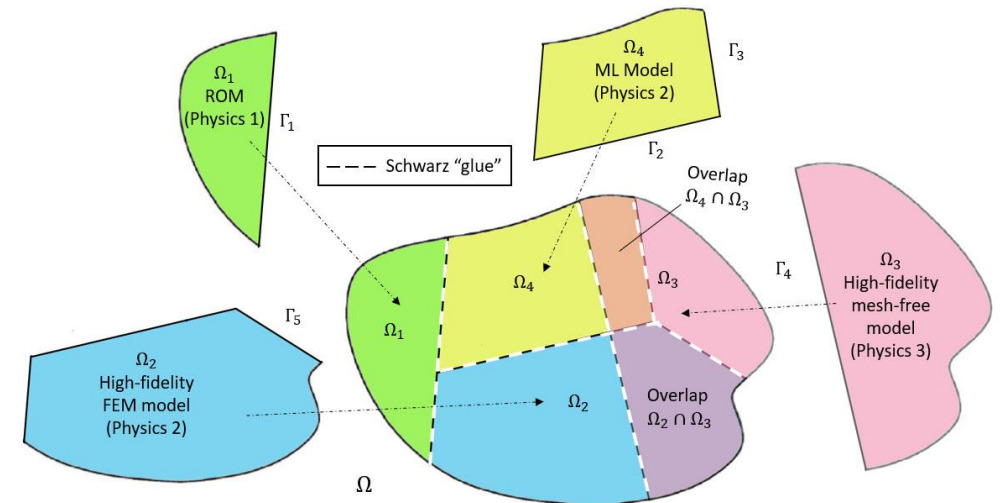
- Motivation & Background
- Quasistatic Formulation
 - Numerical Examples
- Extension to Dynamics
 - Numerical Examples



2. Schwarz Alternating Method for FOM-ROM* and ROM-ROM Coupling

- Motivation & Background
- Formulation
- Numerical Examples

3. Summary and Future Work



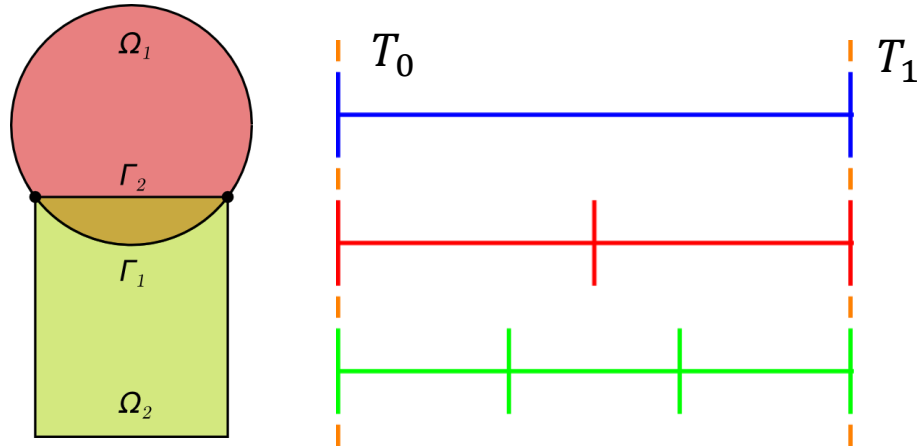
* Projection-based Reduced Order Model

Solid Dynamics Formulation



- Kinetic energy: $T(\dot{\boldsymbol{\varphi}}) := \frac{1}{2} \int_{\Omega} \rho \dot{\boldsymbol{\varphi}} \cdot \dot{\boldsymbol{\varphi}} dV$
- Potential energy: $V(\boldsymbol{\varphi}) := \int_{\Omega} A(\mathbf{F}, \mathbf{Z}) dV - \int_{\Omega} \rho \mathbf{B} \cdot \boldsymbol{\varphi} dV$
- Lagrangian: $L(\boldsymbol{\varphi}, \dot{\boldsymbol{\varphi}}) := T(\dot{\boldsymbol{\varphi}}) - V(\boldsymbol{\varphi})$
- Action functional: $S[\boldsymbol{\varphi}] := \int_I L(\boldsymbol{\varphi}, \dot{\boldsymbol{\varphi}}) dt$
- Euler-Lagrange equations:
$$\begin{cases} \text{Div } \mathbf{P} + \rho \mathbf{B} = \rho \ddot{\boldsymbol{\varphi}}, & \text{in } \Omega \times I \\ \boldsymbol{\varphi}(\mathbf{X}, t_0) = \mathbf{x}_0, & \text{in } \Omega \\ \dot{\boldsymbol{\varphi}}(\mathbf{X}, t_0) = \mathbf{v}_0, & \text{in } \Omega \\ \boldsymbol{\varphi}(\mathbf{X}, t) = \boldsymbol{\chi}, & \text{on } \partial\Omega \times I \end{cases}$$
- Semi-discrete problem following FEM discretization in space:

$$\mathbf{M}\ddot{\mathbf{u}} + \mathbf{f}_{\text{int}}(\mathbf{u}, \dot{\mathbf{u}}) = \mathbf{f}_{\text{ext}}$$



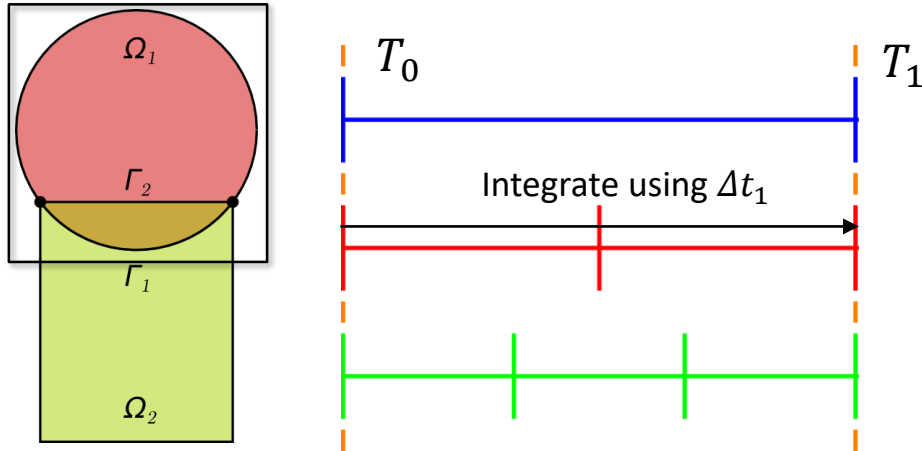
Controller time stepper

Time integrator for Ω_1

Time integrator for Ω_2

Step 0: Initialize $i = 0$ (controller time index).

$$\text{Model PDE: } \begin{cases} M\ddot{\mathbf{u}} + \mathbf{f}_{\text{int}}(\mathbf{u}, \dot{\mathbf{u}}) = \mathbf{f}_{\text{ext}} \\ \mathbf{u}(\mathbf{x}, 0) = \mathbf{u}_0 \end{cases}$$



Controller time stepper

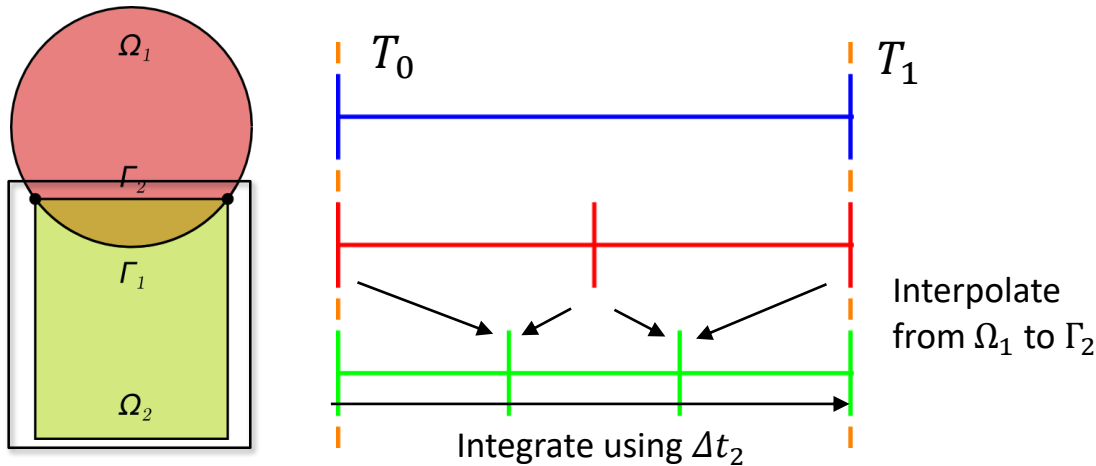
Time integrator for Ω_1

Time integrator for Ω_2

Step 0: Initialize $i = 0$ (controller time index).

Step 1: Advance Ω_1 solution from time T_i to time T_{i+1} using time-stepper in Ω_1 with time-step Δt_1 , using solution in Ω_2 interpolated to Γ_1 at times $T_i + n\Delta t_1$.

$$\text{Model PDE: } \begin{cases} M\ddot{\mathbf{u}} + \mathbf{f}_{\text{int}}(\mathbf{u}, \dot{\mathbf{u}}) = \mathbf{f}_{\text{ext}} \\ \mathbf{u}(\mathbf{x}, 0) = \mathbf{u}_0 \end{cases}$$



Controller time stepper

Time integrator for Ω_1

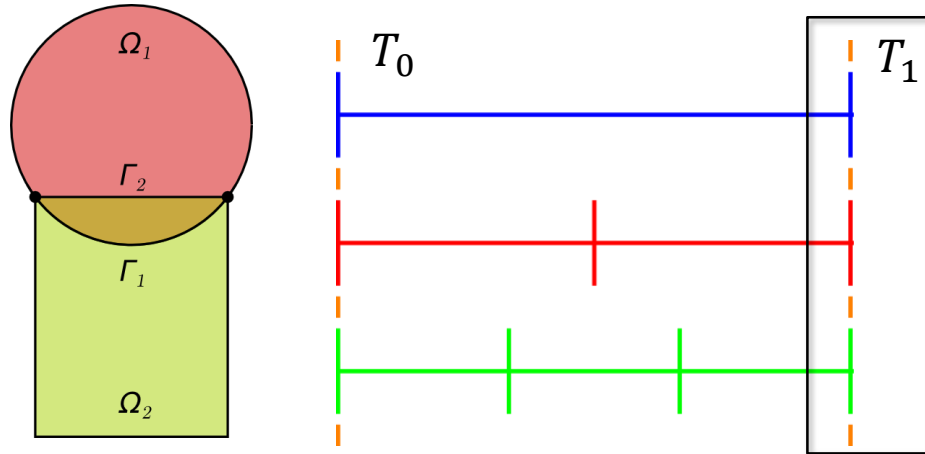
Time integrator for Ω_2

Step 0: Initialize $i = 0$ (controller time index).

Step 1: Advance Ω_1 solution from time T_i to time T_{i+1} using time-stepper in Ω_1 with time-step Δt_1 , using solution in Ω_2 interpolated to Γ_1 at times $T_i + n\Delta t_1$.

Step 2: Advance Ω_2 solution from time T_i to time T_{i+1} using time-stepper in Ω_2 with time-step Δt_2 , using solution in Ω_1 interpolated to Γ_2 at times $T_i + n\Delta t_2$.

$$\text{Model PDE: } \begin{cases} M\ddot{\mathbf{u}} + \mathbf{f}_{\text{int}}(\mathbf{u}, \dot{\mathbf{u}}) = \mathbf{f}_{\text{ext}} \\ \mathbf{u}(\mathbf{x}, 0) = \mathbf{u}_0 \end{cases}$$



Controller time stepper

Time integrator for Ω_1

Time integrator for Ω_2

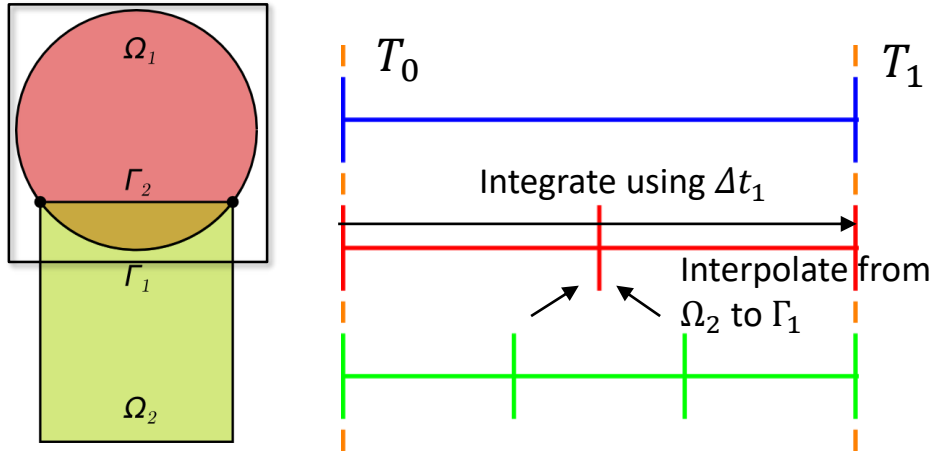
Step 0: Initialize $i = 0$ (controller time index).

Step 1: Advance Ω_1 solution from time T_i to time T_{i+1} using time-stepper in Ω_1 with time-step Δt_1 , using solution in Ω_2 interpolated to Γ_1 at times $T_i + n\Delta t_1$.

Step 2: Advance Ω_2 solution from time T_i to time T_{i+1} using time-stepper in Ω_2 with time-step Δt_2 , using solution in Ω_1 interpolated to Γ_2 at times $T_i + n\Delta t_2$.

Step 3: Check for convergence at time T_{i+1} .

$$\text{Model PDE: } \begin{cases} M\ddot{\mathbf{u}} + \mathbf{f}_{\text{int}}(\mathbf{u}, \dot{\mathbf{u}}) = \mathbf{f}_{\text{ext}} \\ \mathbf{u}(\mathbf{x}, 0) = \mathbf{u}_0 \end{cases}$$



Controller time stepper

Time integrator for Ω_1

Time integrator for Ω_2

Step 0: Initialize $i = 0$ (controller time index).

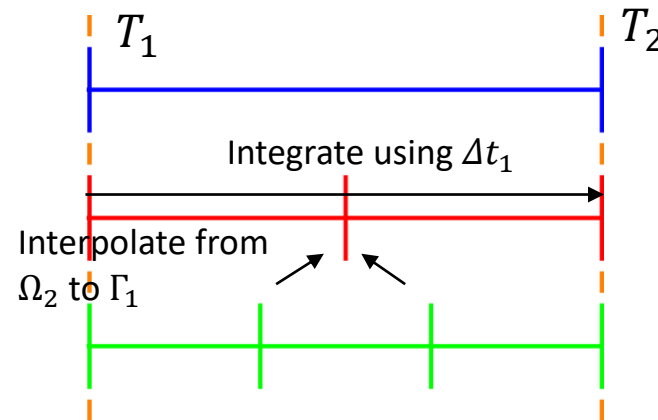
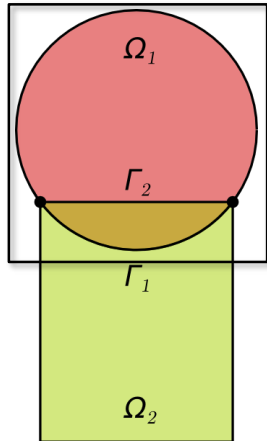
Step 1: Advance Ω_1 solution from time T_i to time T_{i+1} using time-stepper in Ω_1 with time-step Δt_1 , using solution in Ω_2 interpolated to Γ_1 at times $T_i + n\Delta t_1$.

Step 2: Advance Ω_2 solution from time T_i to time T_{i+1} using time-stepper in Ω_2 with time-step Δt_2 , using solution in Ω_1 interpolated to Γ_2 at times $T_i + n\Delta t_2$.

Step 3: Check for convergence at time T_{i+1} .

➤ If unconverged, return to Step 1.

$$\text{Model PDE: } \begin{cases} M\ddot{\mathbf{u}} + \mathbf{f}_{\text{int}}(\mathbf{u}, \dot{\mathbf{u}}) = \mathbf{f}_{\text{ext}} \\ \mathbf{u}(\mathbf{x}, 0) = \mathbf{u}_0 \end{cases}$$



Controller time stepper

Time integrator for Ω_1

Time integrator for Ω_2

Can use *different integrators* with *different time steps* within each domain!

Step 0: Initialize $i = 0$ (controller time index).

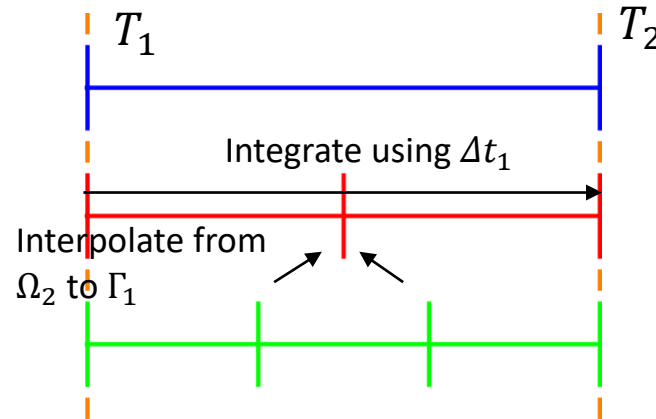
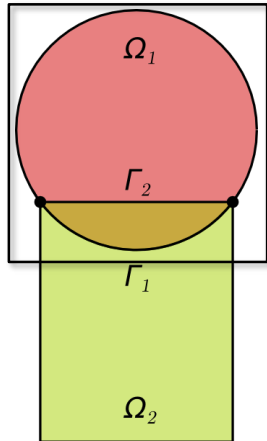
Step 1: Advance Ω_1 solution from time T_i to time T_{i+1} using time-stepper in Ω_1 with time-step Δt_1 , using solution in Ω_2 interpolated to Γ_1 at times $T_i + n\Delta t_1$.

Step 2: Advance Ω_2 solution from time T_i to time T_{i+1} using time-stepper in Ω_2 with time-step Δt_2 , using solution in Ω_1 interpolated to Γ_2 at times $T_i + n\Delta t_2$.

Step 3: Check for convergence at time T_{i+1} .

- If unconverged, return to Step 1.
- If converged, set $i = i + 1$ and return to Step 1.

$$\text{Model PDE: } \begin{cases} M\ddot{\mathbf{u}} + \mathbf{f}_{\text{int}}(\mathbf{u}, \dot{\mathbf{u}}) = \mathbf{f}_{\text{ext}} \\ \mathbf{u}(\mathbf{x}, 0) = \mathbf{u}_0 \end{cases}$$



Controller time stepper

Time integrator for Ω_1

Time integrator for Ω_2

Time-stepping procedure is **equivalent** to doing Schwarz on **space-time domain** [Mota *et al.* 2022].

Step 0: Initialize $i = 0$ (controller time index).

Step 1: Advance Ω_1 solution from time T_i to time T_{i+1} using time-stepper in Ω_1 with time-step Δt_1 , using solution in Ω_2 interpolated to Γ_1 at times $T_i + n\Delta t_1$.

Step 2: Advance Ω_2 solution from time T_i to time T_{i+1} using time-stepper in Ω_2 with time-step Δt_2 , using solution in Ω_1 interpolated to Γ_2 at times $T_i + n\Delta t_2$.

Step 3: Check for convergence at time T_{i+1} .

- If unconverged, return to Step 1.
- If converged, set $i = i + 1$ and return to Step 1.

$$\text{Model PDE: } \begin{cases} M\ddot{\mathbf{u}} + \mathbf{f}_{\text{int}}(\mathbf{u}, \dot{\mathbf{u}}) = \mathbf{f}_{\text{ext}} \\ \mathbf{u}(\mathbf{x}, 0) = \mathbf{u}_0 \end{cases}$$



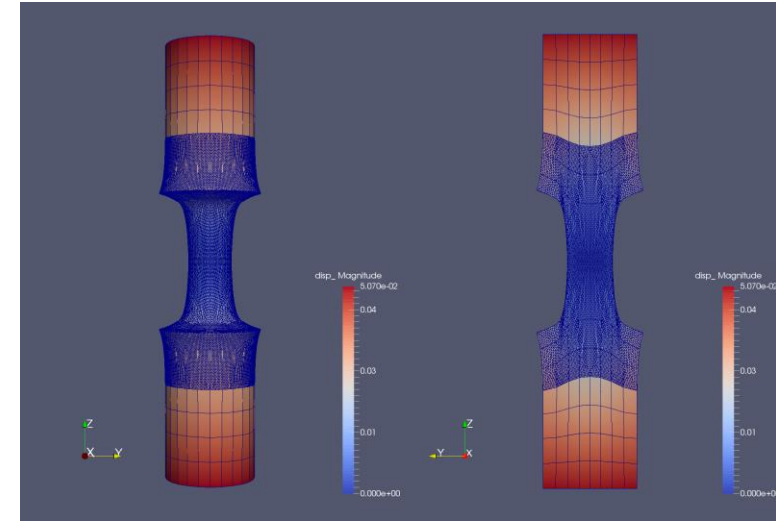
- Like for quasistatics, dynamic alternating Schwarz method converges provided each single-domain problem is **well-posed** and **overlap region** is **non-empty**, under some **conditions** on Δt .
- **Well-posedness** for the dynamic problem requires that action functional $S[\boldsymbol{\varphi}] := \int_I \int_{\Omega} L(\boldsymbol{\varphi}, \dot{\boldsymbol{\varphi}}) dV dt$ be **strictly convex** or **strictly concave**, where $L(\boldsymbol{\varphi}, \dot{\boldsymbol{\varphi}}) := T(\dot{\boldsymbol{\varphi}}) + V(\boldsymbol{\varphi})$ is the Lagrangian.
 - This is studied by looking at its second variation $\delta^2 S[\boldsymbol{\varphi}_h]$
- We can show assuming a **Newmark** time-integration scheme that for the **fully-discrete** problem:

$$\delta^2 S[\boldsymbol{\varphi}_h] = \mathbf{x}^T \left[\frac{\gamma^2}{(\beta \Delta t)^2} \mathbf{M} - \mathbf{K} \right] \mathbf{x}$$

- $\delta^2 S[\boldsymbol{\varphi}_h]$ can always be made positive by choosing a **sufficiently small** Δt
- Numerical experiments reveal that Δt requirements for **stability/accuracy** typically lead to automatic satisfaction of this bound.

1. Schwarz Alternating Method for Coupling of Full Order Models (FOMs) in Solid Mechanics

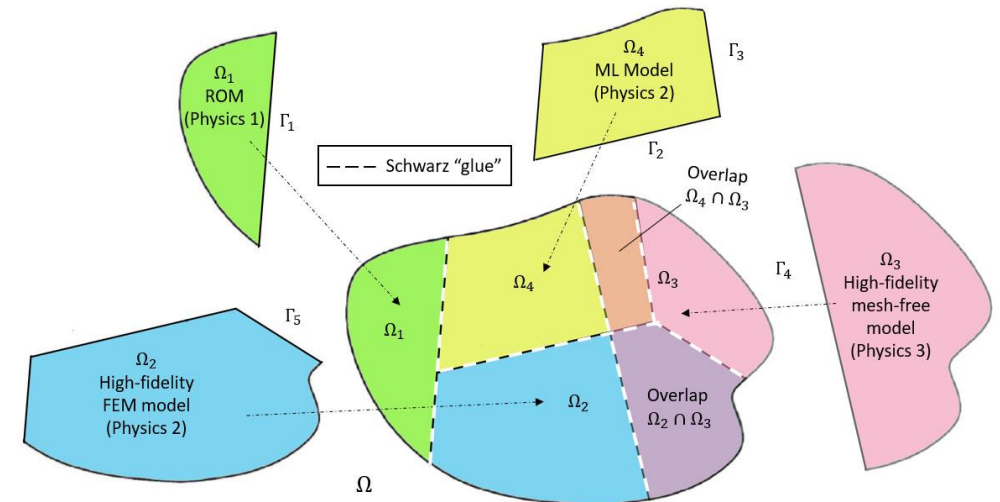
- Motivation & Background
- Quasistatic Formulation
 - Numerical Examples
- Extension to Dynamics
 - Numerical Examples



2. Schwarz Alternating Method for FOM-ROM* and ROM-ROM Coupling

- Motivation & Background
- Formulation
- Numerical Examples

3. Summary and Future Work

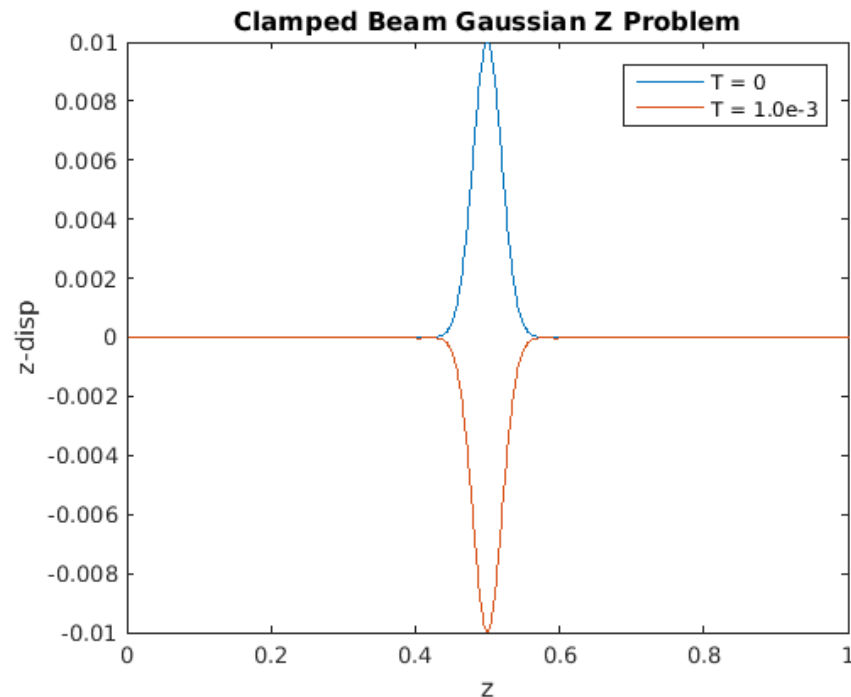


* Projection-based Reduced Order Model

Elastic Wave Propagation



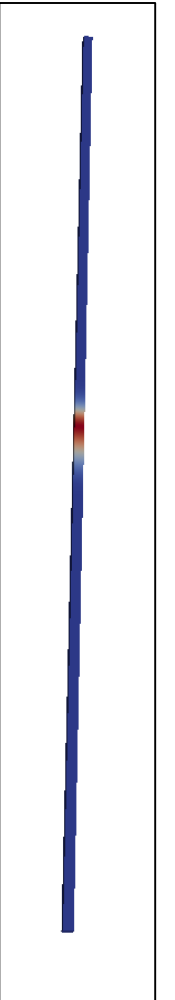
- Linear elastic *clamped beam* with Gaussian initial condition for the z -displacement.
- Simple problem with analytical exact solution but very *stringent test* for discretization methods.
- Test Schwarz with **2 subdomains**: $\Omega_0 = (0,0.001) \times (0,0.001) \times (0,0.75)$, $\Omega_1 = (0,0.001) \times (0,0.001) \times (0.25,1)$.



Left: Initial condition (blue) and final solution (red). Wave profile is negative of initial profile at time $T = 1.0e-3$.

Time-discretizations:
Newmark (implicit, explicit).

Meshes: HEX, TET



Elastic Wave: Different Integrators, Same Δt s

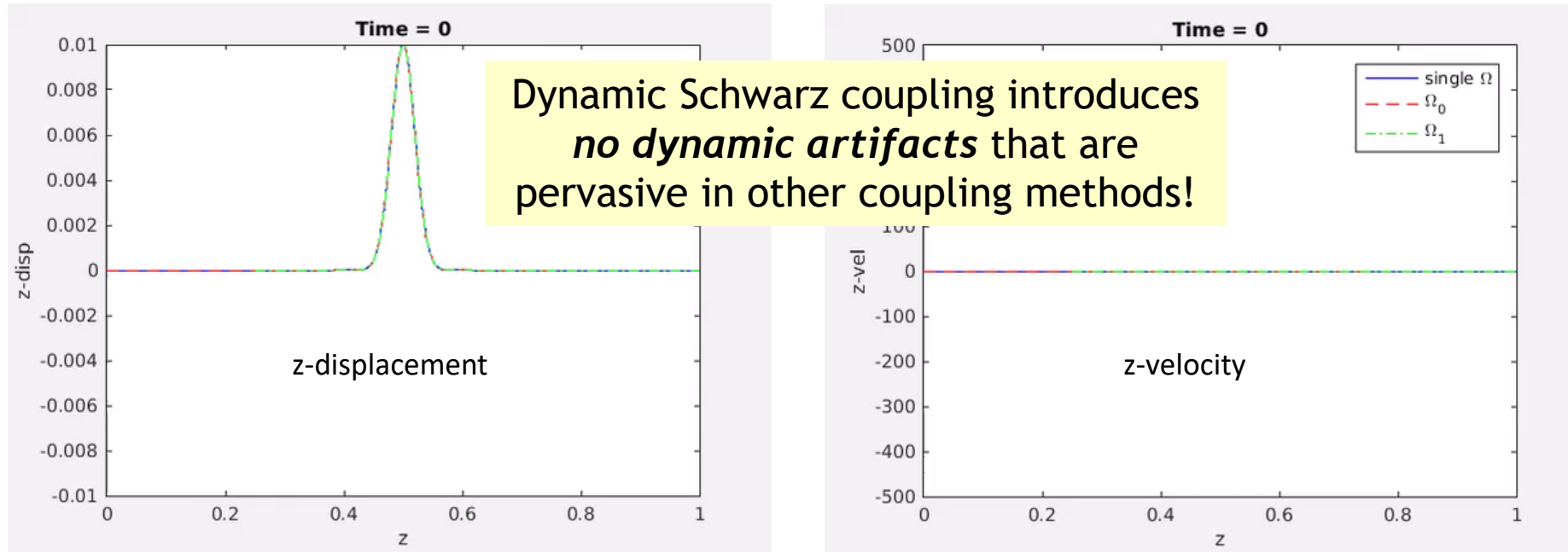
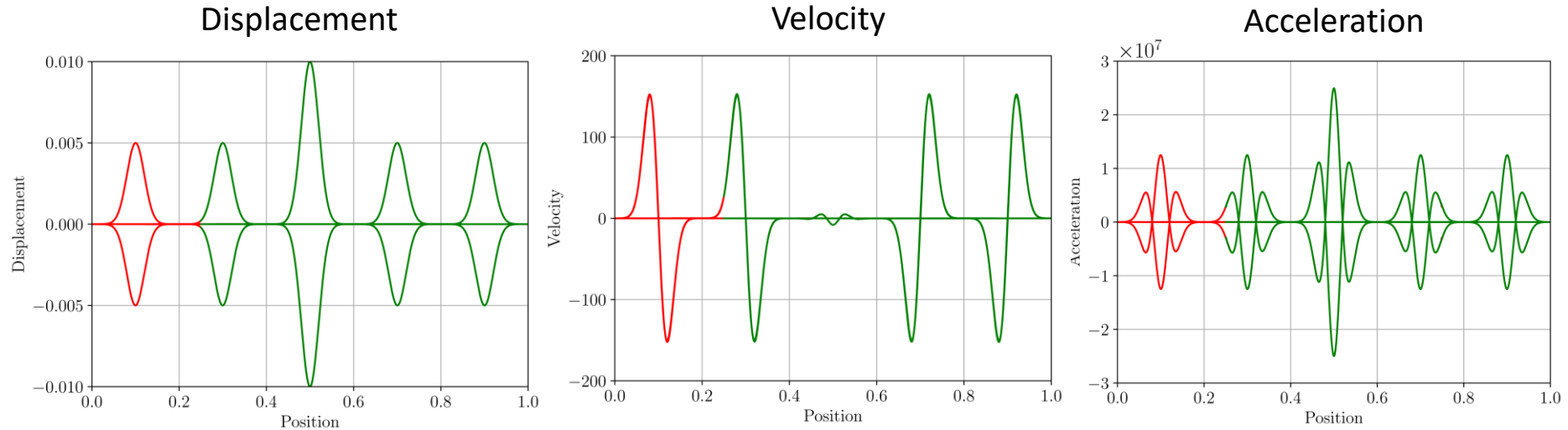


Table 1: Averaged (over times + domains) relative errors in **z-displacement** (blue) and **z-velocity** (green) for several different Schwarz couplings, 50% overlap volume fraction

	Implicit-Implicit		Explicit(CM)-Implicit		Explicit(LM)-Implicit	
Conformal HEX - HEX	2.79e-3	7.32e-3	3.53e-3	8.70e-3	4.72e-3	1.19e-2
Nonconformal HEX - HEX	2.90e-3	7.10e-3	2.82e-3	7.29e-3	2.84e-3	7.33e-3
TET - HEX	2.79e-3	7.58e-3	3.52e-3	8.92e-3	4.72e-3	1.19e-2

Elastic Wave: Different Integrators, Different Δt s

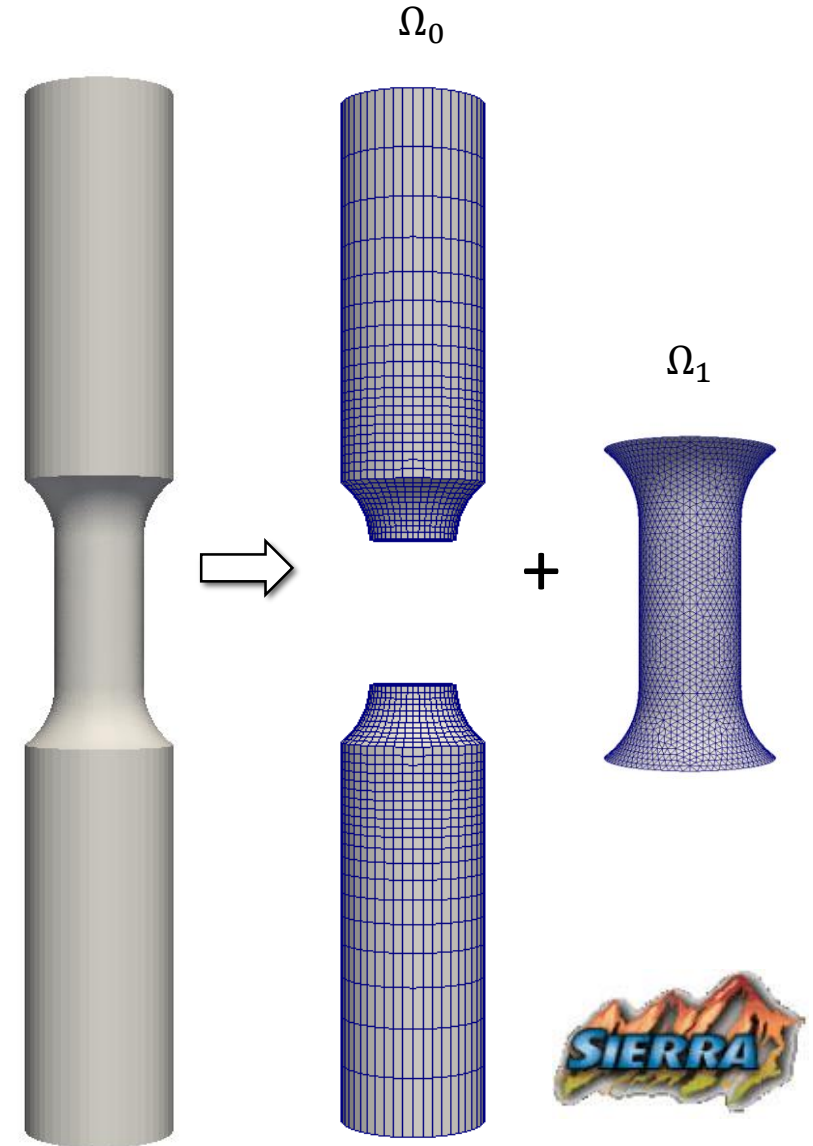


Figures above: Plots of displacement, velocity and acceleration for the elastic wave propagation problem using different time integrators (implicit and explicit) and different time steps ($1e-2s$ and $2e-7s$) for each subdomain, superimposed over the analytic single domain solution.

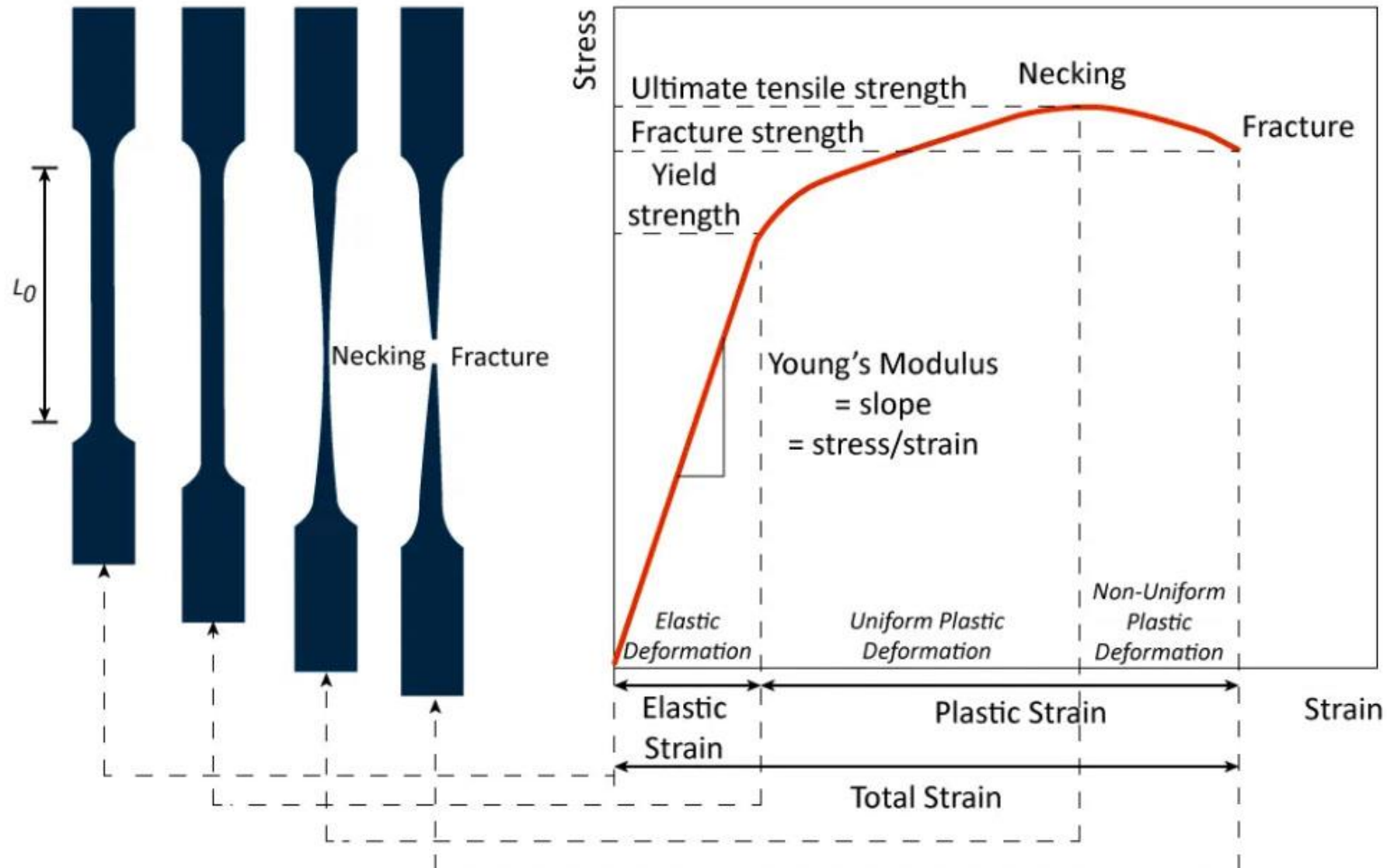
The analytic solution is *indistinguishable* from Schwarz solutions (hidden behind the solutions for Ω_0 (red) and Ω_1 (green))!

Tension Specimen

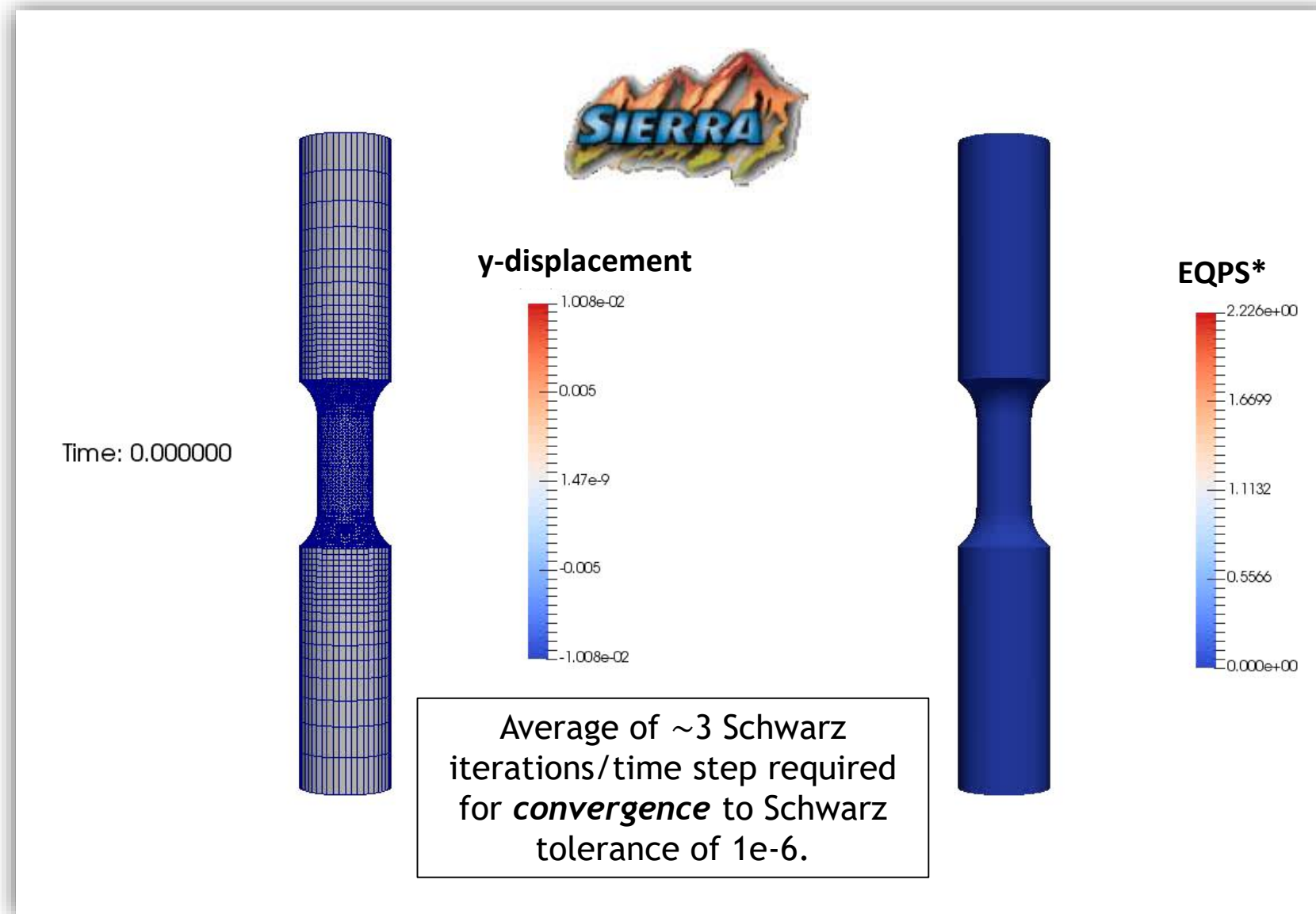
- Uniaxial aluminum cylindrical tensile specimen with *inelastic J_2 material model*.
- Domain decomposition into *two subdomains* (right): Ω_0 = ends, Ω_1 = gauge.
- *Nonconformal HEX + composite TET10* coupling via Schwarz.
- *Implicit* Newmark time-integration with *adaptive time-stepping* algorithm employed in both subdomains.
- Slight *imperfection* introduced at center of gauge to force *necking* upon pulling in vertical direction.



Tension Specimen: Expected Result



Tension Specimen: Displacement & EQPS*



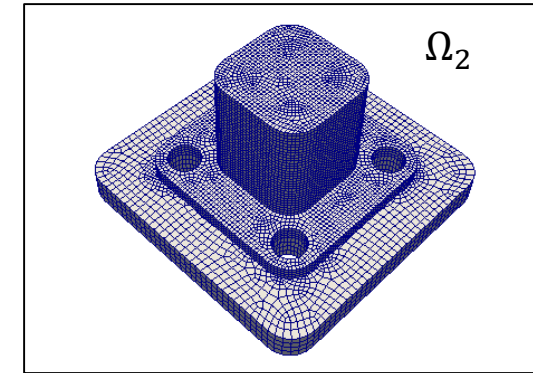
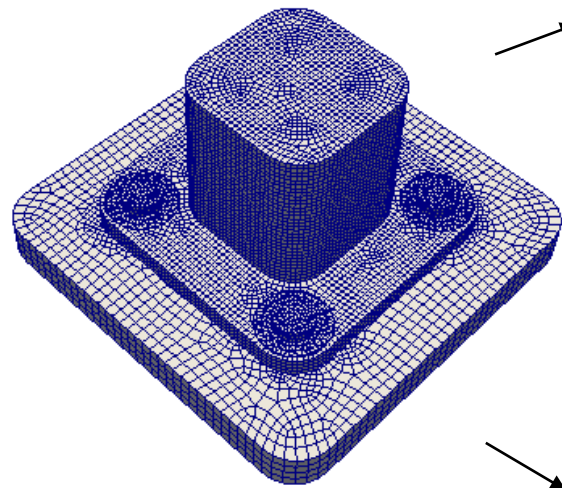
*EQPS = Equivalent Plastic Strain

Bolted Joint Problem



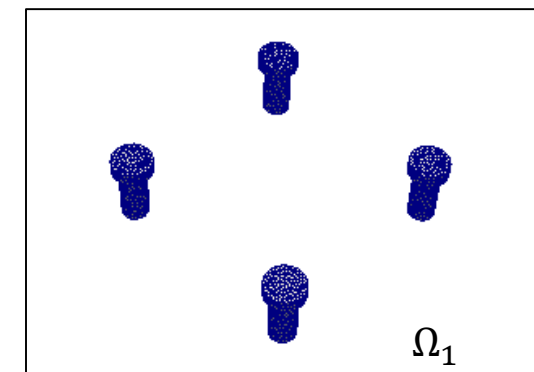
Problem of *practical scale*.

- Schwarz solution compared to single-domain solution on composite TET10 mesh.

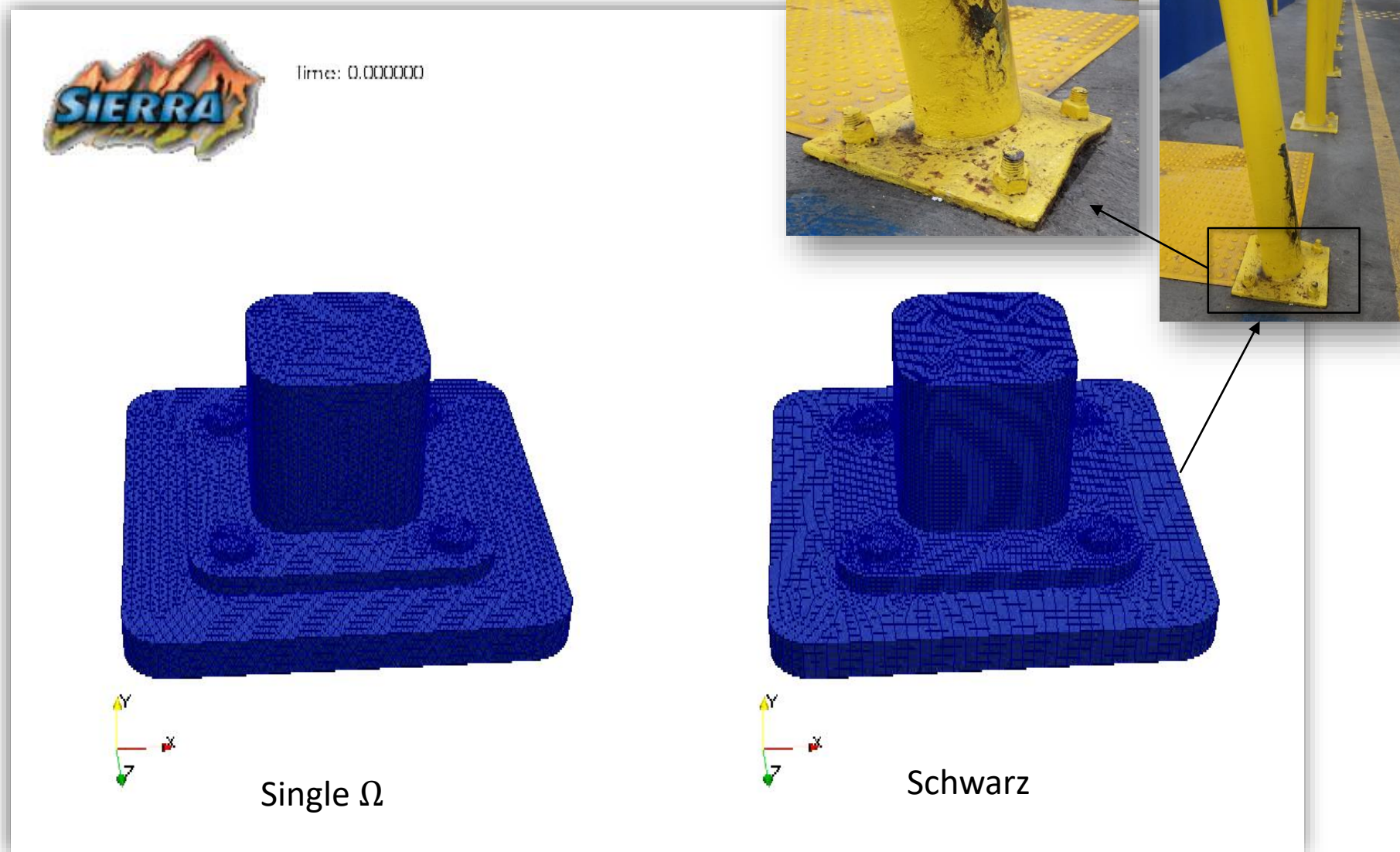


- BC: $x\text{-disp} = 0.02$ at $T = 1.0e-3$ on top of parts.
- Run until $T = 5.0e-4$ w/ $dt = 1e-5$ + implicit Newmark with analytic mass matrix for composite tet 10s.

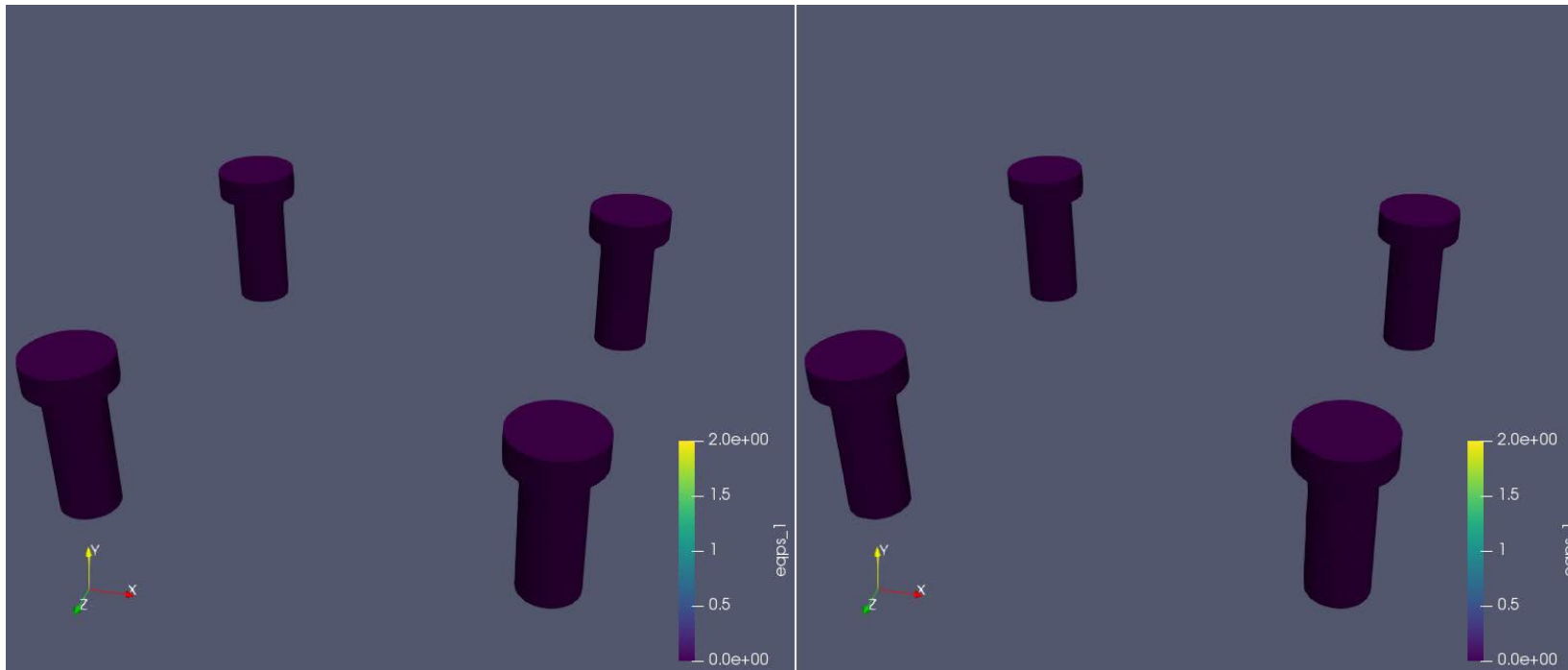
- Ω_1 = bolts (Composite TET10), Ω_2 = parts (HEX).
- Inelastic J_2 material model** in both subdomains.
 - Ω_1 : steel
 - Ω_2 : steel component, aluminum (bottom) plate



Bolted Joint Problem: Displacement



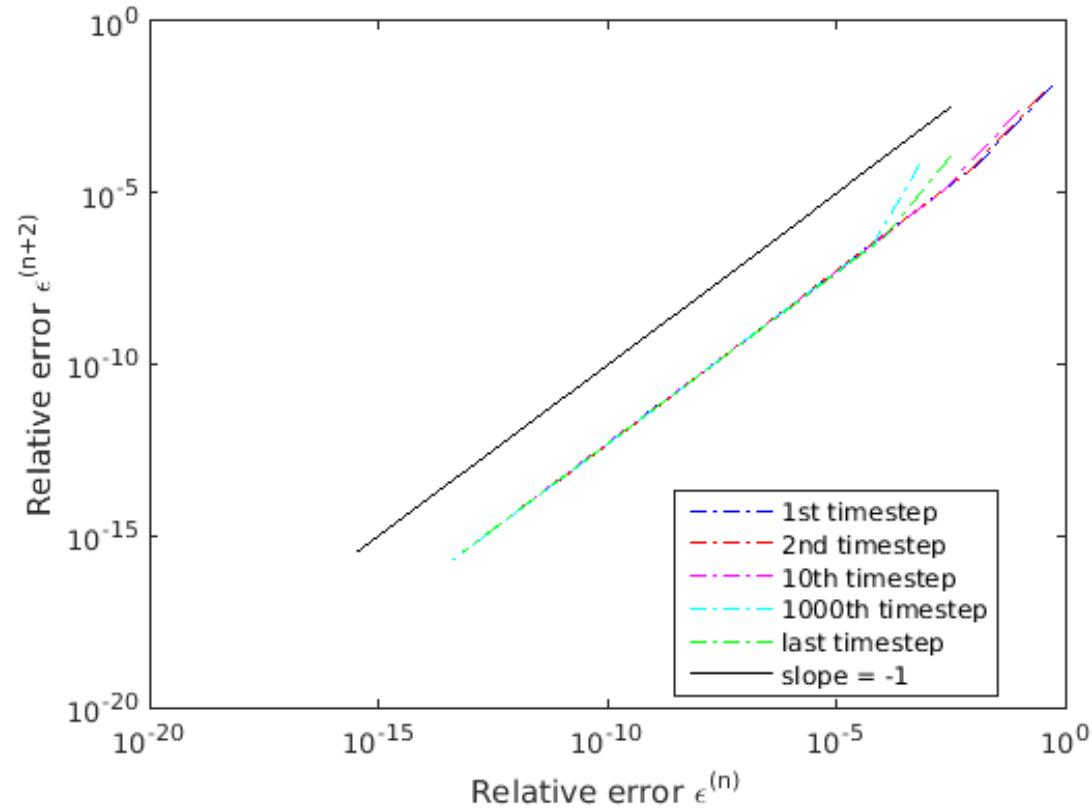
Bolted Joint Problem: Equivalent Plastic Strain (EQPS)



Single Ω

Schwarz

Bolted Joint Problem: Convergence Rate



Linear convergence rate is observed for *dynamic* Schwarz algorithm, as for the quasistatic Schwarz algorithm.

Figure above: Convergence behavior of the dynamic Schwarz algorithm for the bolted joint problem

Bolted Joint Problem: Performance



	CPU times (64 procs*)	Avg # Schwarz iters	Max # Schwarz iters
Single Domain	3h 34m	—	—
Schwarz	2h 42m	3.22	4
Single Domain (finer)	17h 00m	—	—
Schwarz (finer mesh of bolts)	29h 29m	3.28	4



* On SNL ascicgpu15, 16, 17 machines (Intel Skylake CPU processor), Schwarz tol = 1e-6.

Bolted Joint Problem: Performance



	CPU times (64 procs*)	Avg # Schwarz iters	Max # Schwarz iters
Single Domain	3h 34m	–	–
Schwarz	2h 42m	3.22	4
Single Domain (finer)	17h 00m	–	–
Schwarz (finer mesh of bolts)	29h 29m	3.28	4



- Despite its iterative nature, Schwarz can actually be *faster* than single domain run for discretizations having comparable # of elements in the bolts.

* On SNL ascicgpu15, 16, 17 machines (Intel Skylake CPU processor), Schwarz tol = 1e-6.

Bolted Joint Problem: Performance



	CPU times (64 procs*)	Avg # Schwarz iters	Max # Schwarz iters
Single Domain	3h 34m	—	—
Schwarz	2h 42m	3.22	4
Single Domain (finer)	17h 00m	—	—
Schwarz (finer mesh of bolts)	29h 29m	3.28	4



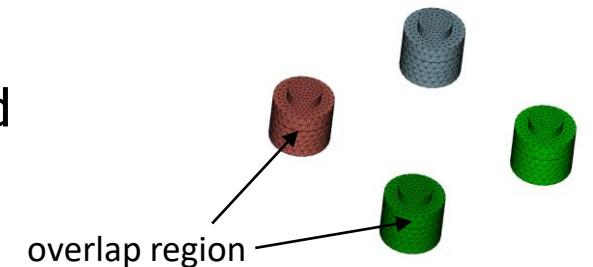
- Despite its iterative nature, Schwarz can actually be *faster* than single domain run for discretizations having comparable # of elements in the bolts.
 - Even if the method is more computationally expensive for some resolutions, it may be preferred for its ability to *rapidly change* and *evaluate* a *variety* of *engineering designs* (our typical use case).

* On SNL ascicgpu15, 16, 17 machines (Intel Skylake CPU processor), Schwarz tol = 1e-6.

	CPU times (64 procs*)	Avg # Schwarz iters	Max # Schwarz iters
Single Domain	3h 34m	—	—
Schwarz	2h 42m	3.22	4
Single Domain (finer)	17h 00m	—	—
Schwarz (finer mesh of bolts)	29h 29m	3.28	4



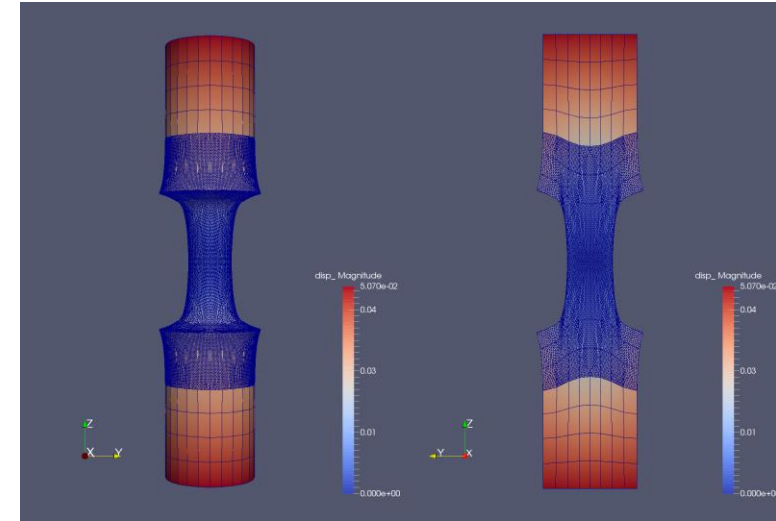
- Despite its iterative nature, Schwarz can actually be *faster* than single domain run for discretizations having comparable # of elements in the bolts.
 - Even if the method is more computationally expensive for some resolutions, it may be preferred for its ability to *rapidly change* and *evaluate* a *variety* of *engineering designs* (our typical use case).
- Dynamic Schwarz converges in between *2-4 Schwarz iterations* per time-step despite the *overlap* region being *very small* for this problem.



* On SNL ascicgpu15, 16, 17 machines (Intel Skylake CPU processor), Schwarz tol = 1e-6.

1. Schwarz Alternating Method for Coupling of Full Order Models (FOMs) in Solid Mechanics

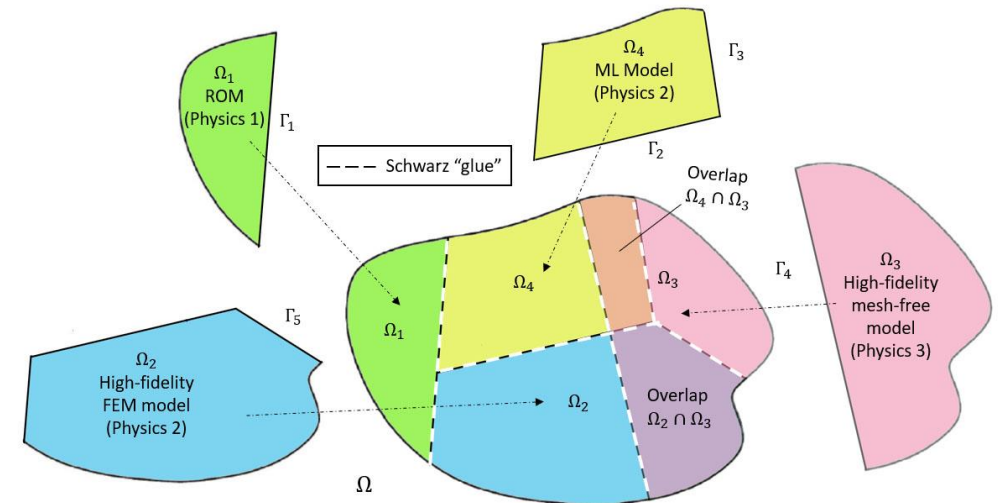
- Motivation & Background
- Quasistatic Formulation
 - Numerical Examples
- Extension to Dynamics
 - Numerical Examples



2. Schwarz Alternating Method for FOM-ROM* and ROM-ROM Coupling

- Motivation & Background
- Formulation
- Numerical Examples

3. Summary and Future Work

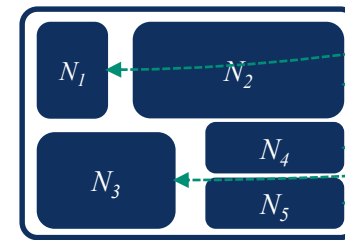
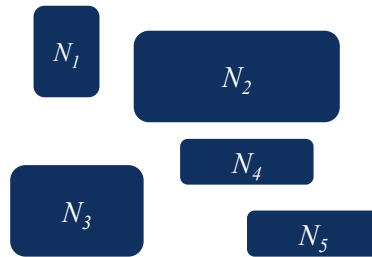
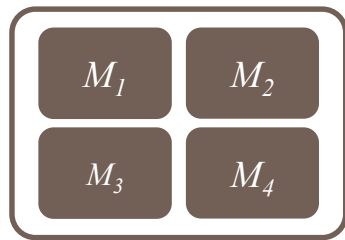


* Projection-based Reduced Order Model

Motivation for ROM-ROM/ROM-FOM Couplings

The past decades have seen tremendous investment in **simulation frameworks for coupled multi-scale and multi-physics problems.**

- Frameworks rely on **established mathematical theories** to couple physics components.
- Most existing coupling frameworks are based on **traditional discretization methods.**



Complex System Model

- PDEs, ODEs
- Nonlocal integral
- Classical DFT
- Atomistic, ...

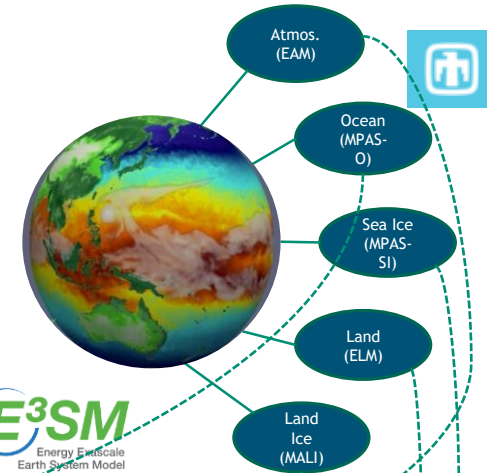
Traditional Methods

- Mesh-based (FE, FV, FD)
- Meshless (SPH, MLS)
- Implicit, explicit
- Eulerian, Lagrangian...

Coupled Numerical Model

- Monolithic (Lagrange multipliers)
- Partitioned (loose) coupling
- Iterative (Schwarz, optimization)

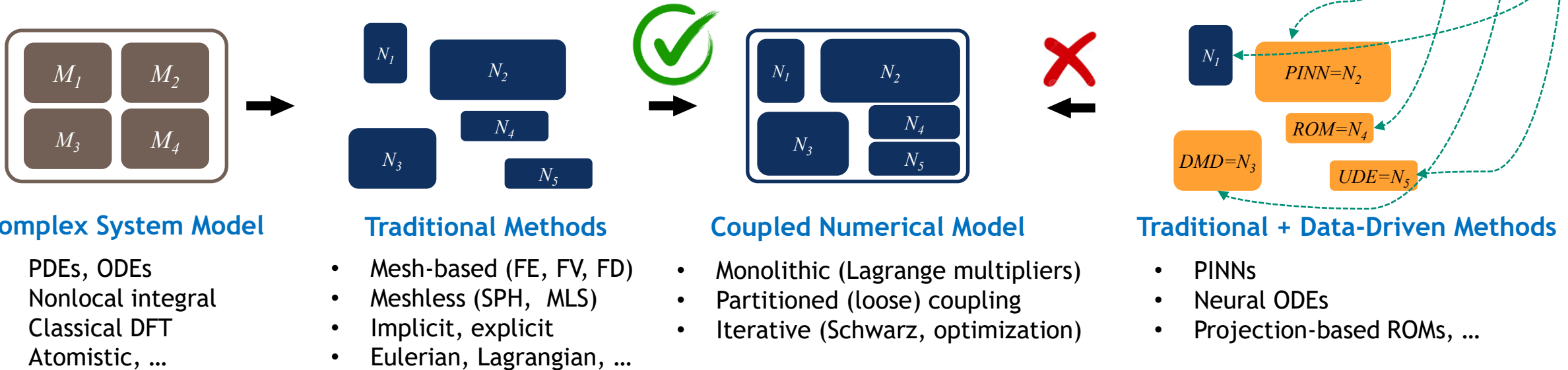
E³SM
Energy-Euscale
Earth System Model



Motivation for ROM-ROM/ROM-FOM Couplings

The past decades have seen tremendous investment in **simulation frameworks for coupled multi-scale and multi-physics problems.**

- Frameworks rely on **established mathematical theories** to couple physics components.
- Most existing coupling frameworks are based on **traditional discretization methods.**



- There is currently a big push to integrate **data-driven methods** into modeling & simulation toolchains.

Unfortunately, existing algorithmic and software infrastructures are **ill-equipped** to handle plug-and-play integration of **non-traditional, data-driven models!**

Principal research objective:

- Discover mathematical principles guiding the assembly of standard and data-driven numerical models in stable, accurate and physically consistent ways.

Principal research challenges: we lack mathematical and algorithmic understanding of how to

- “Mix-and-match” standard and data-driven models from three-classes

➤ **Class A:** projection-based reduced order models (ROMs) *This talk.*

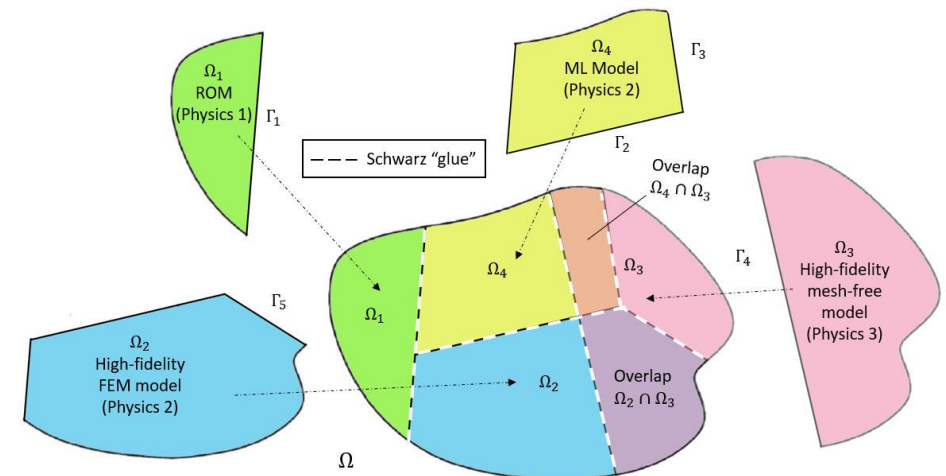
➤ **Class B:** machine-learned models, i.e., Physics-Informed Neural Networks (PINNs)

➤ **Class C:** flow map approximation models, i.e., dynamic model decomposition (DMD) models

- Ensure well-posedness & physical consistency of resulting heterogeneous models.
- Solve such heterogeneous models efficiently.

Three coupling methods:

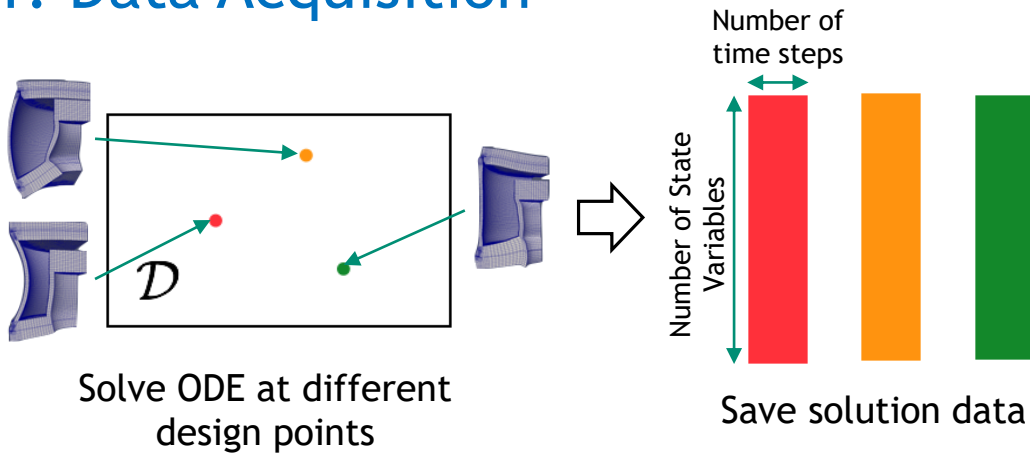
- Alternating Schwarz-based coupling *This talk.*
- Optimization-based coupling
- Coupling via generalized mortar methods



Full Order Model (FOM): $\frac{\partial q}{\partial t} = f(q, t; \mu)$

*Least-Squares Petrov-Galerkin

1. Data Acquisition



2. Learning of Reduced Basis

Proper Orthogonal Decomposition (POD):

$$\mathbf{X} = \begin{bmatrix} \text{red} & \text{orange} & \text{green} \end{bmatrix} = \begin{bmatrix} \text{brown} & \text{light blue} \end{bmatrix} \mathbf{U} \quad \Sigma \quad \begin{bmatrix} \text{light blue} \end{bmatrix} \mathbf{V}^T$$

ROM = projection-based Reduced Order Model

3. Projection-Based Reduction

Discretize FOM in time

$$\dot{q} = f(q, t; \mu)$$

$$\Downarrow$$

$$\mathbf{r}^n(\mathbf{q}^n; \mu) = \mathbf{0}, \quad n = 1, \dots, T$$

Reduce the number of unknowns

$$\mathbf{q}(t) \approx \tilde{\mathbf{q}}(t) = \Phi \hat{\mathbf{q}}(t)$$

The diagram shows three vertical bars representing unknowns. The first is a tall black bar, the second is a shorter grey bar, and the third is a very short green bar. This illustrates the reduction of the number of unknowns.

Apply hyper-reduction and minimize residual

$$\text{minimize}_{\hat{\mathbf{v}}} \|\mathbf{A} \mathbf{r}^n(\Phi \hat{\mathbf{v}}; \mu)\|_2$$

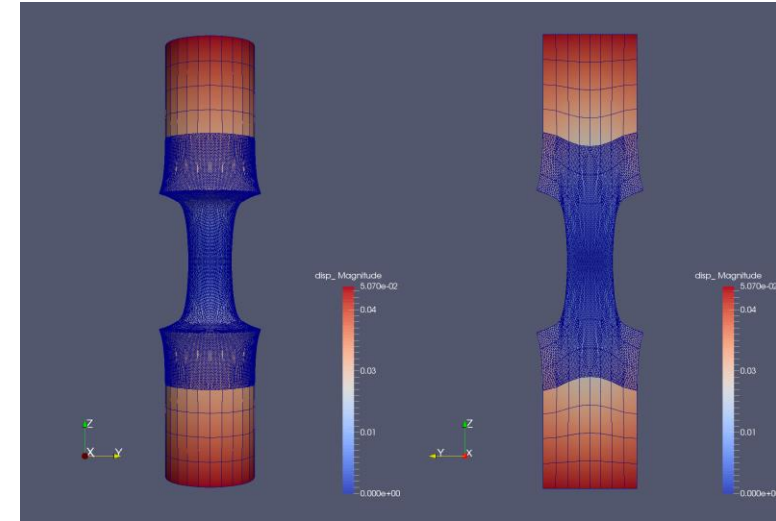


The diagram shows a purple rectangular matrix \mathbf{A} multiplied by a vector $\mathbf{r}^n(\Phi \hat{\mathbf{v}}; \mu)$. The result is a vector with a black bar, a grey bar, and a red bar, representing the residual.

HROM = Hyper-reduced ROM

1. Schwarz Alternating Method for Coupling of Full Order Models (FOMs) in Solid Mechanics

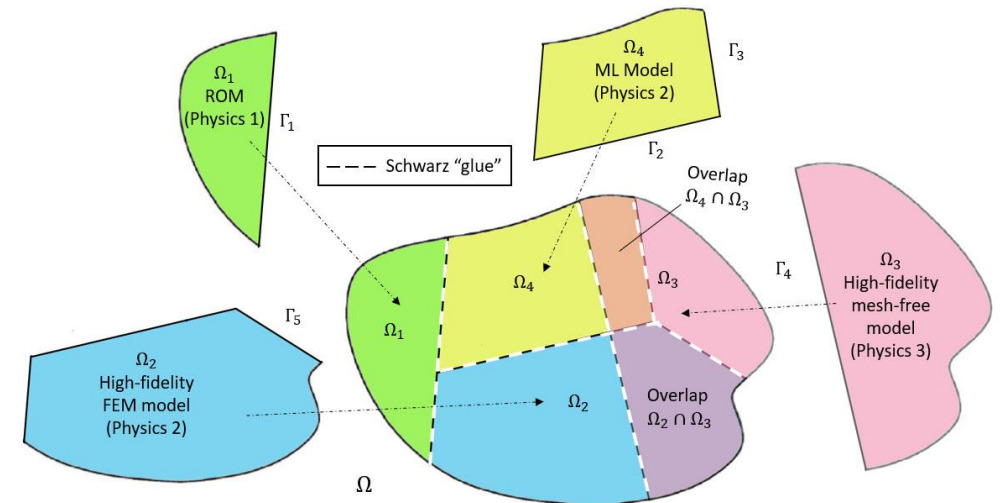
- Motivation & Background
- Quasistatic Formulation
 - Numerical Examples
- Extension to Dynamics
 - Numerical Examples



2. Schwarz Alternating Method for FOM-ROM* and ROM-ROM Coupling

- Motivation & Background
- Formulation
- Numerical Examples

3. Summary and Future Work



* Projection-based Reduced Order Model

Choice of domain decomposition

- **Overlapping vs. non-overlapping** domain decomposition?
 - Non-overlapping more flexible but typically requires more Schwarz iterations
- **FOM vs. ROM** subdomain assignment?
 - Do not assign ROM to subdomains where they have no hope of approximating solution

Snapshot collection and reduced basis construction

- Are subdomains **simulated independently** in each subdomains or together?

Enforcement of boundary conditions (BCs) in ROM at Schwarz boundaries

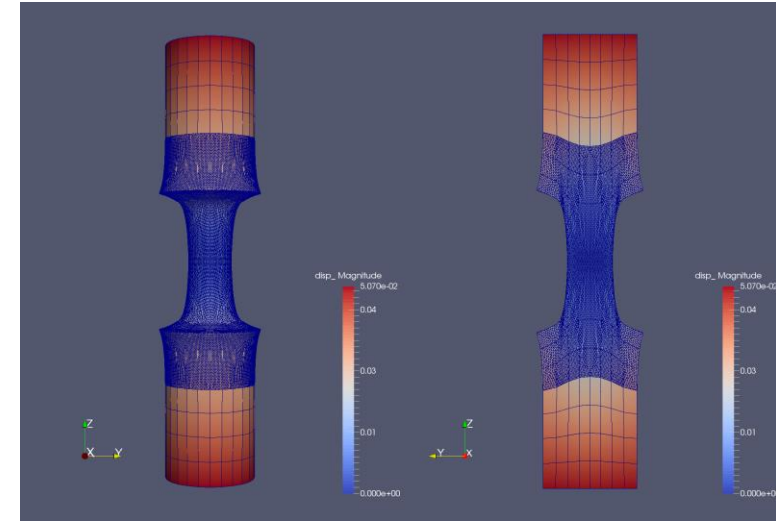
- **Strong vs. weak** BC enforcement?
 - Strong BC enforcement difficult for some models (e.g., cell-centered finite volume, PINNs)
- **Optimizing parameters** in Schwarz BCs for non-overlapping Schwarz?

Choice of hyper-reduction

- What **hyper-reduction** method to use?
 - Application may require particular method (e.g., ECSW for solid mechanics problems)
- How to **sample Schwarz boundaries** in applying hyper-reduction?
 - Need to have enough sample mesh points at Schwarz boundaries to apply Schwarz

1. Schwarz Alternating Method for Coupling of Full Order Models (FOMs) in Solid Mechanics

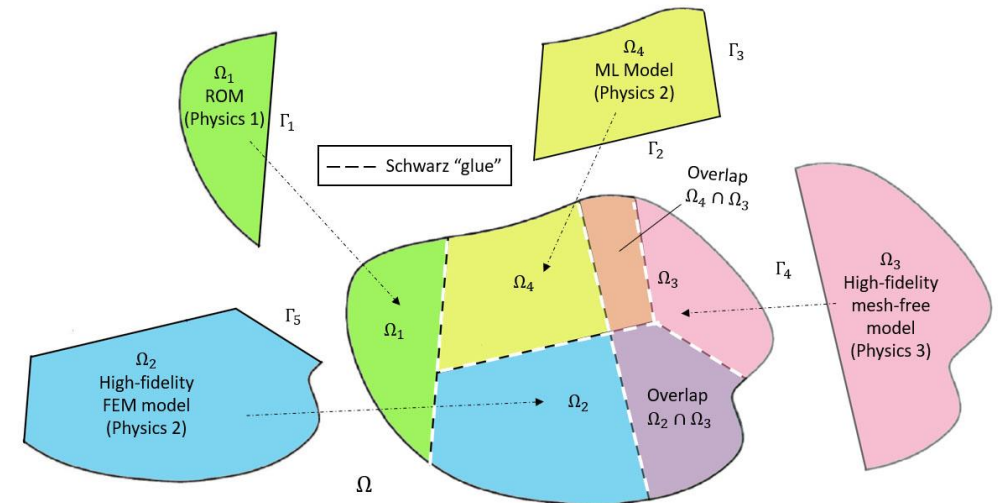
- Motivation & Background
- Quasistatic Formulation
 - Numerical Examples
- Extension to Dynamics
 - Numerical Examples



2. Schwarz Alternating Method for FOM-ROM* and ROM-ROM Coupling

- Motivation & Background
- Formulation
- Numerical Examples

3. Summary and Future Work



* Projection-based Reduced Order Model

2D Inviscid Burgers Equation



Popular analog for fluid problems where **shocks** are possible, and particularly **difficult** for conventional projection-based ROMs

$$\begin{aligned} \frac{\partial u}{\partial t} + \frac{1}{2} \left(\frac{\partial(u^2)}{\partial x} + \frac{\partial(uv)}{\partial y} \right) &= 0.02 \exp(\mu_2 x) \\ \frac{\partial v}{\partial t} + \frac{1}{2} \left(\frac{\partial(vu)}{\partial x} + \frac{\partial(v^2)}{\partial y} \right) &= 0 \\ u(0, y, t; \boldsymbol{\mu}) &= \mu_1 \\ u(x, y, 0) = v(x, y, 0) &= 1 \end{aligned}$$

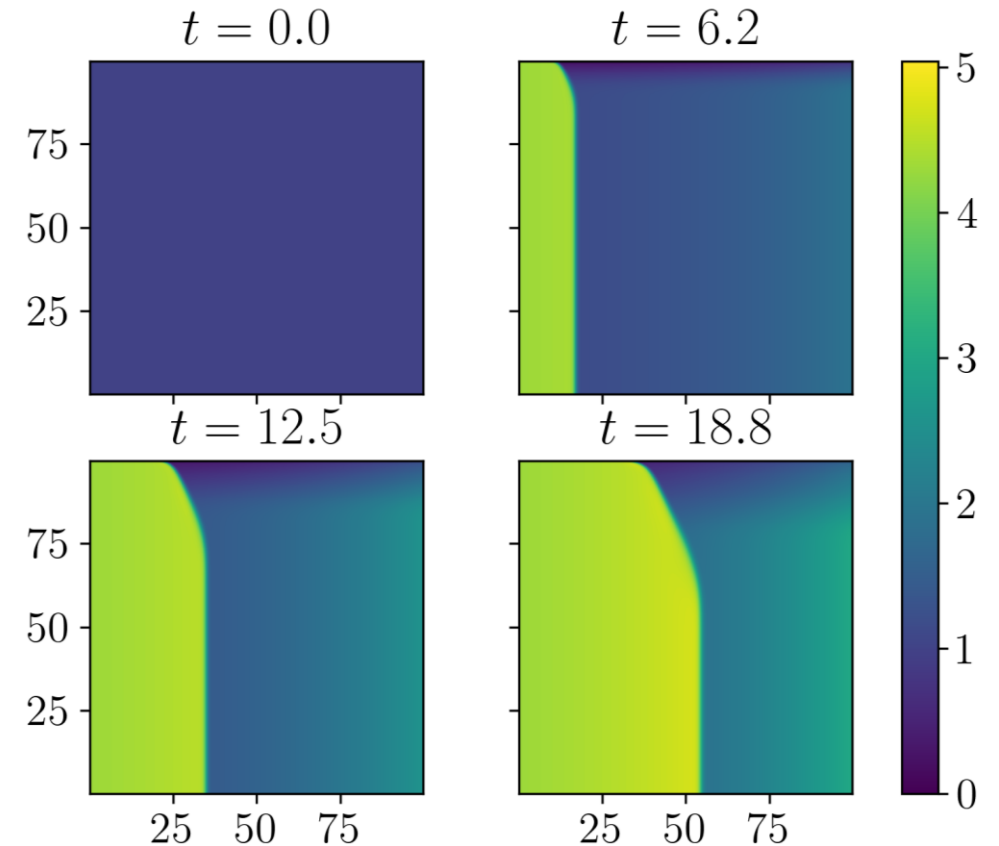
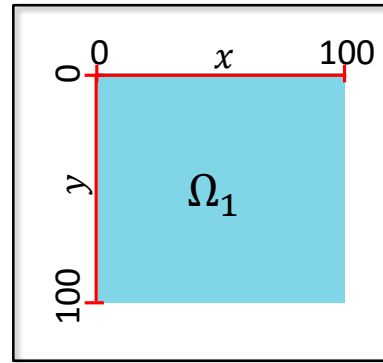


Figure above: solution of u component at various times

Problem setup:

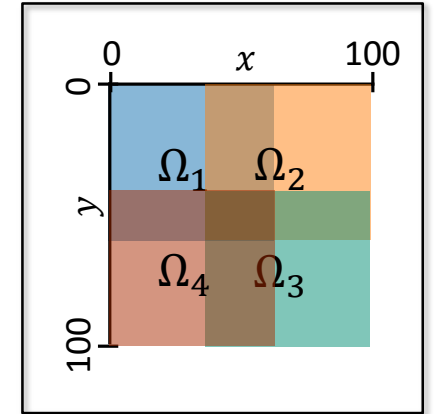
- $\Omega = (0, 100)^2$, $t \in [0, 25]$
- Two parameters $\boldsymbol{\mu} = (\mu_1, \mu_2)$. **Training:** uniform sampling of $\boldsymbol{\mu} \in [4.25, 5.50] \times [0.015, 0.03]$ by a 3×3 grid. **Testing:** query unsampled point $\boldsymbol{\mu} = [4.75, 0.02]$

FOM discretization:

- Spatial discretization given by a **Godunov-type scheme** with $N = 250$ elements in each dimension
- Implicit **trapezoidal method** with fixed $\Delta t = 0.05$

Choice of domain decomposition

- Overlapping DD of Ω into 4 subdomains coupled via multiplicative Schwarz
- Solution in Ω_1 is most difficult to capture by ROM



Snapshot collection and reduced basis construction

- Single-domain FOM on Ω used to generate snapshots/POD modes

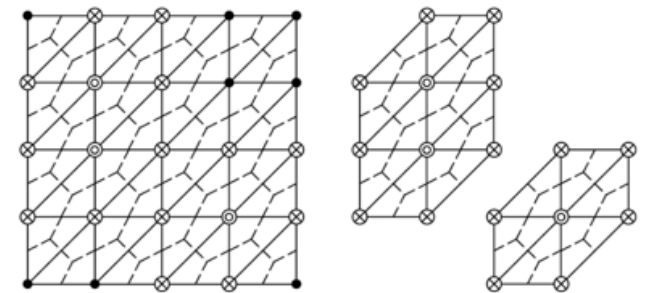
Enforcement of boundary conditions (BCs) in ROM at Schwarz boundaries

- BCs imposed strongly using Method 1 of [Gunzburger *et al.*, 2007] at indices i_{Dir}

$$\mathbf{q}(t) \approx \bar{\mathbf{q}} + \Phi \hat{\mathbf{q}}(t)$$

- POD modes made to satisfy homogeneous DBCs: $\Phi(\mathbf{i}_{\text{Dir}}, :) = \mathbf{0}$

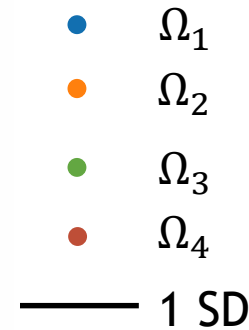
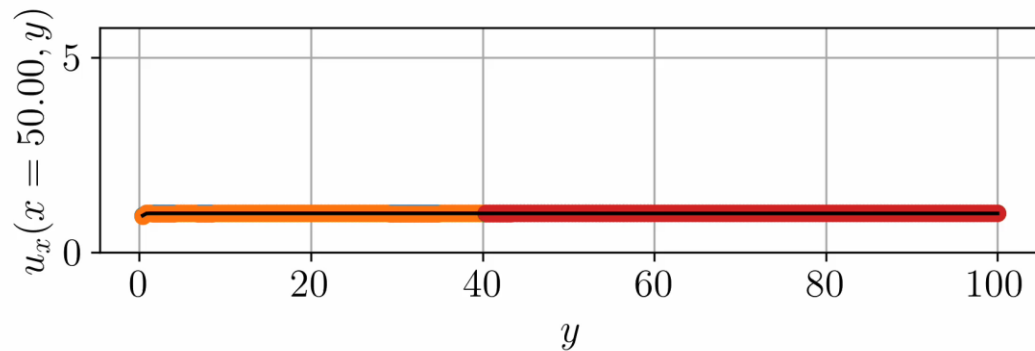
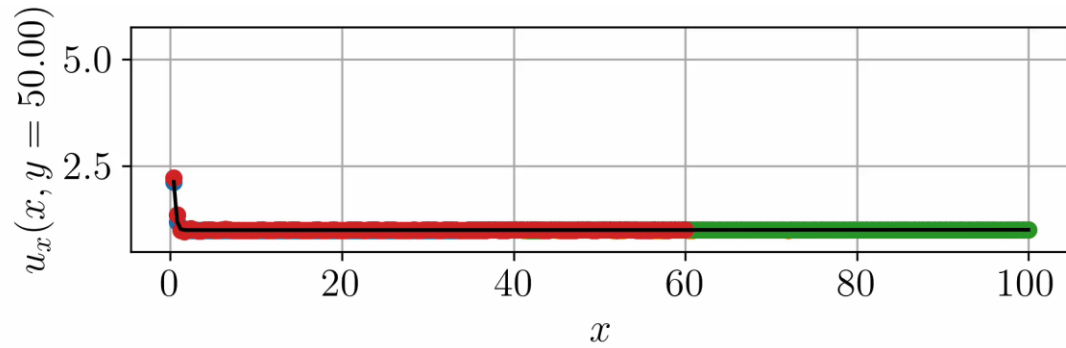
- BCs imposed by modifying $\bar{\mathbf{q}}$: $\bar{\mathbf{q}}(\mathbf{i}_{\text{Dir}}) \leftarrow \chi_q$



Choice of hyper-reduction

- Energy Conserving Sampling & Weighting (ECSW) method for hyper-reduction
- All points on Schwarz boundaries are included in the sample mesh

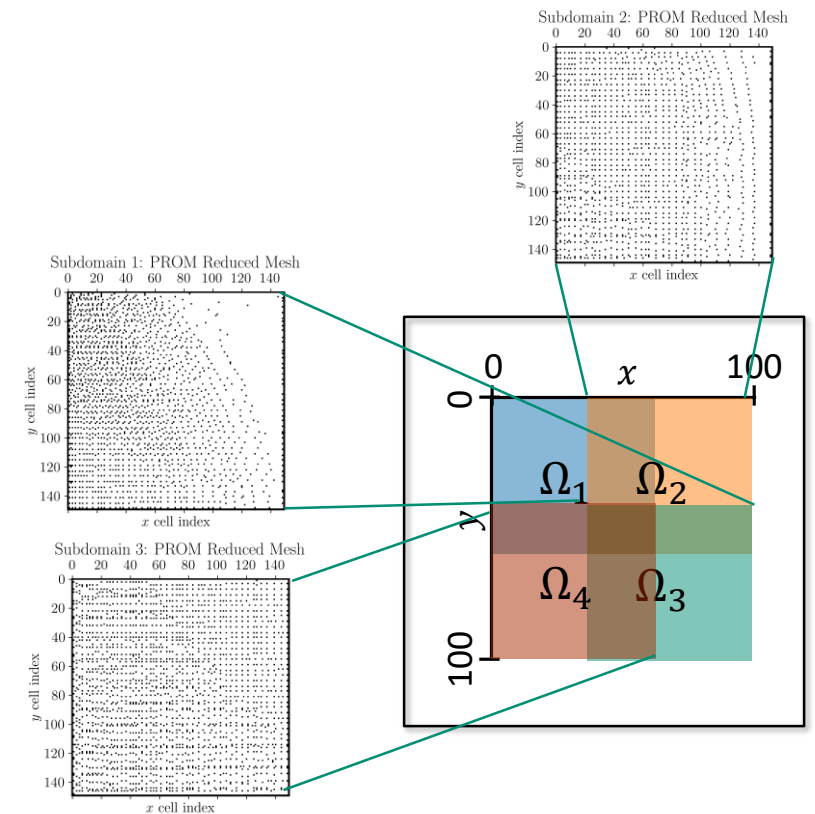
FOM-HROM-HROM-HROM Coupling



- FOM in Ω_1 as this is “hardest” subdomain for ROM
- HROMs in $\Omega_2, \Omega_3, \Omega_4$ capture 99% snapshot energy
- Method converges in 3 Schwarz iterations per controller time-step
- Errors $O(0.1\%)$ with 0 error in Ω_1
- $2.26\times$ speedup achieved over all-FOM coupling

Further speedups possible via code optimizations, additive Schwarz and reduction of # sample mesh points.

Subdomains	99% SV Energy		
	M	MSE (%)	CPU time (s)
Ω_1	—	0.0	95
Ω_2	120	0.26	26
Ω_3	60	0.43	17
Ω_4	66	0.34	21
Total			159



2D Shallow Water Equations (SWE)



Hyperbolic PDEs modeling **wave propagation** below a pressure surface in a fluid (e.g., atmosphere, ocean).

$$\frac{\partial h}{\partial t} + \frac{\partial(hu)}{\partial x} + \frac{\partial(hv)}{\partial y} = 0$$

$$\frac{\partial(hu)}{\partial t} + \frac{\partial}{\partial x} \left(hu^2 + \frac{1}{2}gh^2 \right) + \frac{\partial}{\partial y} (huv) = -\mu v$$

$$\frac{\partial(hv)}{\partial t} + \frac{\partial}{\partial x} (huv) + \frac{\partial}{\partial y} \left(hv^2 + \frac{1}{2}gh^2 \right) = \mu u$$

Problem setup:

- $\Omega = (-5,5)^2$, $t \in [0, 10]$, Gaussian initial condition
- **Coriolis parameter** $\mu \in \{-4, -3, -2, -1, 0\}$ for training, and $\mu \in \{-3.5, -2.5, -1.5, -0.5\}$ for testing

FOM discretization:

- Spatial discretization given by a first-order **cell-centered finite volume** discretization with $N = 300$ elements in each dimension
- Implicit first order temporal discretization: **backward Euler** with fixed $\Delta t = 0.01$
- Implemented in **Pressio-demoapps** (<https://github.com/Pressio/pressio-demoapps>)

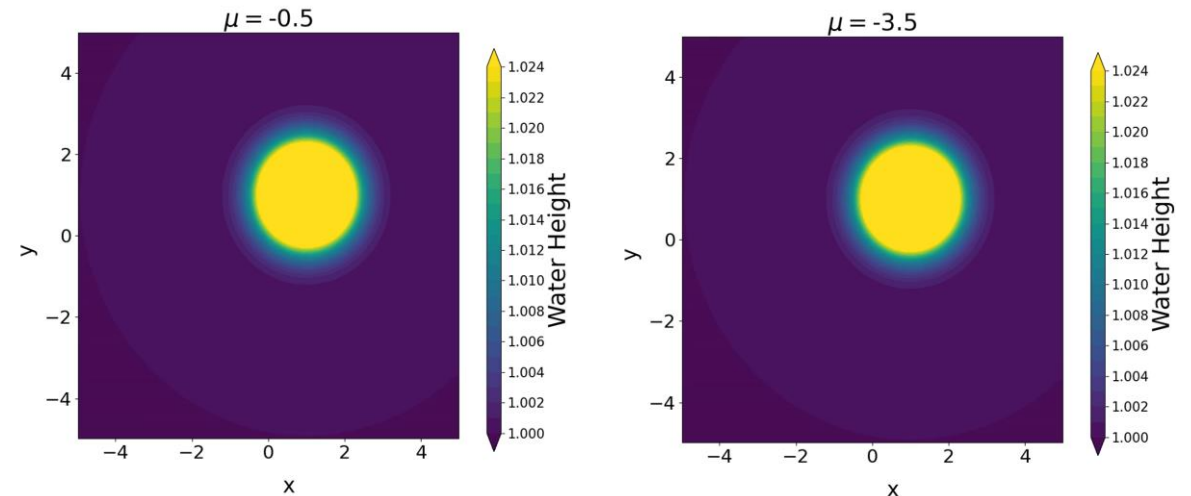


Figure above: FOM solutions to SWE for $\mu = -0.5$ (left) and $\mu = -3.5$ (right).

Schwarz Coupling Details

Green: different from Burgers' problem

Choice of domain decomposition

- **Non-overlapping** DD of Ω into 4 subdomains coupled via **additive Schwarz**
 - **OpenMP parallelism** with 1 thread/subdomain
- **All-ROM** or **All-HROM** coupling via Pressio*

Snapshot collection and reduced basis construction

- **Single-domain FOM** on Ω used to generate snapshots/POD modes

Enforcement of boundary conditions (BCs) in ROM at Schwarz boundaries

- BCs are imposed **approximately** by fictitious ghost cell states
 - Implementing Neumann and Robin BCs is **challenging**
- **Ghost cells** introduce some overlap even with non-overlapping DD
 - \Rightarrow **Dirichlet-Dirichlet non-overlapping Schwarz is stable/convergent!**

Choice of hyper-reduction

- **Collocation** for hyper-reduction: min residual at small subset DOFs
- Assume **fixed budget of sample mesh points** at Schwarz boundaries

*<https://github.com/Pressio/pressio-demoapps>

Figure right: non-overlapping DD w/ ghost cells creating overlap

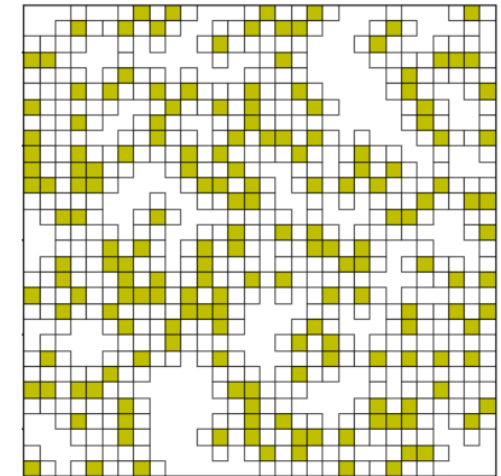
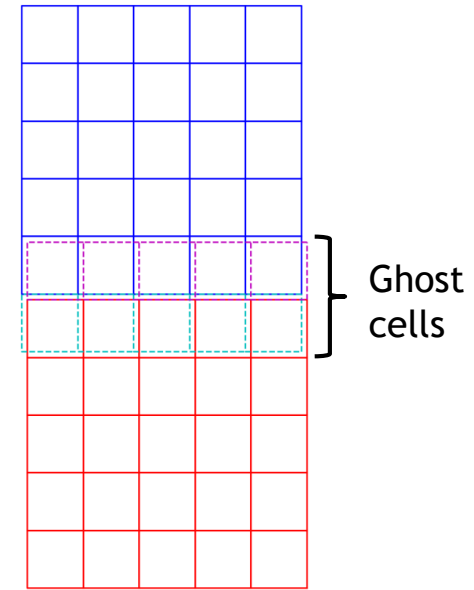
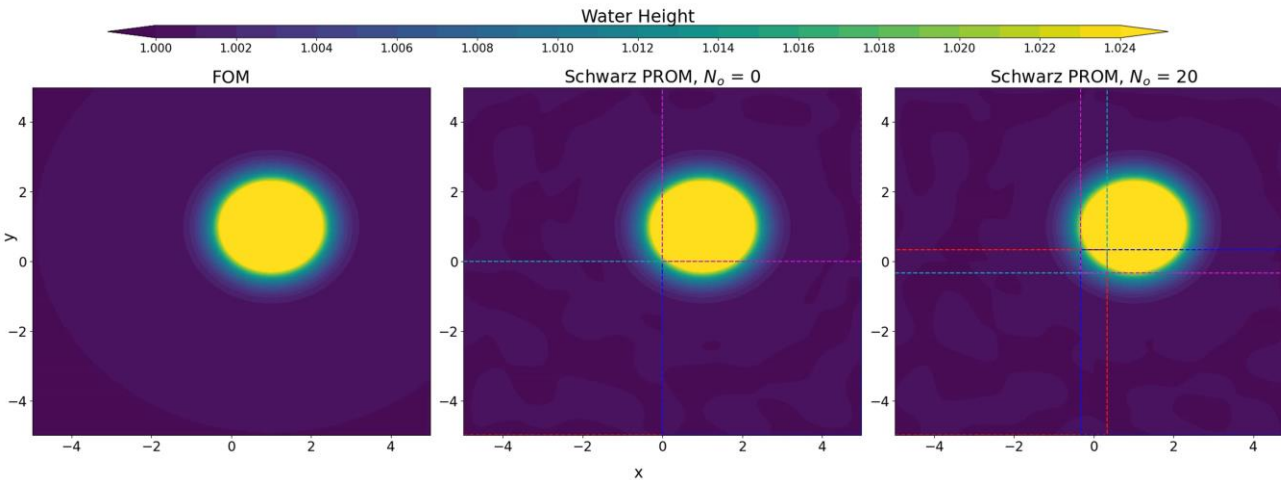


Figure above: sample mesh (yellow) and stencil (white) cells

Schwarz All-ROM Domain Overlap Study



Study of Schwarz convergence for all-ROM coupling as a function of $N_o :=$ cell width of overlap region (not including ghost cells).

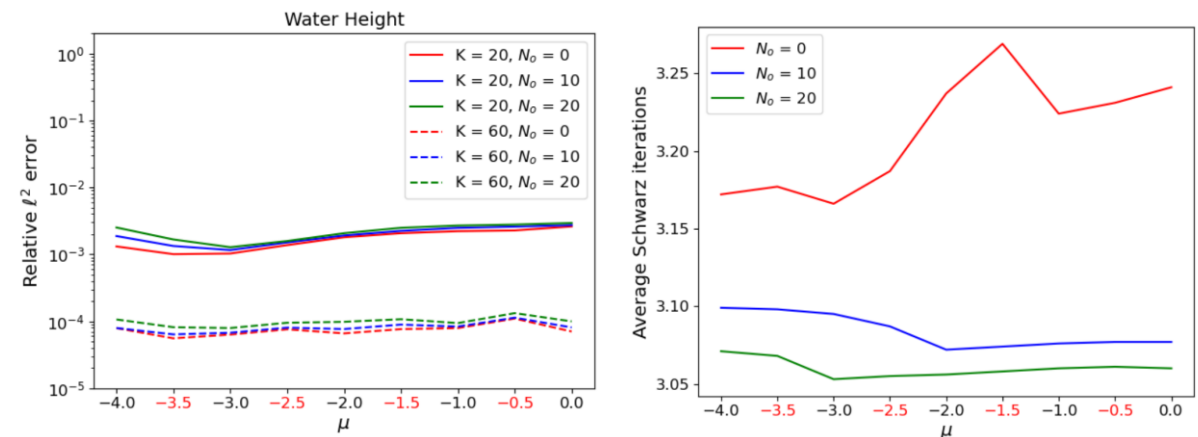


Movie above: FOM (left), 4 subdomain ROM coupled via non-overlapping Schwarz (middle), and 4 subdomain ROM coupled via overlapping Schwarz (right) for predictive SWE problem with $\mu = -0.5$. All ROMs have $K = 80$ POD modes.

- Schwarz iterations decrease (very roughly) with $N_o^{0.25}$ (figure, right) whereas evaluating $r(q)$ scales with N_o^2

➤ \Rightarrow there is no reason not to do **non-overlapping coupling** for this problem

- Dirichlet-Dirichlet coupling with **no-overlap** ($N_o = 0$) performs well with **no convergence issues** (movie, left) and **errors comparable to Dirichlet-Dirichlet coupling with overlap** (figure below, left)



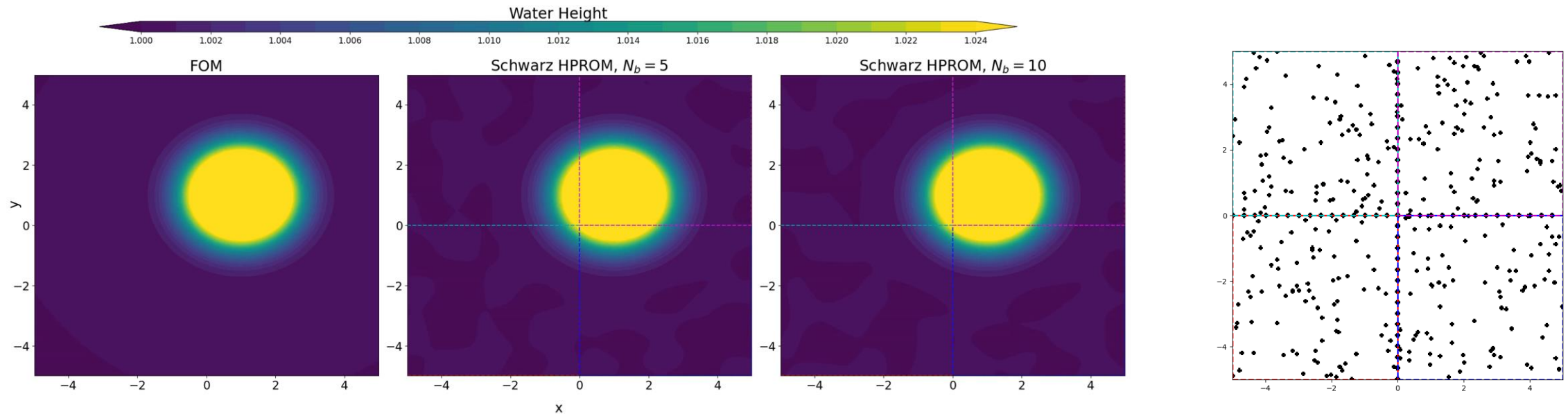
Figures above: relative error and average # Schwarz iterations as a function of μ and N_o . Black μ : training, red μ : testing.

Schwarz Boundary Sampling for All-HROM Coupling



Key question: how many Schwarz boundary points need to be included in **sample mesh** when performing HROM coupling?

- Naïve/sparse-sampled Schwarz boundary results in **failure** to transmit coupling information during Schwarz

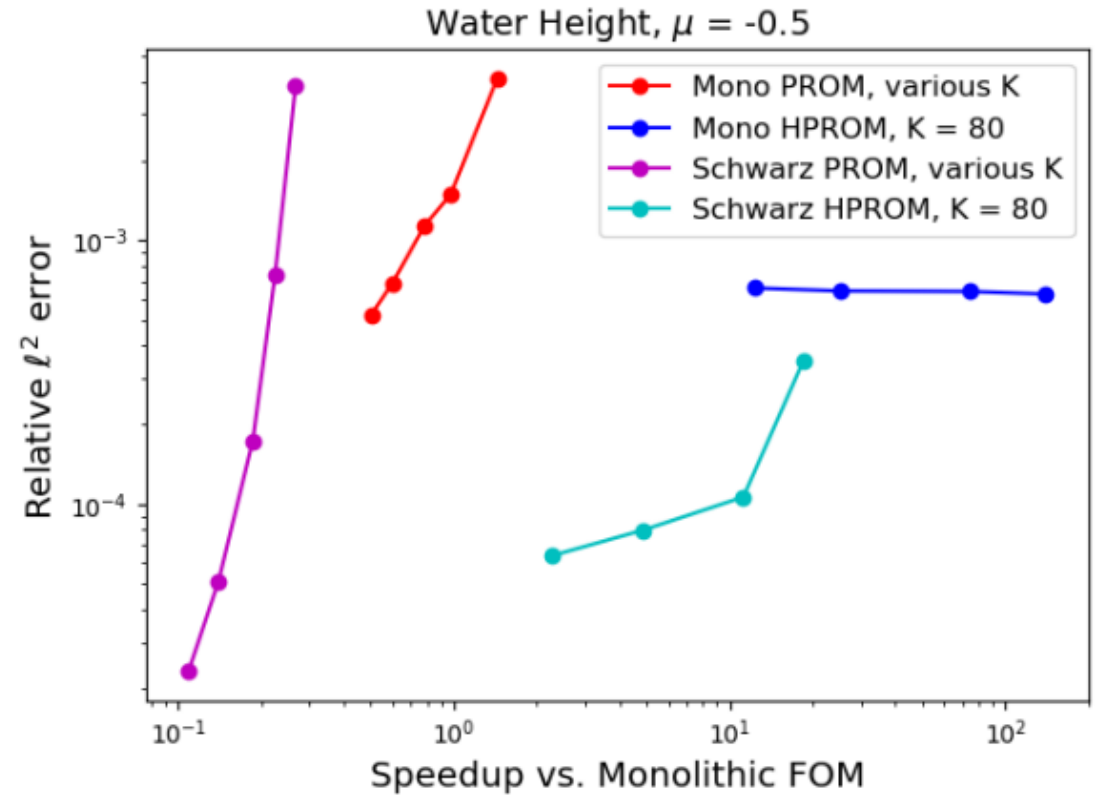
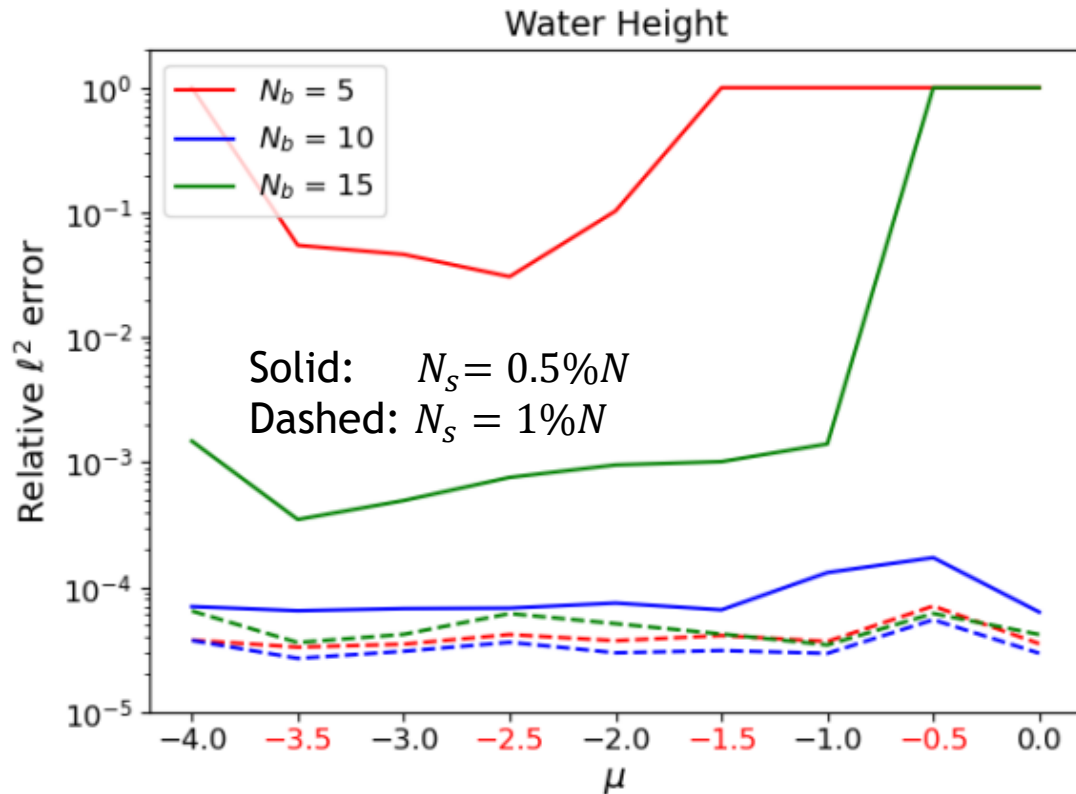


Movie above: FOM (left), all HROM with $N_b = 5\%$ (middle) and all HROM with $N_b = 10\%$ (left). ROMs have $K = 100$ modes and $N_s = 0.5\%N$ sample mesh points.

Figure above: example sample mesh with sampling rate $N_b = 10\%$

- Including too many Schwarz boundary points (N_b) in sample mesh given fixed budget of N_s sample mesh points may lead to too few sample mesh points in interior
- For SWE problem, we can get away with $\sim 10\%$ boundary sampling (movie above, right-most frame)

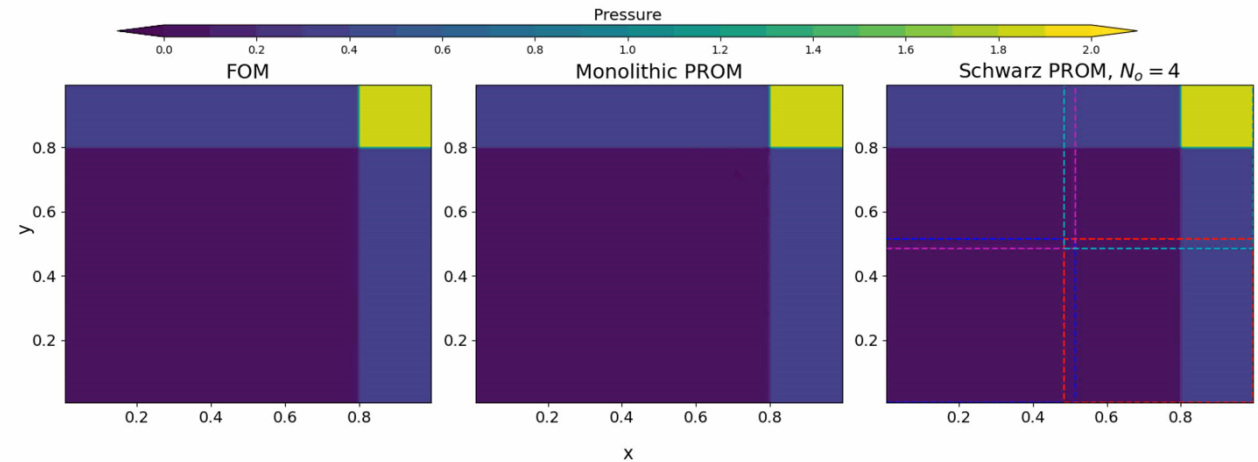
Coupled HRROM Performance



- For a fixed ROM dimension, Schwarz delivers **lower error and comparable cost!**
- There are noticeable **cost savings** relative to monolithic FOM!
- Accuracy similar for **predictive μ** (red) and **non-predictive μ** (black) cases.

$$\frac{\partial}{\partial t} \begin{pmatrix} \rho \\ \rho u \\ \rho v \\ \rho E \end{pmatrix} + \frac{\partial}{\partial x} \begin{pmatrix} \rho u \\ \rho u^2 + p \\ \rho uv \\ (E + p)u \end{pmatrix} + \frac{\partial}{\partial y} \begin{pmatrix} \rho v \\ \rho uv \\ \rho v^2 + p \\ (E + p)v \end{pmatrix} = \mathbf{0}$$

$$p = (\gamma - 1) \left(\rho E - \frac{1}{2} \rho (u^2 + v^2) \right)$$



Problem setup:

- $\Omega = (0,1)^2$, $t \in [0, 0.8]$, homogeneous Neumann BCs
- Fix $\rho_1 = 1.5$, $u_1 = v_1 = 0$, $p_3 = 0.029$
- Vary p_1 ; IC from compatibility conditions*
 - Training: $p_1 \in [1.0, 1.25, 1.5, 1.75, 2.0]$
 - Testing: $p_1 \in [1.125, 1.375, 1.625, 1.875]$

FOM discretization:

- Spatial discretization given by a first-order **cell-centered finite volume** discretization with $N = 300$ or $N = 100$ elements in each dimension
- Implicit first order temporal discretization: **backward Euler** with fixed $\Delta t = 0.005$
- Implemented in **Pressio-demoapps** (<https://github.com/Pressio/pressio-demoapps>)

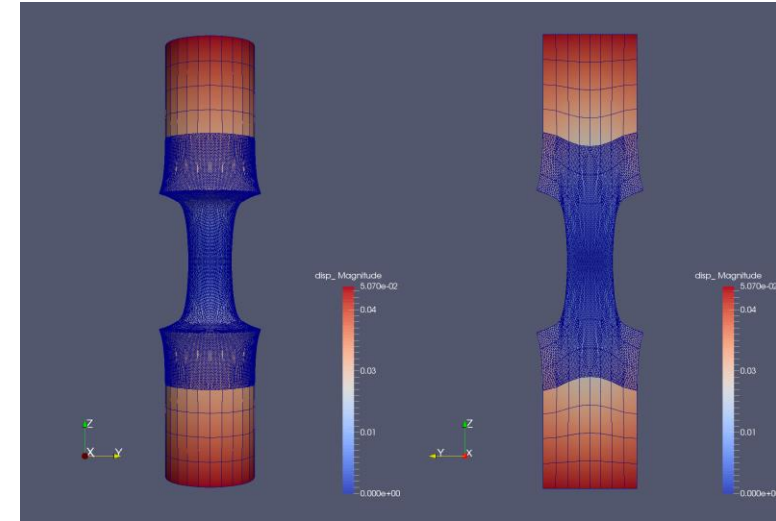
Preliminary results:

- Schwarz can **stabilize** unstable monolithic ROM for fixed dimension K (above)
- Since shock traverses all parts of domain, achieving **speedups** with Schwarz is **more difficult**

*Schulz-Rinne, 1993.

1. Schwarz Alternating Method for Coupling of Full Order Models (FOMs) in Solid Mechanics

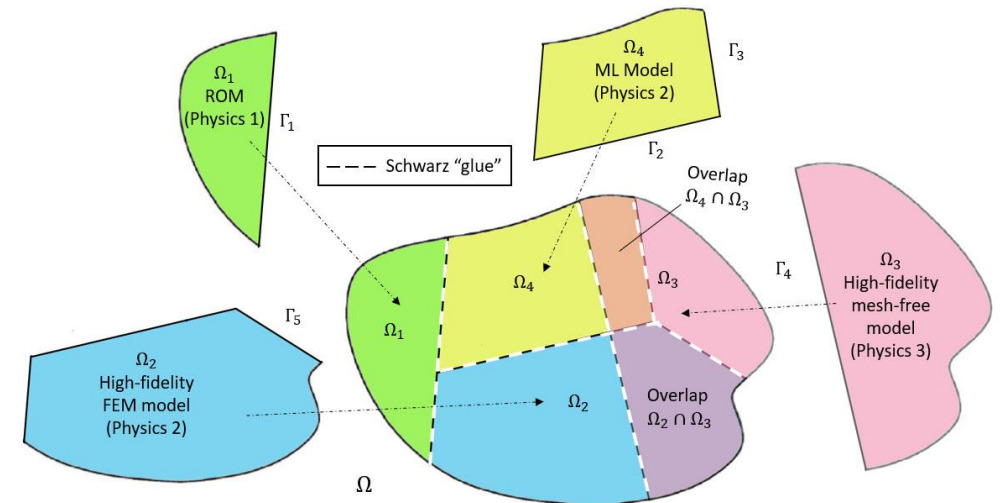
- Motivation & Background
- Quasistatic Formulation
 - Numerical Examples
- Extension to Dynamics
 - Numerical Examples



2. Schwarz Alternating Method for FOM-ROM* and ROM-ROM Coupling

- Motivation & Background
- Formulation
- Numerical Examples

3. Summary and Future Work



* Projection-based Reduced Order Model

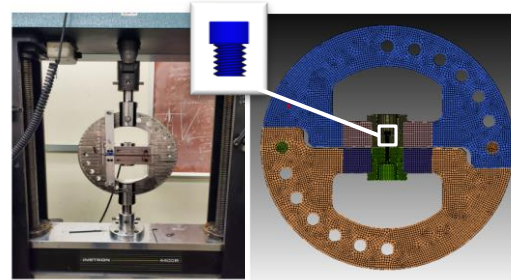


The **Schwarz alternating method** has been developed for concurrent multi-scale coupling of **conventional** and **data-driven models**.

- ☺ Coupling is *concurrent* (two-way).
- ☺ *Ease of implementation* into existing massively-parallel HPC codes.
- ☺ “*Plug-and-play*” *framework*: simplifies task of meshing complex geometries!
 - ☺ Ability to couple regions with *different non-conformal meshes*, *different element types* and *different levels of refinement*.
 - ☺ Ability to use *different solvers (including ROM/FOM)* and *time-integrators* in different regions.
- ☺ *Scalable, fast, robust* on *real* engineering problems
- ☺ Coupling does not introduce *nonphysical artifacts*.
- ☺ *Theoretical* convergence properties/guarantees.

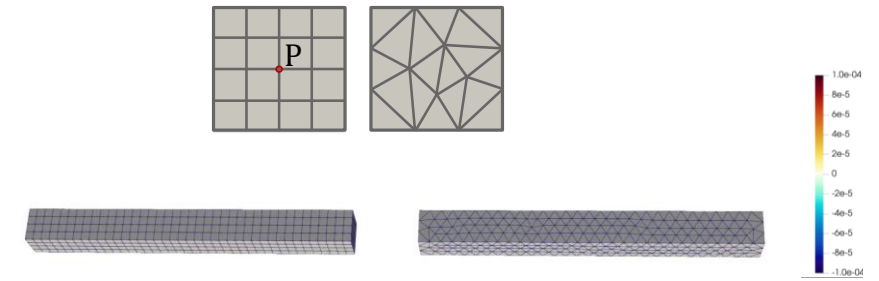
Ongoing & Future Work

- Development fundamentally new approach for simulating multi-scale mechanical contact using the Dirichlet-Neumann Schwarz alternating method
 - Contact constraints are replaced with boundary conditions applied iteratively at contact boundaries
- Implementation of non-overlapping Schwarz in Sierra/SM
- Working with analysts to apply Schwarz to problems of interest to Sandia missions
 - Laser welds
 - Fastener modeling for joints
 - Salt caverns for oil storage
- Rigorous analysis of why Dirichlet-Dirichlet BC “work” when employing non-overlapping Schwarz with discretizations that employ ghost cells
- Extension to coupling of non-intrusive ROMs (dynamic mode decomposition, operator inference, neural networks)
- Development of automated criteria to determine appropriate use of less refined or reduced-order models w/o sacrificing accuracy, enabling real-time transitions between different model fidelities

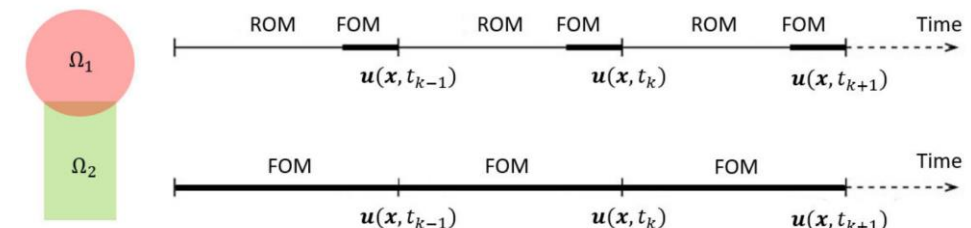
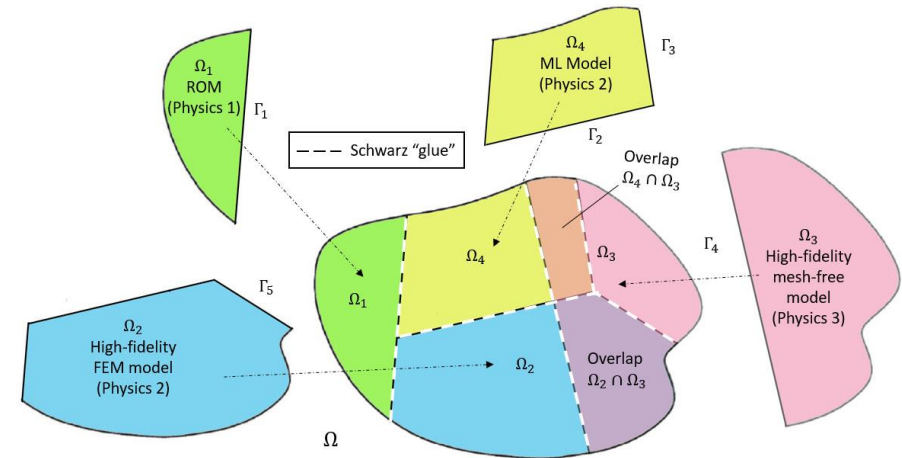


From Murugesan *et al.*, 2020.

Contact boundaries Γ^1 and Γ^2



Impact of two 3D beams having different meshes with Schwarz contact method. From [Mota *et al.*, 2023].



Team & Acknowledgments



Irina Tezaur



Joshua Barnett



Alejandro Mota



Chris Wentland



Francesco Rizzi



Coleman Alleman



Greg Phlipot





- [1] A. Mota, I. Tezaur, C. Alleman. “The Schwarz Alternating Method in Solid Mechanics”, *Comput. Meth. Appl. Mech. Engng.* 319 (2017), 19-51.
- [2] A. Mota, I. Tezaur, G. Phlipot. “The Schwarz Alternating Method for Dynamic Solid Mechanics”, *Comput. Meth. Appl. Mech. Engng.* 121 (21) (2022) 5036-5071.
- [3] J. Barnett, I. Tezaur, A. Mota. “The Schwarz alternating method for the seamless coupling of nonlinear reduced order models and full order models”, ArXiv pre-print, 2022.
<https://arxiv.org/abs/2210.12551>
- [4] W. Snyder, I. Tezaur, C. Wentland. “Domain decomposition-based coupling of physics-informed neural networks via the Schwarz alternating method”, ArXiv pre-print, 2023.
<https://arxiv.org/abs/2311.00224>
- [5] A. Mota, D. Koliesnikova, I. Tezaur. “A Fundamentally New Coupled Approach to Contact Mechanics via the Dirichlet-Neumann Schwarz Alternating Method”, ArXiv pre-print, 2023.
<https://arxiv.org/abs/2311.05643>

Email: ikalash@sandia.gov
URL: www.sandia.gov/~ikalash

Start of Backup Slides

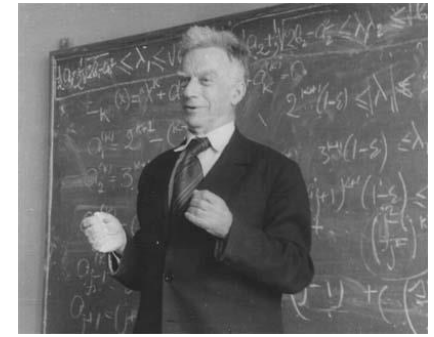
Theoretical Foundation

Using the Schwarz alternating as a *discretization method* for PDEs is natural idea with a sound *theoretical foundation*.

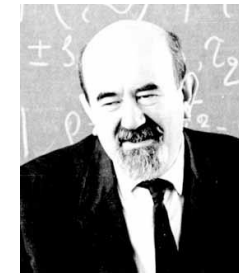
- [S.L. Sobolev \(1936\)](#): posed Schwarz method for *linear elasticity* in variational form and *proved method's convergence* by proposing a convergent sequence of energy functionals.
- [S.G. Mikhlin \(1951\)](#): *proved convergence* of Schwarz method for general linear elliptic PDEs.
- [P.-L. Lions \(1988\)](#): studied convergence of Schwarz for *nonlinear monotone elliptic problems* using max principle.
- [A. Mota, I. Tezaur, C. Alleman \(2017\)](#): proved *convergence* of the alternating Schwarz method for *finite deformation quasi-static nonlinear PDEs* (with energy functional $\Phi[\varphi]$) with a *geometric convergence rate*.

$$\Phi[\varphi] = \int_B A(\mathbf{F}, \mathbf{Z}) dV - \int_B \mathbf{B} \cdot \boldsymbol{\varphi} dV$$

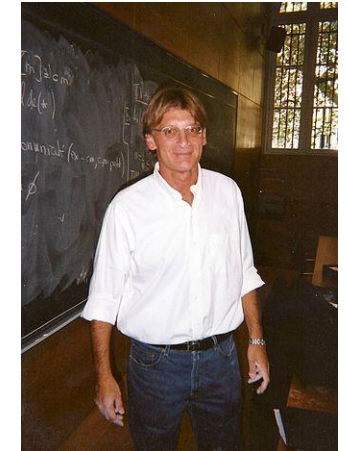
$$\nabla \cdot \mathbf{P} + \mathbf{B} = \mathbf{0}$$



S.L. Sobolev (1908 - 1989)



S.G. Mikhlin
(1908 - 1990)



P.- L. Lions (1956-)



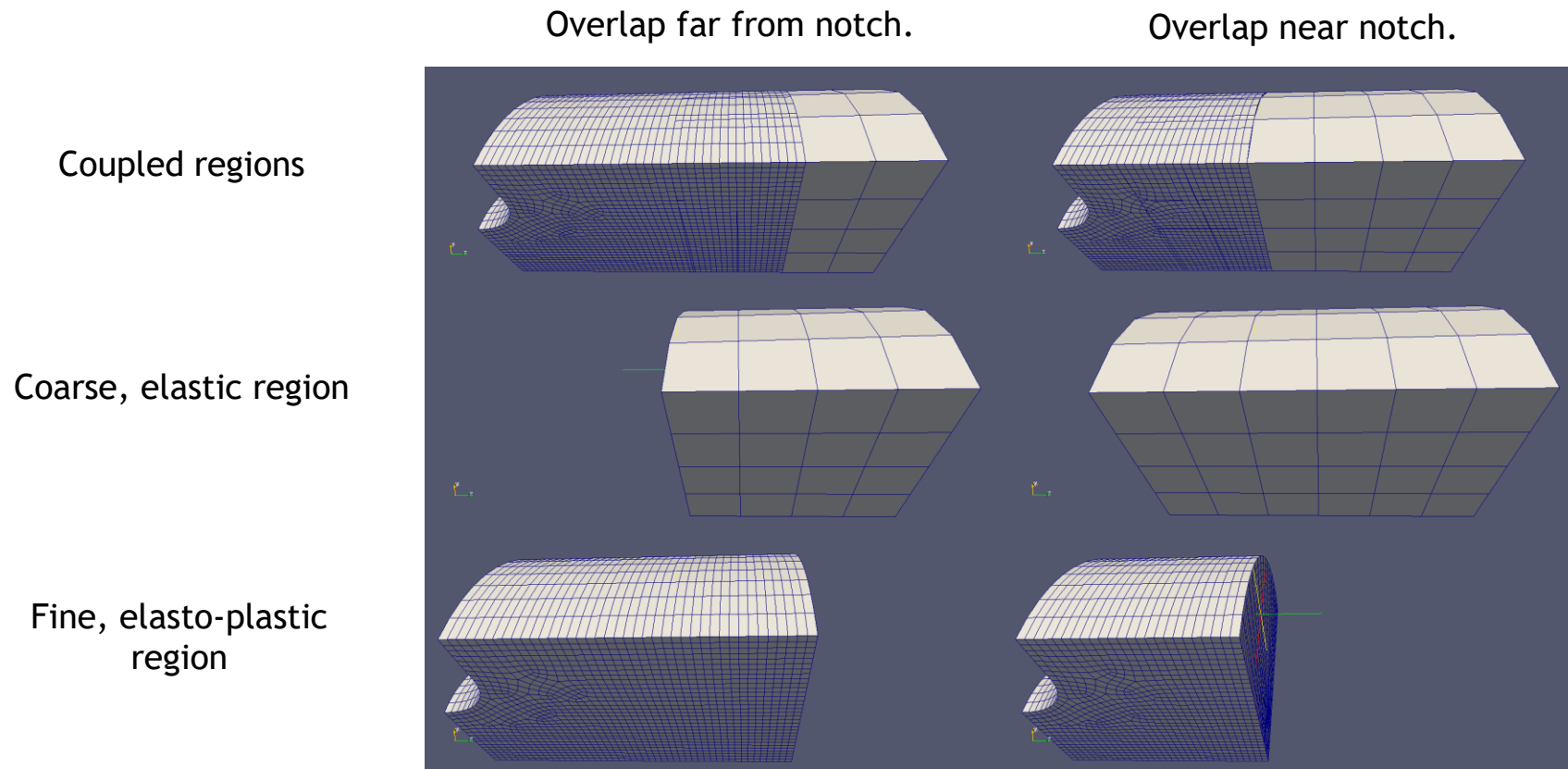
A. Mota, I. Tezaur, C. Alleman

Notched Cylinder: Coupling Different Materials



The Schwarz method is capable of coupling regions with *different material models*.

- Notched cylinder subjected to tensile load with an *elastic* and *J2 elasto-plastic* regions.
- *Coarse* region is *elastic* and *fine* region is *elasto-plastic*.
- The *overlap region* in the first mesh is nearer the notch, where plastic behavior is expected.

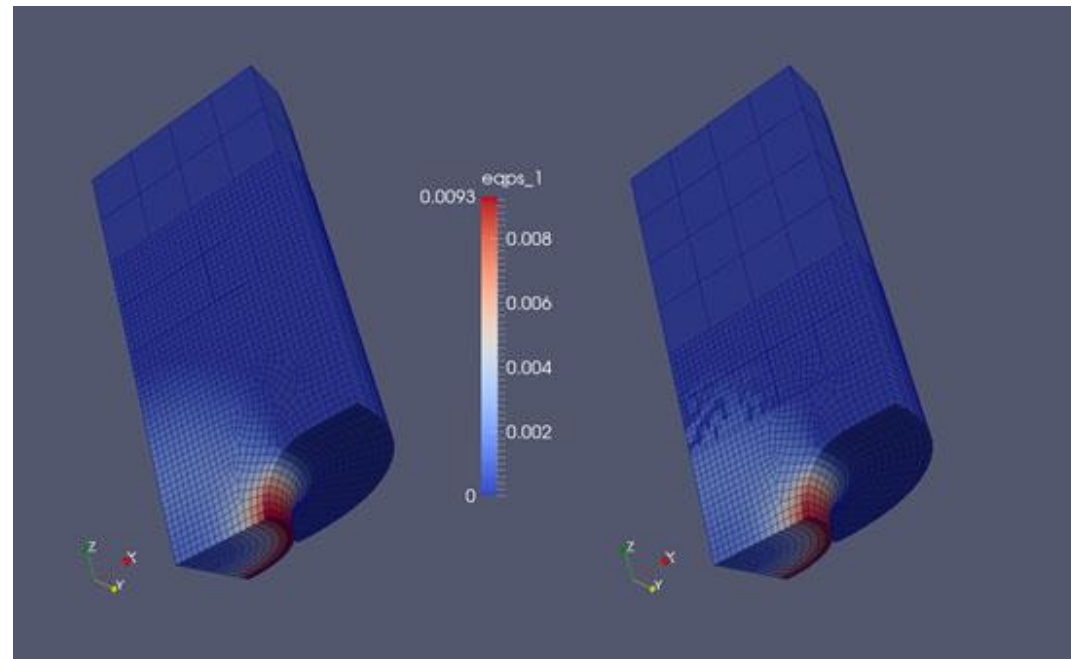


Notched Cylinder: Coupling Different Materials



Need to be careful to do domain decomposition so that material models are *consistent* in overlap region.

- When the *overlap* region is *far from the notch*, no plastic deformation exists in it: the coarse and fine regions predict the *same behavior*.
- When the *overlap* region is *near the notch*, plastic deformation spills onto it and the two models predict different behavior, affecting convergence *adversely*.



Overlap far from notch.

Overlap near notch.

Single Domain Predictive ROM

- **Uniform sampling** of $\mathcal{D} = [4.25, 5.50] \times [0.015, 0.03]$ by a 3×3 grid
 \Rightarrow 9 training parameters characterized by $\Delta\mu_1 = 0.625$, $\Delta\mu_2 = 0.0075$
 - > 200 POD modes required to capture 99% snapshot energy
- Queried but **unsampled parameter point** $\mu = [4.75, 0.02]$
- **Reduced mesh** resulting from solving non-negative least squares problem defining ECSW gives $n_e = 5,689$ elements (9.1% of $N_e = 62,500$ elements).

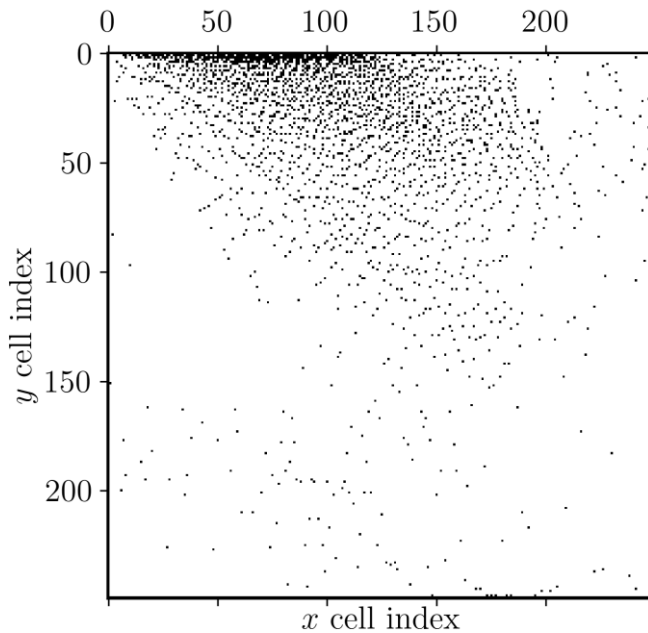
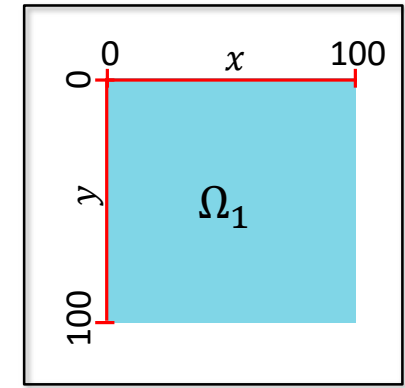


Figure above: Reduced mesh of single domain HROM

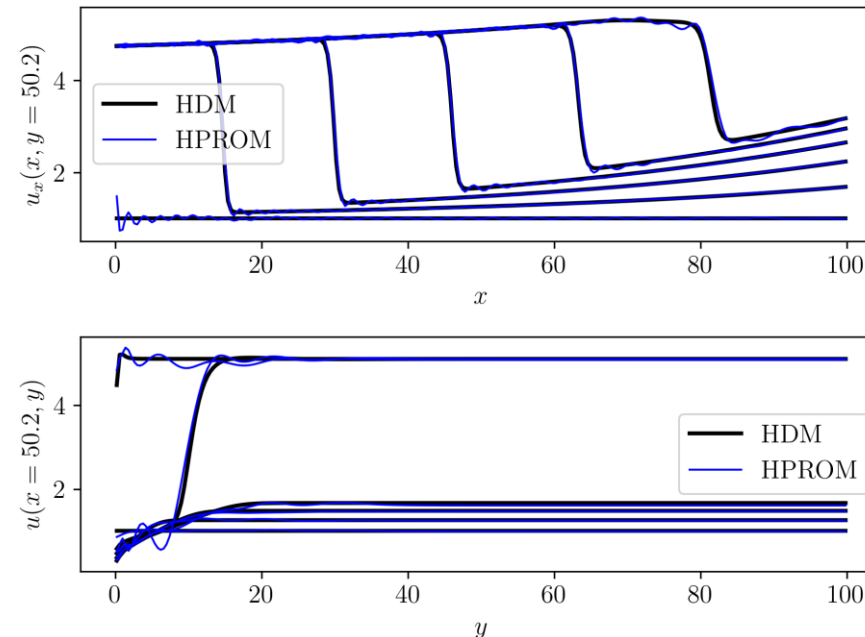
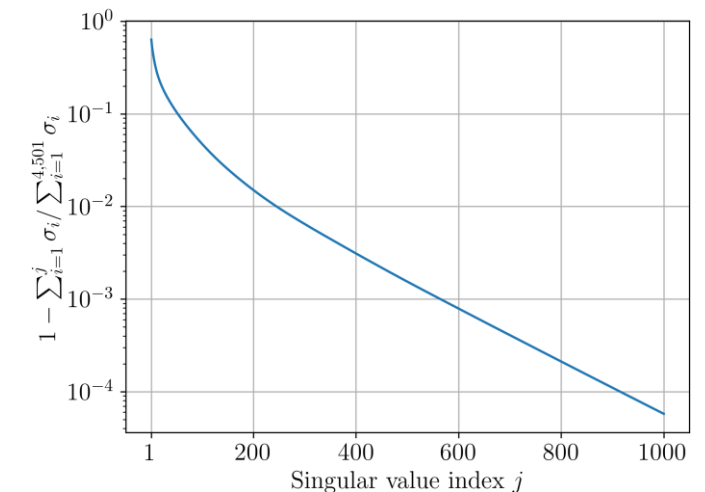
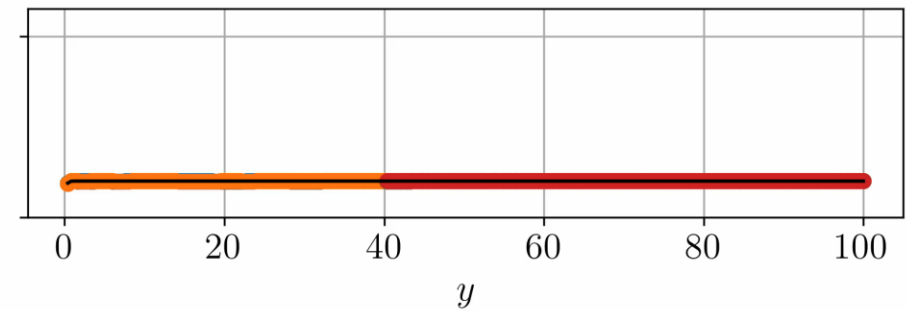
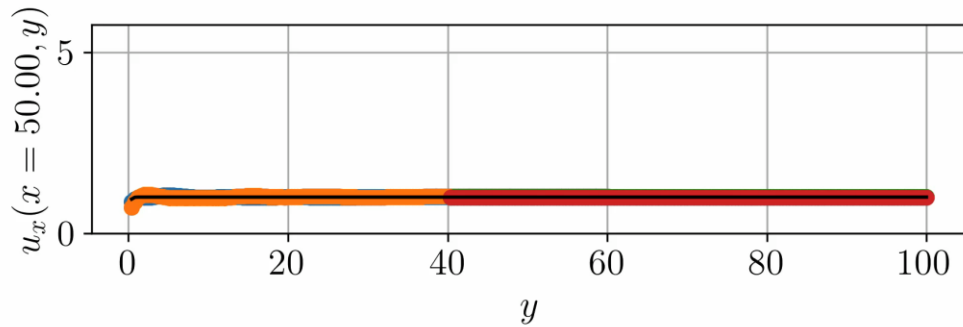
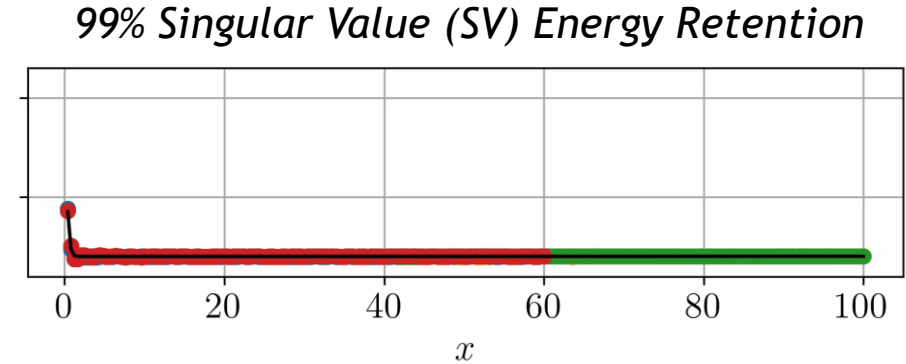
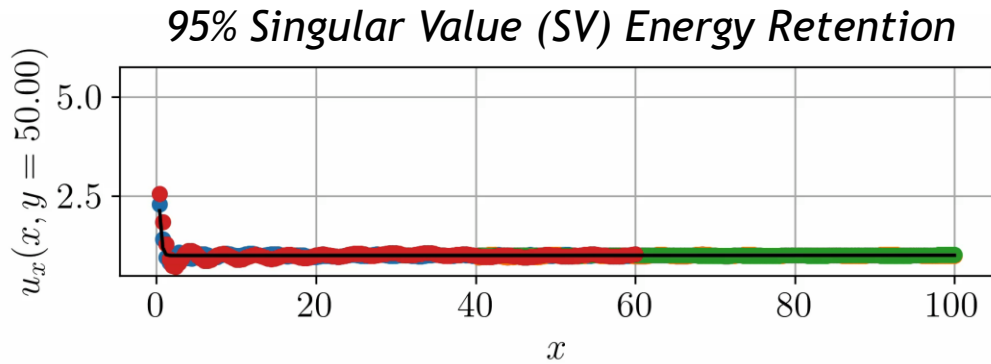
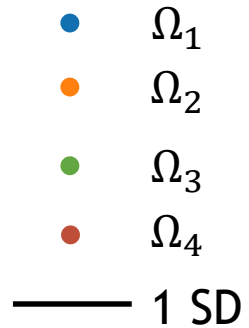


Figure above: HROM and FOM results at various time steps

% SV Energy	M	MSE* (%)	CPU time* (s)
95	69	1.1	138
99	177	0.17	447

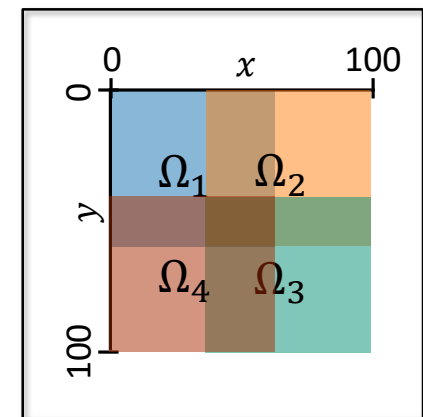
* Numbers in table are w/o hyper-reduction





- Method converges in **only 3 Schwarz iterations** per controller time-step
- Errors $O(1\%)$ or less
- 1.47 \times speedup** over all-FOM coupling for 95% SV energy retention case

Subdomains	95% SV Energy			99% SV Energy		
	M	MSE (%)	CPU time (s)	M	MSE (%)	CPU time (s)
Ω_1	57	1.1	85	146	0.18	295
Ω_2	44	1.2	56	120	0.18	216
Ω_3	24	1.4	43	60	0.16	89
Ω_4	32	1.9	61	66	0.25	100
Total			245			700



Schwarz Boundary Sampling for All-HROM Coupling



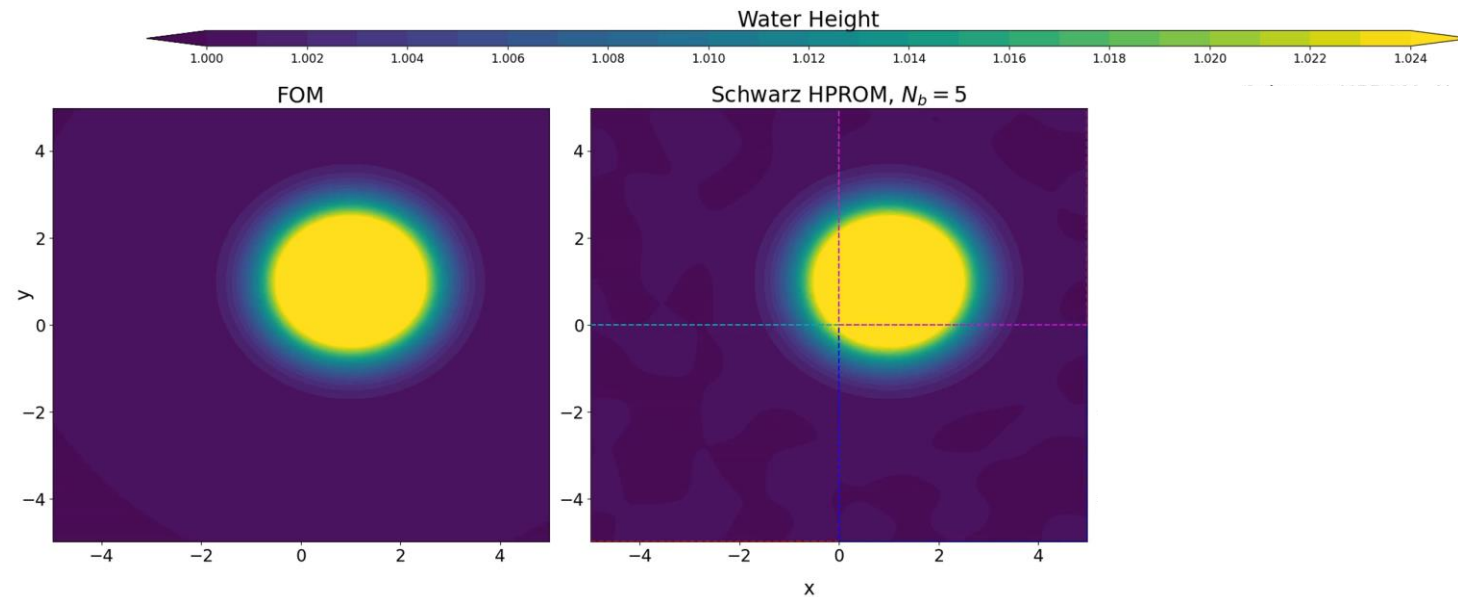
Key question: how many **Schwarz boundary points** need to be included in **sample mesh** when performing HROM coupling?

Schwarz Boundary Sampling for All-HROM Coupling



Key question: how many Schwarz boundary points need to be included in **sample mesh** when performing HROM coupling?

- Naïve/sparsely-sampled Schwarz boundary results in **failure** to transmit coupling information during Schwarz



Movie above: FOM (left) and all HROM with $N_b = 5\%$ (right).
ROMs have $K = 100$ modes and $N_s = 0.5\%N$ sample mesh points.

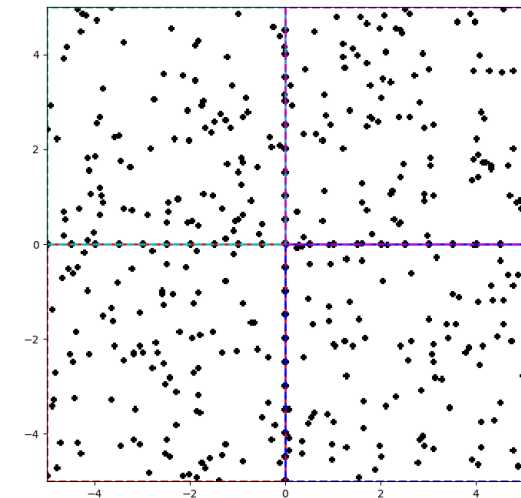


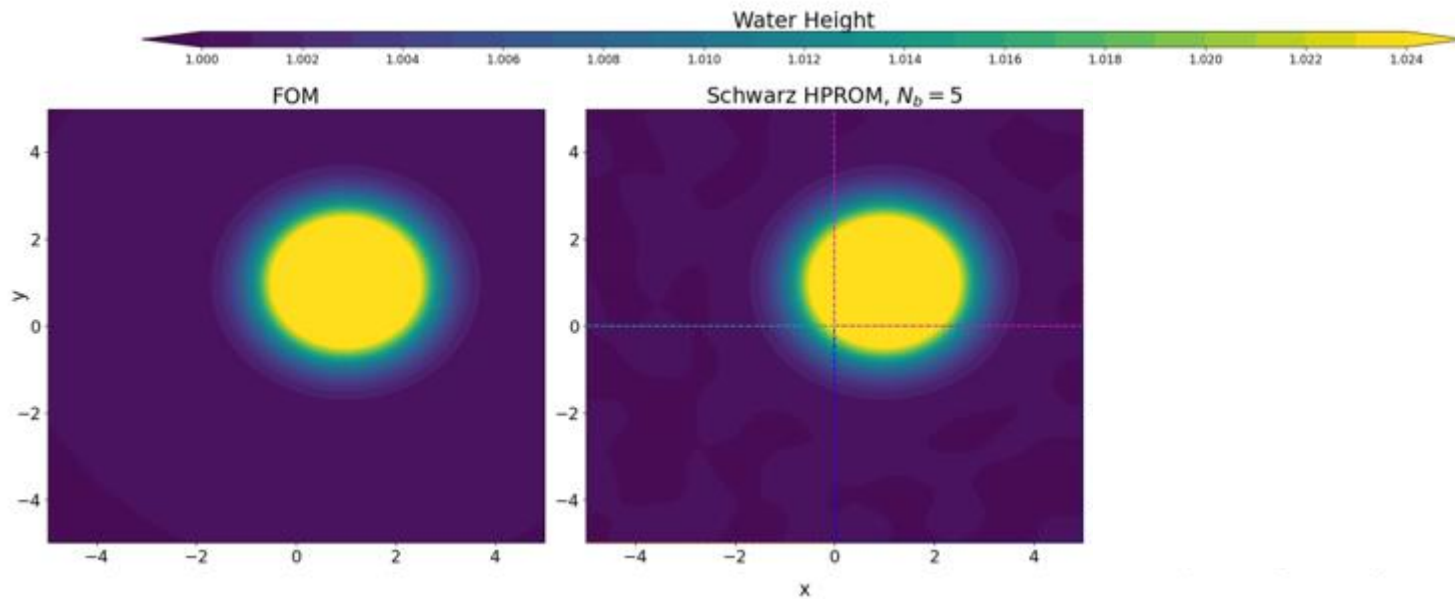
Figure above: example sample mesh with sampling rate $N_b = 5\%$.

Schwarz Boundary Sampling for All-HROM Coupling



Key question: how many Schwarz boundary points need to be included in **sample mesh** when performing HROM coupling?

- Naïve/sparse-sampled Schwarz boundary results in **failure** to transmit coupling information during Schwarz



Movie above: FOM (left) and all HROM with $N_b = 5\%$ (right).
ROMs have $K = 100$ modes and $N_s = 0.5\%N$ sample mesh points.

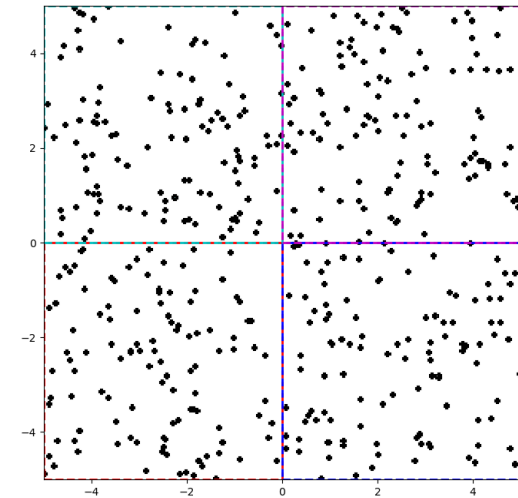


Figure above: example sample mesh with sampling rate $N_b = 0$.

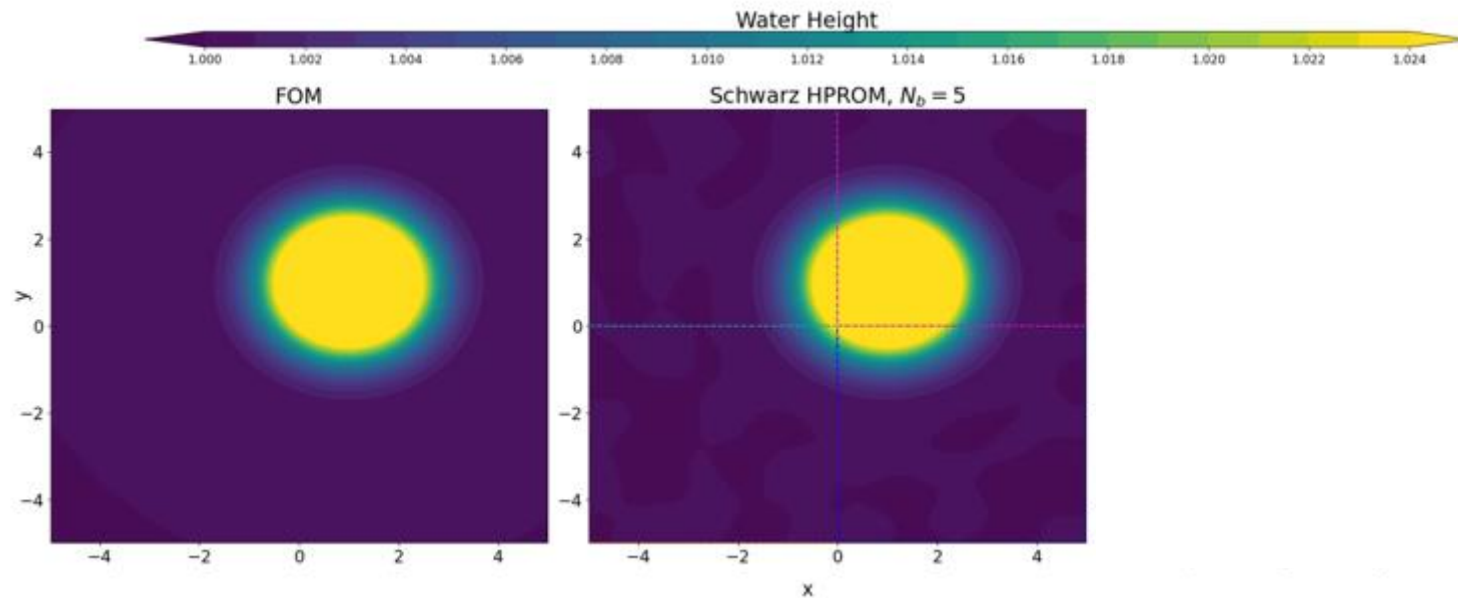
- Including too many Schwarz boundary points (N_b) in sample mesh given **fixed budget** of N_s sample mesh points may lead to **too few sample mesh points in interior**

Schwarz Boundary Sampling for All-HROM Coupling



Key question: how many Schwarz boundary points need to be included in **sample mesh** when performing HROM coupling?

- Naïve/sparse-sampled Schwarz boundary results in **failure** to transmit coupling information during Schwarz



Movie above: FOM (left) and all HROM with $N_b = 5\%$ (right).
ROMs have $K = 100$ modes and $N_s = 0.5\%N$ sample mesh points.

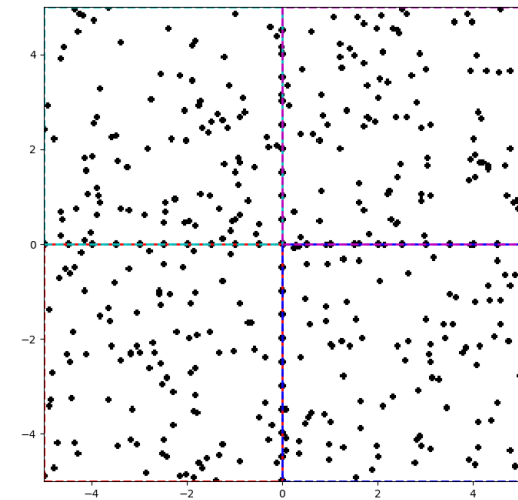


Figure above: example sample mesh with sampling rate $N_b = 5\%$.

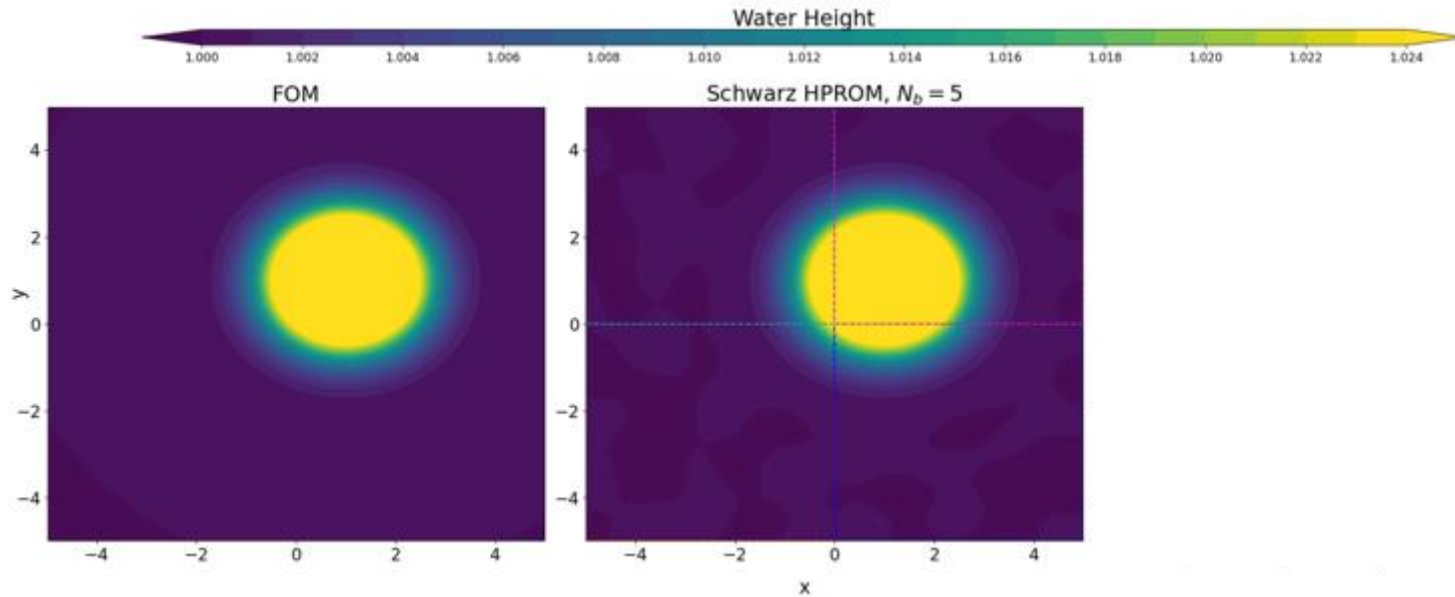
- Including too many Schwarz boundary points (N_b) in sample mesh given **fixed budget** of N_s sample mesh points may lead to **too few sample mesh points in interior**

Schwarz Boundary Sampling for All-HROM Coupling



Key question: how many Schwarz boundary points need to be included in **sample mesh** when performing HROM coupling?

- Naïve/sparse-sampled Schwarz boundary results in **failure** to transmit coupling information during Schwarz



Movie above: FOM (left) and all HROM with $N_b = 5\%$ (right).
ROMs have $K = 100$ modes and $N_s = 0.5\%N$ sample mesh points.

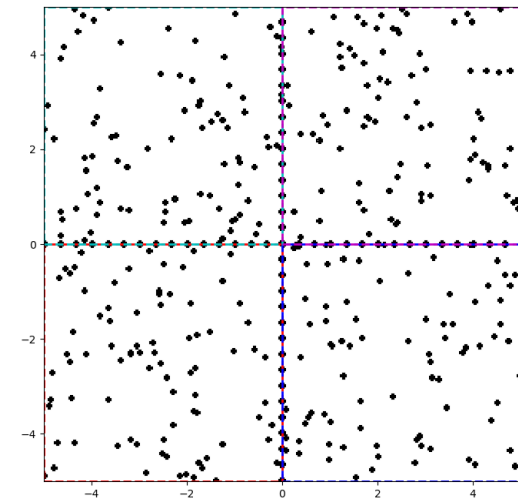


Figure above: example sample mesh with sampling rate $N_b = 10\%$.

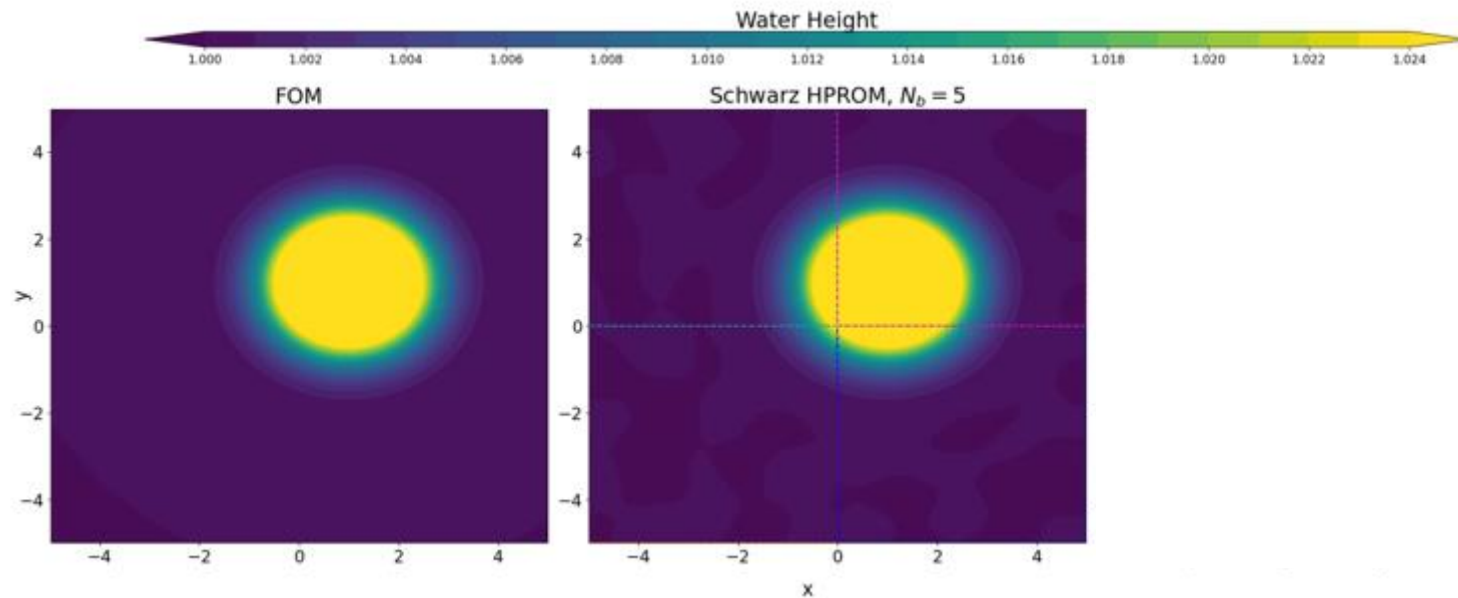
- Including too many Schwarz boundary points (N_b) in sample mesh given **fixed budget** of N_s sample mesh points may lead to **too few sample mesh points in interior**

Schwarz Boundary Sampling for All-HROM Coupling



Key question: how many Schwarz boundary points need to be included in **sample mesh** when performing HROM coupling?

- Naïve/sparse-sampled Schwarz boundary results in **failure** to transmit coupling information during Schwarz



Movie above: FOM (left) and all HROM with $N_b = 5\%$ (right).
ROMs have $K = 100$ modes and $N_s = 0.5\%N$ sample mesh points.

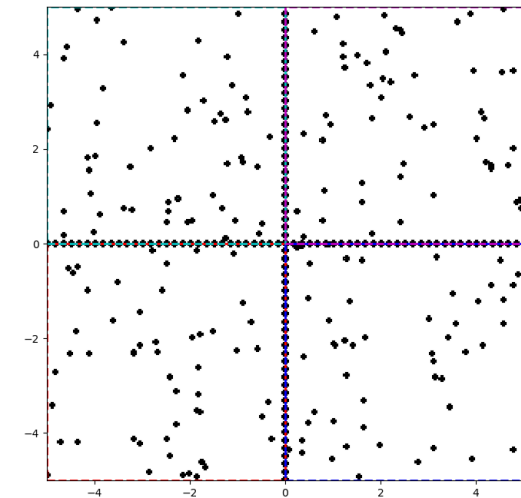


Figure above: example sample mesh with sampling rate $N_b = 15\%$.

- Including too many Schwarz boundary points (N_b) in sample mesh given **fixed budget** of N_s sample mesh points may lead to **too few** sample mesh points in interior

$$\frac{\partial}{\partial t} \begin{pmatrix} \rho \\ \rho u \\ \rho v \\ \rho E \end{pmatrix} + \frac{\partial}{\partial x} \begin{pmatrix} \rho u \\ \rho u^2 + p \\ \rho uv \\ (E + p)u \end{pmatrix} + \frac{\partial}{\partial y} \begin{pmatrix} \rho v \\ \rho uv \\ \rho v^2 + p \\ (E + p)v \end{pmatrix} = \mathbf{0}$$

$$p = (\gamma - 1) \left(\rho E - \frac{1}{2} \rho (u^2 + v^2) \right)$$

Problem setup:

- $\Omega = (0,1)^2$, $t \in [0, 0.8]$, homogeneous Neumann BCs
- Fix $\rho_1 = 1.5$, $u_1 = v_1 = 0$, $p_3 = 0.029$
- Vary p_1 ; IC from compatibility conditions*
 - Training: $p_1 \in [1.0, 1.25, 1.5, 1.75, 2.0]$
 - Testing: $p_1 \in [1.125, 1.375, 1.625, 1.875]$

FOM discretization:

- Spatial discretization given by a first-order **cell-centered finite volume** discretization with $N = 300$ or $N = 100$ elements in each dimension
- Implicit first order temporal discretization: **backward Euler** with fixed $\Delta t = 0.005$
- Implemented in **Pressio-demoapps** (<https://github.com/Pressio/pressio-demoapps>)

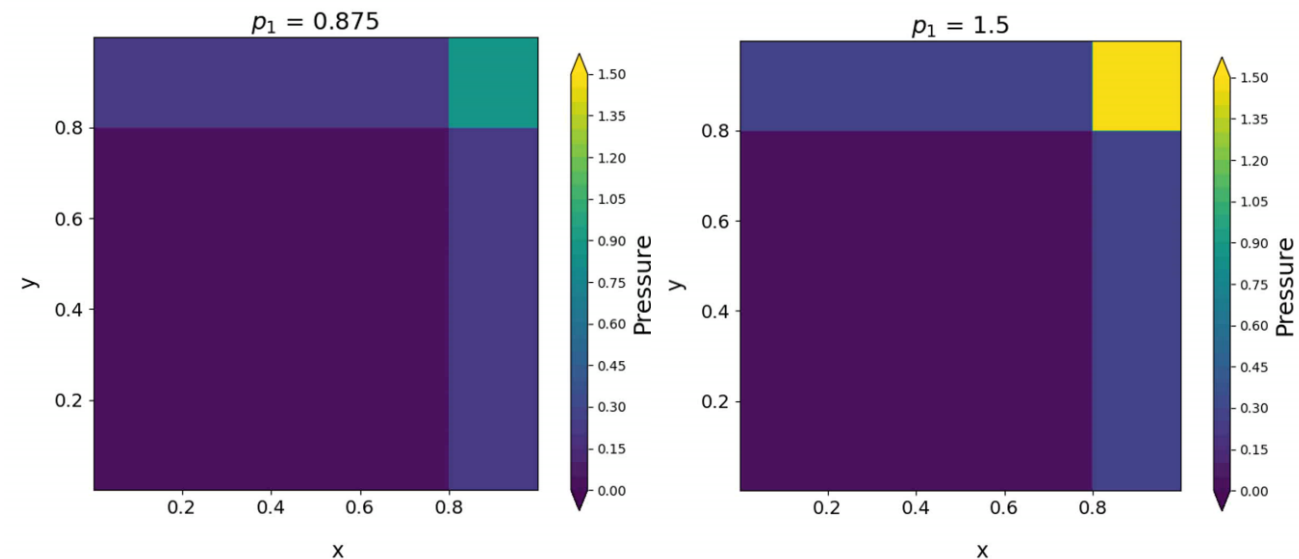


Figure above: FOM solutions to Euler Riemann problem for $p_1 = 0.875$ (left) and $p_1 = 1.5$ (right).

Preliminary results (WIP)

*Schulz-Rinne, 1993.

Schwarz Coupling Details

Choice of domain decomposition

- Overlapping and non-overlapping DD of Ω into 4 subdomains coupled via additive/multiplicative Schwarz
- All-ROM or All-HROM coupling via Pressio*



Snapshot collection and reduced basis construction

- Single-domain FOM on Ω used to generate snapshots/POD modes

Enforcement of boundary conditions (BCs) in ROM at Schwarz boundaries

- BCs are imposed approximately by fictitious ghost cell states
- Dirichlet-Dirichlet BCs for both overlapping and non-overlapping

Choice of hyper-reduction

- Collocation and gappy POD for hyper-reduction
- Assume fixed budget of sample mesh points at Schwarz boundaries

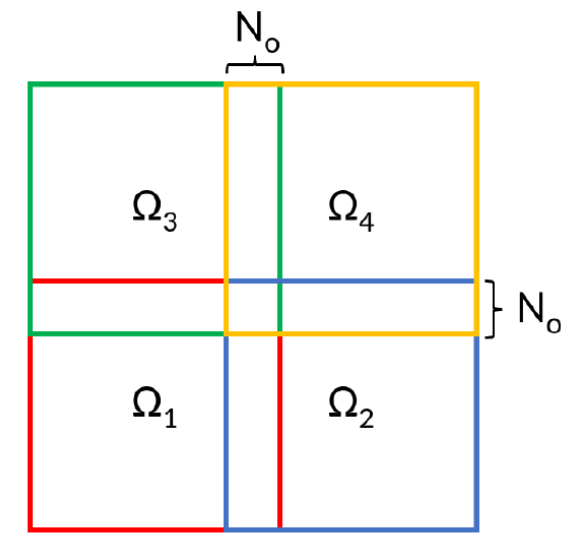


Figure above: DD of Ω into 4 subdomains

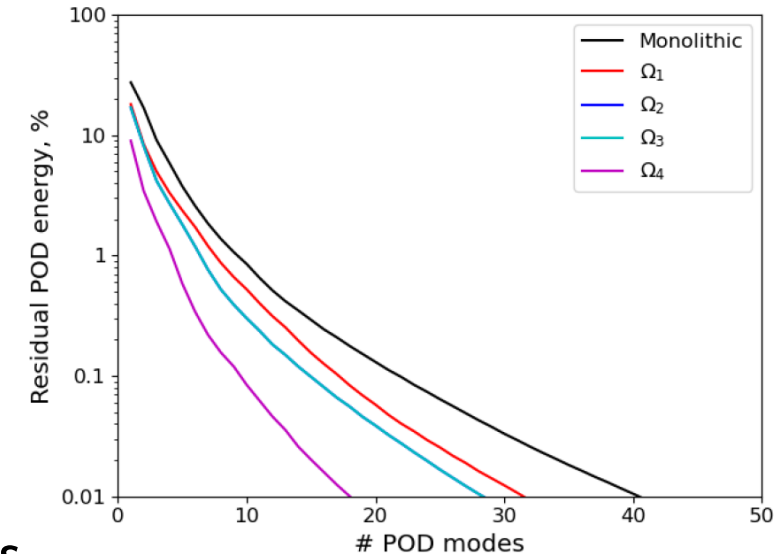
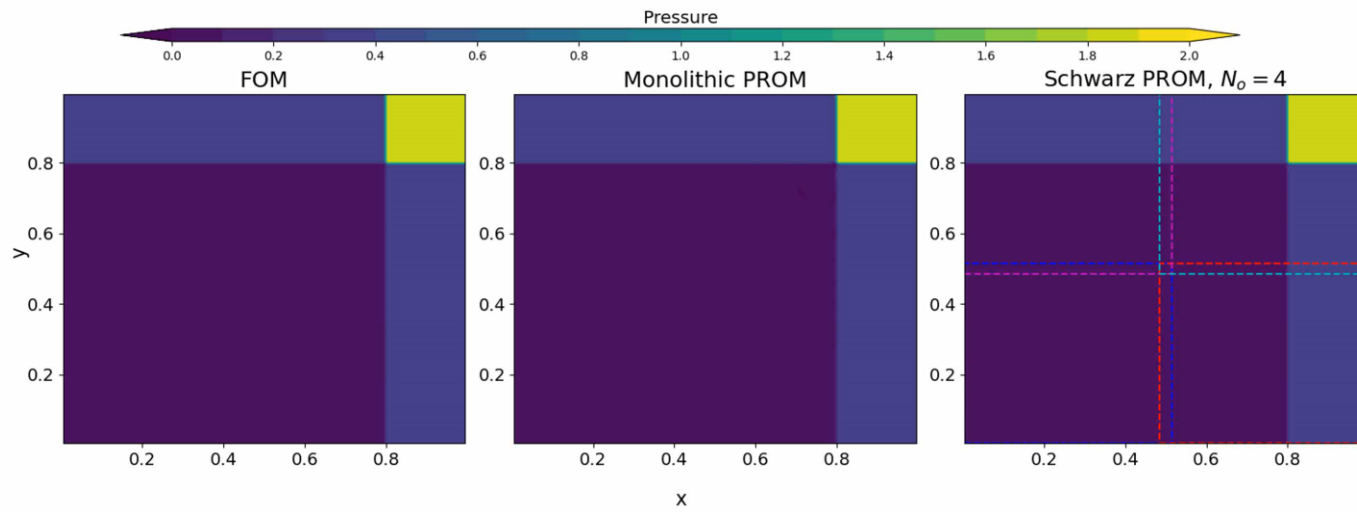


Figure above: Slow decay of POD energy for Euler problem

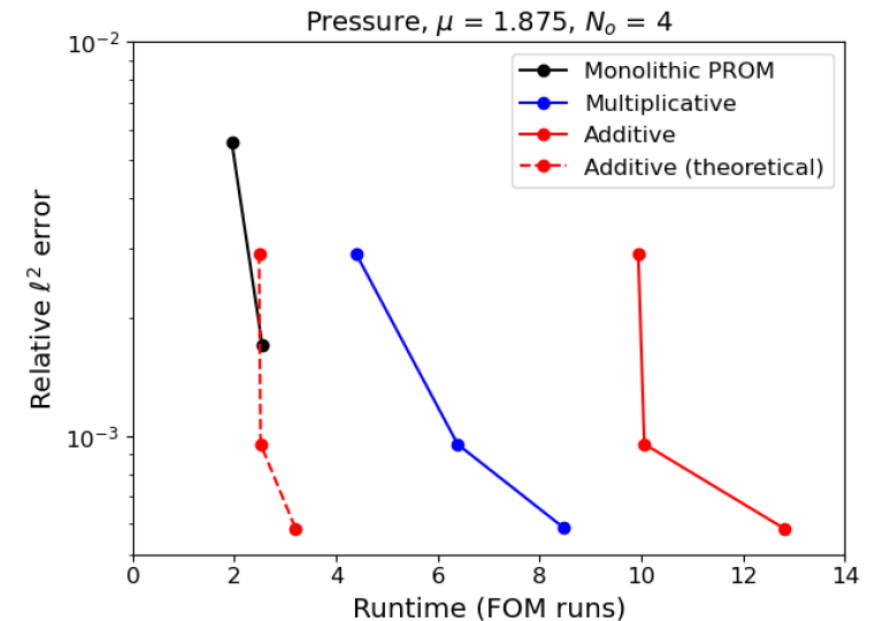
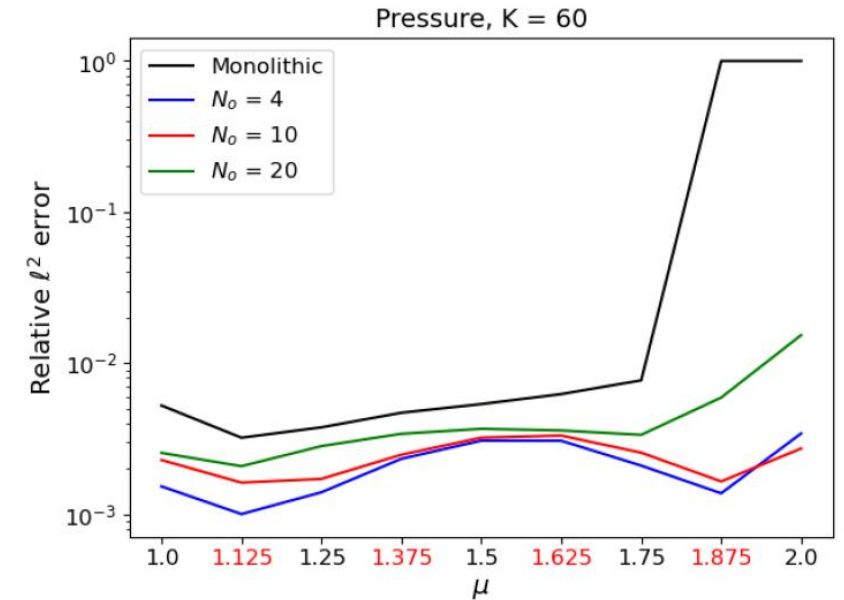
Model Problem 3: All-ROM Coupling + Overlapping Schwarz



- For smaller basis sizes and larger p_1 , monolithic ROM is **unstable** whereas **Schwarz ROM** gives accurate solution!
- Increased **overlap** degrades accuracy (top right)
- Shock transmission **error significantly increases with overlap**
- **~4.4 average # Schwarz iterations** with additive Schwarz vs. **~3.6** for multiplicative Schwarz
- With **additive Schwarz**, can achieve **lower error** than monolithic ROM for **same CPU time** (bottom right)



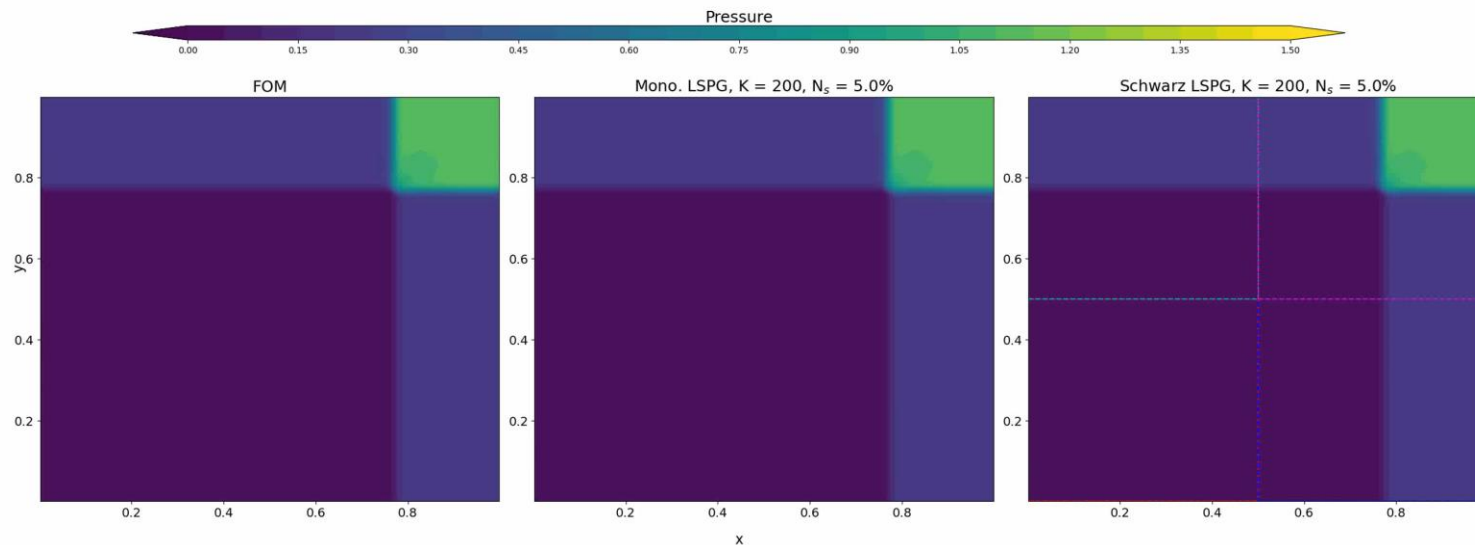
Movie above: FOM (left), $K = 50$ monolithic ROM (middle), and $K = 50$ overlapping Schwarz ROM with $N_o = 4$ (left) for $p_1 = 1.875$.



Model Problem 3: All-HROM Coupling + Non-Overlapping Schwarz



- Hyper-reduction via collocation works better than gappy POD
- Schwarz can give **improved accuracy** relative to monolithic ROM
- Achieving **cost-savings** w.r.t. monolithic FOM is WIP



Movie above: FOM (left), HROM (middle) and Schwarz All-HROM (right) solution. HROMs have 5% sampling rate and 200 POD modes.

Preliminary results (WIP)

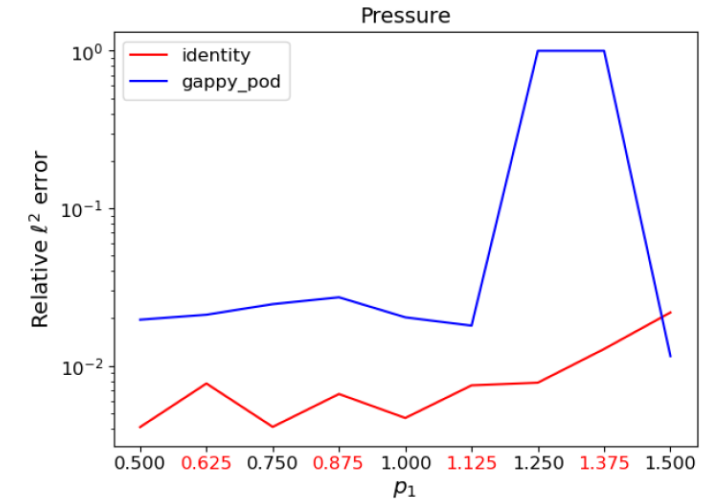


Figure above: collocation and gappy POD relative errors for $K=200$, 1% sampling rate.

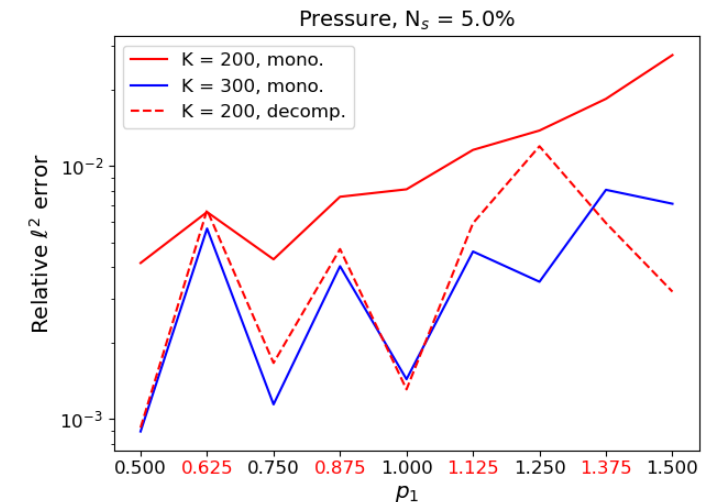


Figure above: monolithic vs. decomposed HROM errors with 5% sampling rate no overlap.

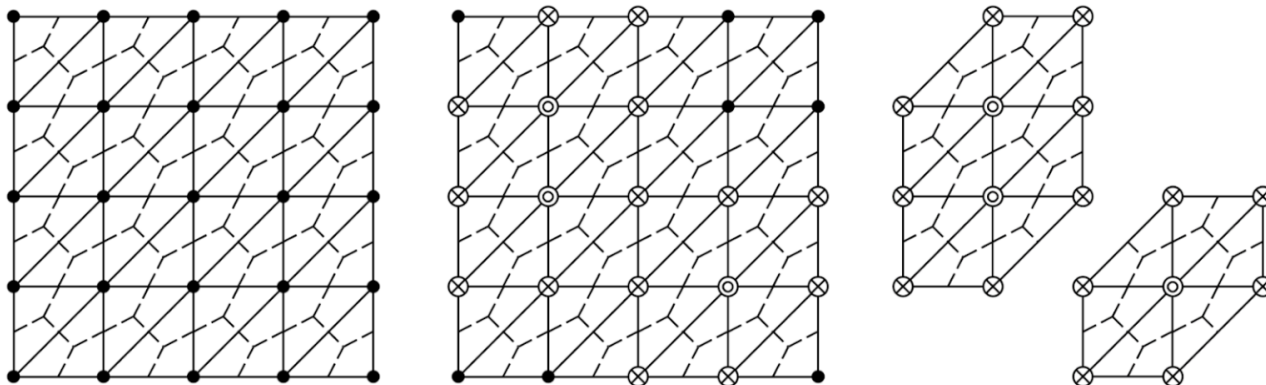
Energy-Conserving Sampling and Weighting (ECSW)



- **Project-then-approximate** paradigm (as opposed to approximate-then-project)

$$\begin{aligned} r_k(q_k, t) &= W^T r(\tilde{u}, t) \\ &= \sum_{e \in \mathcal{E}} W^T L_e^T r_e(L_{e+} \tilde{u}, t) \end{aligned}$$

- $L_e \in \{0,1\}^{d_e \times N}$ where d_e is the **number of degrees of freedom** associated with each mesh element (this is in the context of meshes used in first-order hyperbolic problems where there are N_e mesh elements)
- $L_{e+} \in \{0,1\}^{d_e \times N}$ selects degrees of freedom necessary for **flux reconstruction**
- Equality can be **relaxed**



Augmented reduced mesh: \odot represents a selected node attached to a selected element; and \otimes represents an added node to enable the full representation of the computational stencil at the selected node/element

ECSW: Generating the Reduced Mesh and Weights



- Using a subset of the same snapshots $u_i, i \in 1, \dots, n_h$ used to generate the **state basis** V , we can train the reduced mesh
- Snapshots are first **projected** onto their associated basis and then **reconstructed**

$$c_{se} = W^T L_e^T r_e \left(L_e + \left(u_{ref} + V V^T (u_s - u_{ref}) \right), t \right) \in \mathbb{R}^n$$

$$d_s = r_k(\tilde{u}, t) \in \mathbb{R}^n, \quad s = 1, \dots, n_h$$

- We can then form the **system**

$$\mathbf{C} = \begin{pmatrix} c_{11} & \dots & c_{1N_e} \\ \vdots & \ddots & \vdots \\ c_{n_h 1} & \dots & c_{n_h N_e} \end{pmatrix}, \quad \mathbf{d} = \begin{pmatrix} d_1 \\ \vdots \\ d_{n_h} \end{pmatrix}$$

- Where $\mathbf{C}\xi = \mathbf{d}$, $\xi \in \mathbb{R}^{N_e}$, $\xi = \mathbf{1}$ must be the solution
- Further relax the equality to yield **non-negative least-squares problem**:

$$\xi = \arg \min_{x \in \mathbb{R}^n} \|\mathbf{C}x - \mathbf{d}\|_2 \text{ subject to } x \geq \mathbf{0}$$

- Solve the above optimization problem using a **non-negative least squares solver** with an **early termination condition** to promote sparsity of the vector ξ